ISSN 1016-6254

Österreichische Beiträge zu Meteorologie und Geophysik

Heft 29

Scientific Contributions of Austria to the Mesoscale Alpine Programme (MAP)

Wien 2003

Österreichische Beiträge zu
Meteorologie und Geophysik

Heft 29

Scientific Contributions of Austria to the Mesoscale Alpine Programme (MAP)

Wien 2003

Zentralanstalt für Meteorologie und Geodynamik, Wien

Publ.Nr. 409

ISSN 1016-6254

I M P R E S S U M

Herausgeber: Zentralanstalt für Meteorologie und Geodynamik (ZAMG), Wien
Institut für Meteorologie und Geophysik (IMG), Universität Graz
Institut für Meteorologie und Geophysik (IMG), Universität Innsbruck
Institut für Meteorologie und Geophysik (IMG), Universität Wien
Institut für Angewandte Geophysik (IAG), Montanuniversität Leoben
Institut für Meteorologie und Physik (IMP), Univ. für Bodenkultur, Wien
Institut für Theoretische Geodäsie und Geophysik (IGG), Technische Univ., Wien

Leitender Redakteur: Peter Steinhauser, ZAMG, Wien
Redaktionskomitee: Ewald Brückl, IGG, Wien
Michael Hantel, IMG, Wien
Helga Kromp-Kolb, IMP, Wien
Michael Kuhn, IMG, Innsbruck
Hermann Mauritsch, IAG, Leoben

für den Inhalt verantwortlich:
Kathrin Baumann-Stanzer, Georg Mayr, Reinhold Steinacker

Druck: Grafisches Zentrum HTU GmbH
1040 Wien, Wiedener Hauptstraße 8-10
www.grafischeszentrum.at

Verlag: Zentralanstalt für Meteorologie und Geodynamik
Hohe Warte 38, A-1190 Wien
Austria (Österreich)

PREFACE

The Mesoscale Alpine Programme (MAP), an international research initiative lasting from 1995 until 2004, was established to carry out scientific investigations with regard to the weather in mountains. Several hundred scientists worldwide joined together to obtain important new findings in the filed of mountain meteorology by utilizing synergies. During a field experiment in the Autumn of 1999, where Austria could act as the host country, a unique data set was collected, which is serving since then as important fundament for the relevant scientific research. Besides climatological evaluations the data set originating of standard instrumentation as well as of sophisticated special observing platforms allows a better insight into the mechanisms of alpine weather phenomena and last not least a validation of high resolution prediction models. Especially with regard to extreme weather events which repeatedly lead to severe problems in the Alpine region and which seem to become more frequent in the course of the global change an improved understanding and prediction is of high socio-economic importance. Besides extreme precipitation events with floodings, land slides and avalanches wind storm events are being responsible for much of the weather related damages. The Austrian participants of MAP devoted their work basically to the latter theme. The present volume summarises some of the research activities which have been funded by the Austrian Science Foundation (FWF).

VORWORT

Das Mesoscale Alpine Programme (MAP), eine internationale Forschungsinitiative, hat in dem 10-jährigen Zeitraum 1995 bis 2004 die wissenschaftliche Erforschung des Wettergeschehens im Gebirge zum Ziel. Mehrere hundert Wissenschaftler weltweit haben sich zusammengefunden um durch die Bündelung der Ressourcen wichtige neue Erkenntnisse in der Gebirgsmeteorologie zu erzielen. Während eines Feldexperiments im Herbst 1999, bei dem Österreich die Gastgeberrolle spielen konnte, wurde ein einzigartiger Datensatz gewonnen, der seither als wichtige Basis für die fachbezogene Forschung dient. Neben klimatologischen Arbeiten erlauben die gesammelten Daten aus Routine-Mess-systemen und zahlreichen modernen Spezial-Mess-Plattformen auch einen besseren Einblick in die Mechanismen alpiner Wetterphänomene und nicht zuletzt eine Validierung hochauflösender Prognosemodelle. Insbesondere in Hinblick auf Extremwetterlagen, die im Alpenraum immer wieder zu großen Problemen führen und die im Zuge des globalen Wandels häufiger werden dürften, ist eine Verbesserung des Verständnisses und der Vorhersage von großer gesellschaftspolitischer Bedeutung. Neben den Extremniederschlägen mit ihren Folgen in Form von Überschwemmungen, Vermurungen und Lawinen sind die Starkwindereignisse hauptverantwortlich für wetterbedingte Schäden. Die österreichischen Teilnehmer an MAP haben sich vor allem letzterem Themenkreis gewidmet. Der vorliegende Band fasst einige Ergebnisse dieser Forschungsvorhaben zusammen, die vom österreichischen Fonds zur Förderung Wissenschaftlicher Forschung (FWF) gefördert wurden.

ROM - RHINE VALLEY OZONE STUDY WITHIN MAP

Kathrin Baumann-Stanzer, Martin Piringer, Gabriele Rau, Ulrike Pechinger

Central Institute for Meteorology and Geodynamics (ZAMG), A-1190 Vienna, Austria

Abstract

Within the Meso-scale Alpine Programme MAP, ZAMG conducted the Rhine valley ozone study, putting additional instrumentation in the area just south of Lake Constance. The vertical structure and the temporal evolution of the planetary boundary layer (PBL) and the ozone concentrations during Foehn episodes were observed by using a tethersonde system carrying up to three meteorological and up to two ozone sondes simultaneously, a sonde mounted on the Pfaender cable car, a sodar as well as an ultrasonic anemometer and one conventional ground-based meteorological station. Additionally, cross-Alpine measurements with the french aircraft ARAT (Fokker 27) were undertaken on selected Foehn days. Analysis of the vertical structure of the PBL from soundings, trajectory analyses and comparisons between measured and modelled sensible heat flux reveal the physical processes going on in the target area during Foehn cases. An overview about the objectives is given and highlights of the results of the Rhine valley ozone study are presented. New insight in the vertical structure of the boundary layer during Foehn events in the target area has been found and is explained.

1 INTRODUCTION

The Rhine valley ozone study is conducted by ZAMG in a joint effort with other Foehn investigations in the Rhine Valley during MAP. ZAMG contributed to the MAP field experiment in autumn 1999 by putting up vertical sounding devices (a cable car sonde, a multi-sonde tethered balloon system, and a boundary-layer sodar) in the Rhine valley just south of Lake Constance (Fig. 1).

Both the tethersonde system and the cable car sonde measure ozone, and thus the vertical structure and the temporal evolution of the PBL and the ozone concentrations during Foehn episodes are investigated (Pechinger et al., 2000a,b; Piringer et al., 2000 and 2001).

On 5 Foehn days, airborne meteorological and air pollution measurements undertaken with the light research aircraft Dimona (Metair) are available.

The measurements of ozone concentrations are used to distinguish air masses within the valley and to assign regions of origin of the advected Foehn air. Trajectory calculations and mesoscale model studies are used to determine the origin of the different air masses involved (Baumann et al., 2001).

Within STAAARTE 99, measurements with the French aircraft ARAT (Fokker 27) were carried out on selected days in the same area to characterise the old air mass in the Rhine valley before the onset of a South Foehn event and to describe the changes caused by the Foehn (Rau and Baumann, 2000a,b,c,d).

Results of all these activities are described in the following.

2 INSTRUMENTATION

The array of instruments, mainly vertical soundings systems, operated by ZAMG during the MAP SOP (September 7 to November 15, 1999), is depicted in Figure 1.

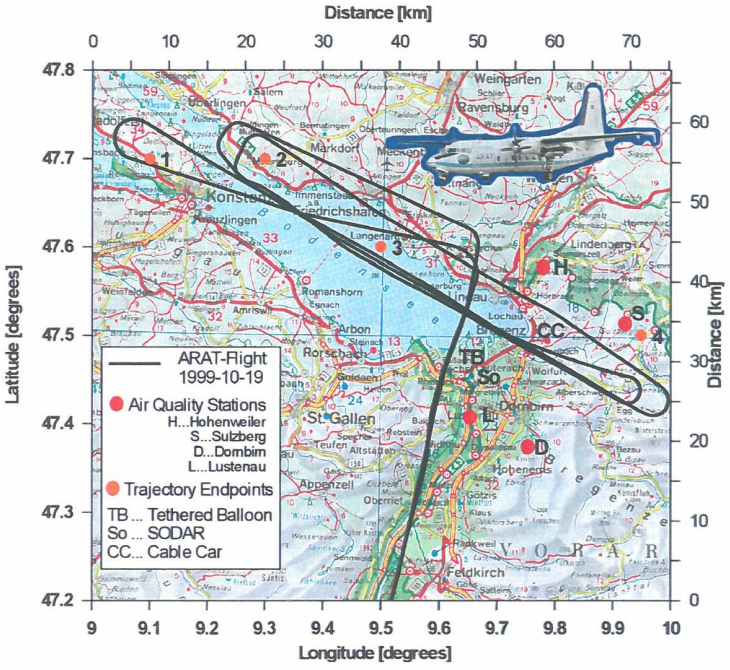

Fig. 1: Map of the Austrian/Swiss Rhine valley south of Lake Constance showing the measurement sites CC: sonde at Pfänder cable car, TB: tethered balloon, meteorological station, So: sodar and ultrasonic anemometer (sonic). Flight track (ARAT) on October 19, endpoints of calculated trajectories and locations of ground-based measurements.

The parameters measured with the different systems in use as well as selected operating parameters are summarised in Tables 1 and 2, respectively.

Site	instrument	T	h	p	dd	ff	gl	O_3
Fussach	meteorological station	X	X	X	X	X	X	
	tethered balloon	X	X	X	X	X		X
Pfänder	cable car sonde	X	X	X				X
Lustenau	sodar				X	X		
	ultrasonic anemometer	X	X	X	X	X		

Tab. 1: Measured parameters temperature T, relative humidity h, air pressure p, wind direction dd, wind speed ff, global radiation gl, ozone O_3.

The tethered balloon system as well as the cable car sonde were in operation on selected Foehn days, whereas the other instruments monitored continuously. The instrumentation is described in detail by Piringer et al. (2001). The special observation periods of tethered balloon system and cable car operation are listed in Pechinger et al. (2000a,b).

Parameter	TMT system	Cable car sonde	Sodar	USA
Frequency	403 MHz	-	2 kHz	40 kHz
Average	-	-	30 min.	10 min.
Vertical range	500 m	550 m	~ 700 m	-
Range resolution	< 10 m	~ 10 m	50 m	-

Tab. 2: Selected operating parameters of the different systems

3 FOEHN BREAKTHROUGH ON OCTOBER 24, 1999

24 October 1999 was the final day of a 4 days lasting Foehn period caused by a prevailing south-westerly airflow in 500 hPa over the Alps. Most of the time, a shallow ground-based cold air pool prevailed below the Foehn flow in the area just south of Lake Constance, in contrast to the situation further south (Piringer et al., 2001; Baumann et al., 2001). Finally, on October 24, a Foehn breakthrough occurred in the area around 11 UTC and Foehn storm was observed at the sites depicted in figure 1 until 16 UTC.

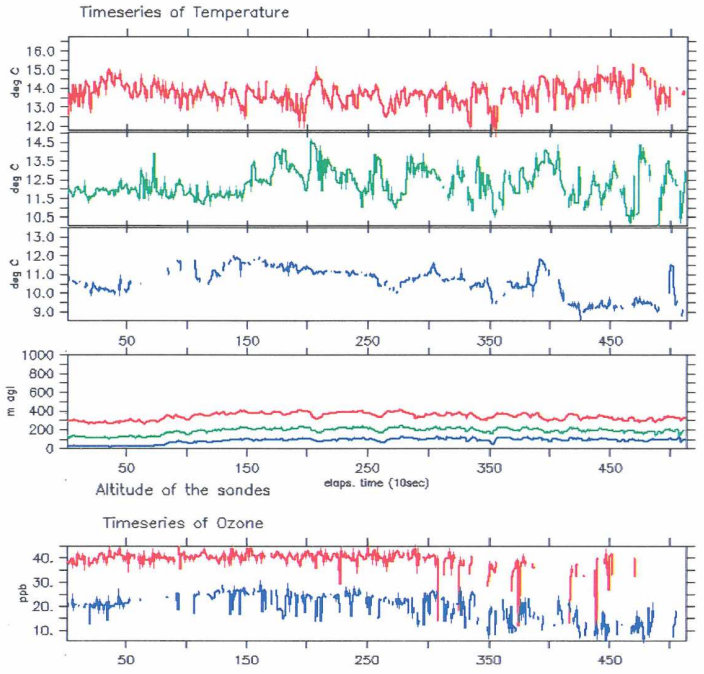

Fig. 2: Time series of temperature (°C), altitudes of the three sondes (in m above ground) and ozone (ppb) measured with 3 tethered balloon sondes at Fussach measured on October 24, 1999 between 7:20 and 9 UTC.

The TMT tethered balloon system at Fussach is able to give insight into the structure of the near-surface boundary layer before the breakthrough of the Foehn to the ground. Because the winds were already strong and gusty before that event, the three meteorological sondes were kept at only approximately 300, 200 and 100 m height to ensure rapid gathering of the sondes in case of anticipated Foehn breakthrough; at the uppermost and lowermost level, the sondes were combined with an ozone sonde. Time series of temperature and ozone between 7:20 and 9 UTC are shown in Fig. 2.

The meteorological and ozone sondes at 300 m are within the Foehn air during the whole period shown in Fig. 2: air temperature ranges between 12 and 15 °C, and ozone is around 40 ppb. The meteorological sonde at 200 m is partly within, partly outside the Foehn air. Especially during the second half of the period shown in Fig. 2, large temperature variations occur at this level. One gets the impression of an undulating boundary between the warm Foehn air above and the cool, moist air pool below, extending only about 200 m above the surface during this period. The lowest sonde is within an easterly flow during the first half of the period. Afterwards, a shift towards north occurs, and successively temperature and ozone drops to lower values.

There are three different effects that might have contributed to the existence of this shallow cold air pool with northerly to easterly flow: the diurnal cycle of the valley wind system, a lake breeze from the Lake of Constance, and possibly advection due to a regional scale pressure gradient caused by the

Foehn flow pattern. From the course of the tethersonde measured, no rapid Foehn break-through to the ground was expected. Instead, a slightly growing ground-based cool layer was supposed to occur, as was experienced during previous Foehn events. The sudden Foehn break-through at about 11 UTC came therefore as a surprise to the crew maintaining the TMT - system, and the balloon got lost. Gusts of up to 24 m s^{-1} occurred in the afternoon.

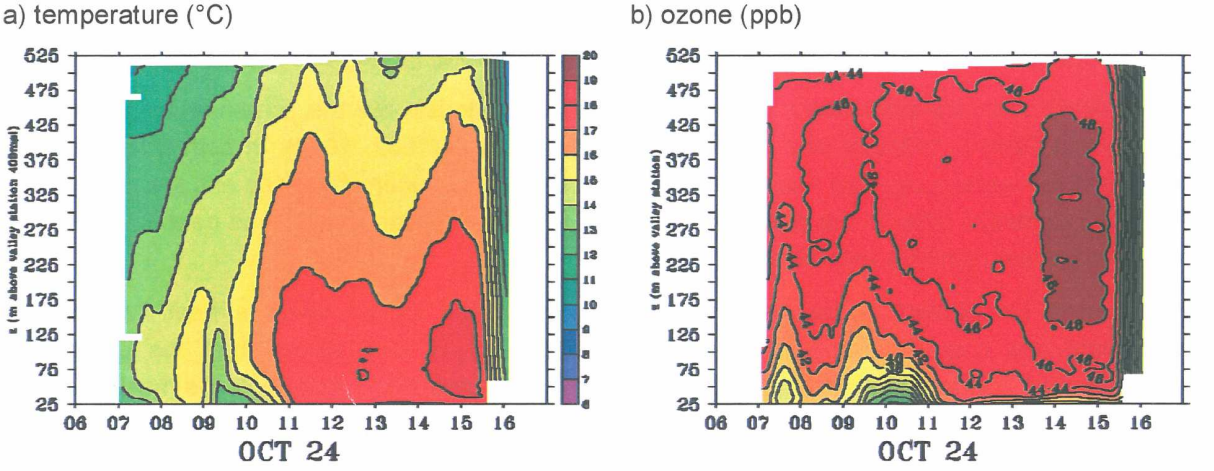

Fig. 3: Time-series of vertical soundings a) of temperature (°C) and b) ozone (ppb) from Pfänder cable car at Bregenz between 400 m and 1053 m above sea level on October 24, 1999.

The cable car sonde measurements give insight into the temporal variation of the vertical ozone and temperature distribution between the morning and the late afternoon on 24 October 1999 (Fig. 3a and b).

Until 11 UTC, strong vertical gradients of ozone and temperature are observed. This is typical for the many Foehn cases when the Foehn air does not reach the ground in the area. The boundary between the cold air pool at the ground and the ozone-rich Foehn air above shows a wavy structure. With the breakthrough of the Foehn after 11 UTC, the inversion disappears, and ozone concentrations up to 40 ppb are observed near the surface.

The results show the ability of the tethered balloon tower system and the cable car sonde to give a comprehensive qualitative picture of the complex structures in the PBL during south Foehn events observed within a rather small area. Based on the profiles from the used sounding devices it is possible to distinguish clearly the cold near-ground air pool from the overlying Foehn air, marked by strong gradients of the meteorological parameters and the ozone concentrations.

4 SIMULATIONS OF THE PBL – FOEHN INTERACTION

As discussed by Baumann et al. (2000, 2002), time series of the sensible heat flux turn out to be good indicators for Foehn air reaching a site. Usually, the advected air is much warmer than the ground below. Thus, the sensible heat flux rapidly turns to negative (ground-directed) values. The absolute values of these fluxes are much larger than those usually observed during night and thus can be easily distinguished from the latter. Measurements of PBL parameters as the sensible heat flux are available from an ultrasonic anemometer which had been operated during the field experiment at a 10 m mast at Lustenau (Fig. 1).

The course of the sensible heat flux observed on a sunny day with weak winds (3 September 1999) and on a Foehn day (24 October 1999) is depicted in Fig. 4. These examples show how the PBL evolution on a Foehn day can differ from the usual conditions observed on a fair-weather day.

Compared to September 3, the breakthrough of the Foehn air on October 24 around 11 UTC causes a reverse diurnal course of the sensible heat flux with strong negative values around noon.

Observations of the PBL parameters as the mixing height and stability are usually not available on a routine basis. Thus, similarity theory is applied in atmospheric dispersion models to calculate necessary dispersion parameters. Surface fluxes of momentum and heat are needed to use the similarity approach. As these turbulent fluxes are also not available on a routine basis, parameterisation schemes have been developed to estimate the surface fluxes from the routine observations of wind speed, temperature, humidity and (if available) global radiation.

Two commonly used pre-processors in European dispersion models are the schemes suggested by Berkowicz and Prahm (1982a,b) and by Holtslag and van Ulden (1982, 1983). In both schemes the calculation of the surface sensible heat flux is based on the surface energy balance and the resistance method. The schemes differ in the parameterisation of the net radiation, the ground heat flux and the partitioning between sensible and latent heat flux.

Both schemes are applied to calculate the temporal evolution of the sensible heat flux at the measurement site (Fig. 4). Hourly measurements of the 10 m wind speed from the ultrasonic anemometer and 2 m temperature and relative humidity measured at the bottom of the mast and the global radiation measured at the meteorological station at Lustenau are used as input to the parameterisation schemes. Some specifications have to be defined to describe the effective underlying surface. Surface roughness is set to 0.25 m, albedo to 15 %, and the leaf area index to 3. The factor for the determination of the ground heat flux is set to 0.15. These values are chosen from empirical values determined in field campaigns over grassland. The Bowen ratio is fixed to 0.35. The results of the parameterisation calculations are depicted as symbols in Figure 4.

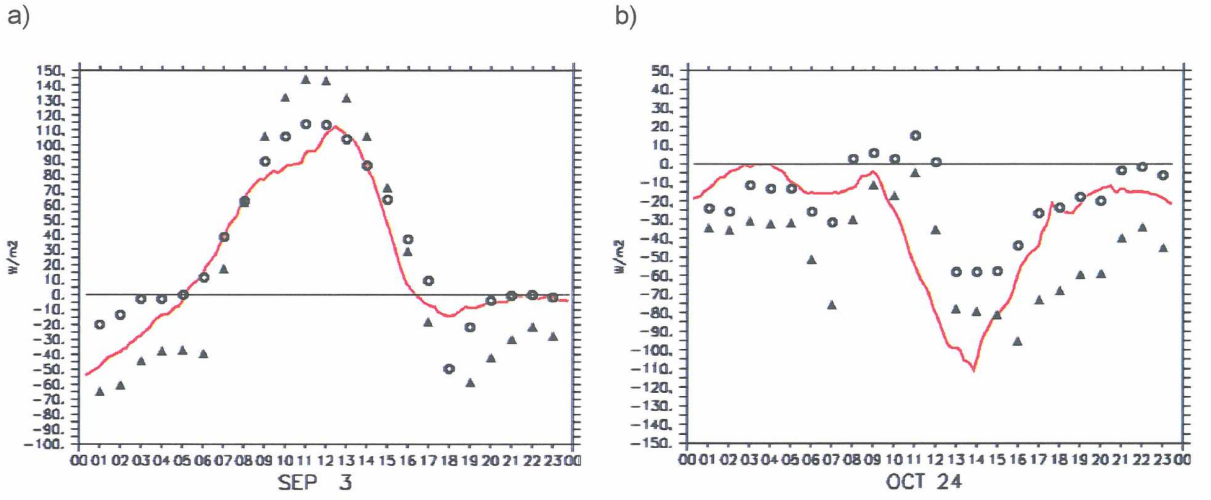

Fig. 4: Time-series of the sensible heat flux from ultrasonic measurements (line) and calculated based on routinely available observations using the scheme after Berkowicz and Prahm (BP, triangles) and after Holtslag and van Ulden (HU, circles); a) on a sunny day with weak winds (3 September 1999), b) under Foehn storm conditions (24 October 1999).

A relatively good agreement is found between the results of the HU scheme and the ultrasonic data on September 3 (Fig. 4a). The BP scheme tends to overestimate the sensible heat flux during daytime and underestimates the nocturnal values. This was also found in other comparison studies (e.g. Erbes and Pechinger, 1999). The ultrasonic anemometer renders a somewhat reduced increase of the surface flux between 8 and 12 UTC which is not found in the model calculations. Both parameterisation schemes render too low values when cooling starts after sunset (between 18 and 20 UTC).

The complex diurnal evolution of the sensible heat flux on 24 October 1999 is quite well reproduced by both schemes (Fig. 4b). Again, the better agreement is achieved with HU, while the results of the BP scheme are too low most of the time. The decrease of the heat flux with the onset of the Foehn flow at the site is simulated about two hours too late. The schemes obviously do not react fast enough to the measured increase of the temperature at 10 UTC (not shown). The model results are in good agreement with the observations for the time period when temperature above 19 °C are recorded (between 12 and 15 UTC).

5 AIR MASS ANALYSES OF TWO FOEHN CASES BASED ON AIRBORNE MEASUREMENTS AND TRAJECTORY CALCULATIONS

As shown before, the onset or breakthrough of Foehn is marked by a sudden increase of ozone. Above the vertical range of the cable car, ozone data are available from airborne measurements undertaken on selected Foehn days by the light research aircraft Dimona (Metair) and by the atmospheric research aircraft ARAT (INSU/CNES). In this section, the Foehn and PBL air masses are analysed based on airborne ozone measurements from the Foehn period between 20 and 24 October 1999 and for the Foehn case of 5 November 1999, when the Foehn air measured by the aircraft did not reach the ground in the area just south of Lake Constance.

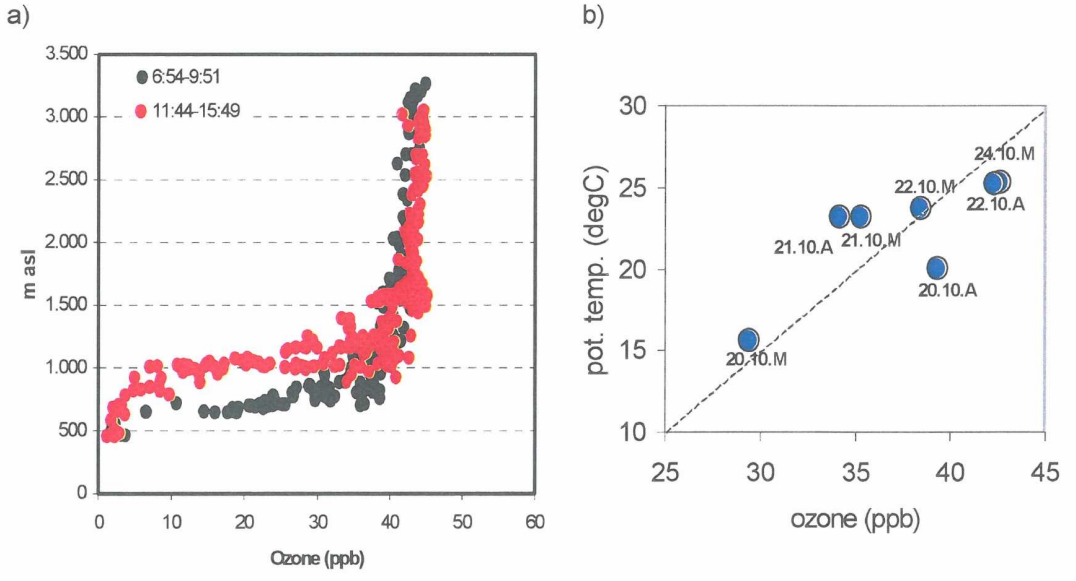

Fig. 5: a) Vertical ozone profiles (ppb) from the Dimona morning (black) and afternoon (red) flight on October 21. Altitudes are given in meters above sealevel. b) Mean ozone concentrations (ppb) plotted against the average potential temperature (°C) within the lowest 2,5 km from Dimona morning (M) and afternoon (A) flights between Sargans and the Lake of Constance on October 20, 21, 22 and 24, 1999.

All ozone measurements conducted with the Dimona aircraft during the period 19 to 24 October 1999 show ozone values below 10 ppb near ground and higher ozone levels above. Typical vertical profiles from the flights on October 21 are depicted in Fig. 5a. The rising of the boundary layer top is well seen in the difference between the morning and afternoon profile. Aloft, the observed ozone concentrations around 45 ppb are more or less constant with height. A significant increase of the potential temperature is often used as Foehn criterion (Duerr, 2000). It is found that the mean ozone concentrations observed by the aircraft during the seven flights are well correlated with the respective average potential temperatures (Fig. 5b).

Since the origin of the ozone-rich air masses is of special interest, trajectories have been calculated backwards for 48 hours travel time based on ECMWF analyses with 0.5 degrees spatial resolution starting at different heights above Bregenz. Two examples, the first day (20 October 1999) when the mean ozone values within the lowest 2,5 km were still relatively low (Fig. 8) and the last day (24 October 1999) of the long lasting Foehn period when maximum ozone values were observed in the Foehn flow by Dimona aircraft (Fig. 5) will be discussed in the following.

Pre-Foehn conditions 19 October 1999

The vertical ozone distribution on 19 October 1999 was observed with the French aircraft ARAT in the frame of the STAAARTE 99 programme. The flight track is depicted in Fig. 1. From the flight data, two vertical ozone profiles were constructed, one representative for the region west of 9.5°E, the other for the region east of 9.65°E (Fig. 6).

The western profile shows a pronounced ozone maximum around 2000 m. The calculation of backward trajectories arriving at the target area at 2000 and 4000 m (Fig. 7) reveals that the air with high ozone values has spent at least two days over the highly industrialised and populated areas of south-western Germany. The air with lower ozone concentrations at higher levels came from northern Europe.

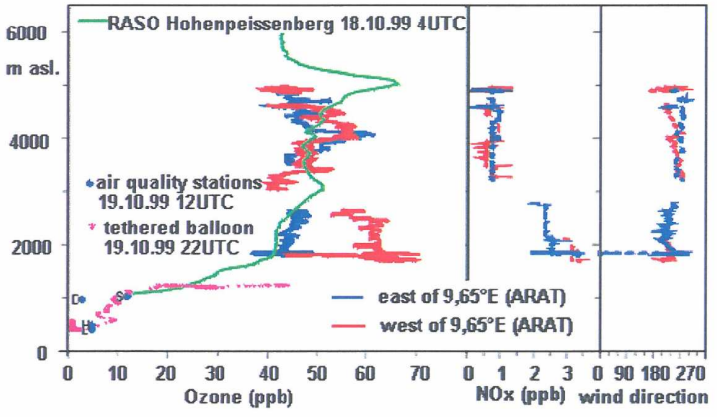

Fig. 6: Vertical ozone profiles (ppb) from the ARAT flight, from Hohenpeissenberg; tethered balloon and air quality network (see Fig. 1); vertical profiles of NOx and wind direction from aircraft data.

The vertical ozone profiles derived from the aircraft data are compared with vertical balloon soundings, data from the regional air quality network and the rawinsonde profile started at Hohenpeissenberg observatory one day before.

The ozone profiles from the different systems depicted in Fig. 6 reveal low ozone values below a low-base elevated inversion and a marked increase over the inversion. The ozone values above the inversion are of the same order of magnitude as the values found by ARAT around noon.

The ozone profile from Hohenpeissenberg from 18 October is in fair good agreement with the aircraft data. At Hohenpeissenberg, an ozone maximum around 5000 m is observed which the aircraft observes at 4000 m a day later. This can be explained by a marked downward movement of the air at higher altitudes shown by trajectory calculations (Fig. 7).

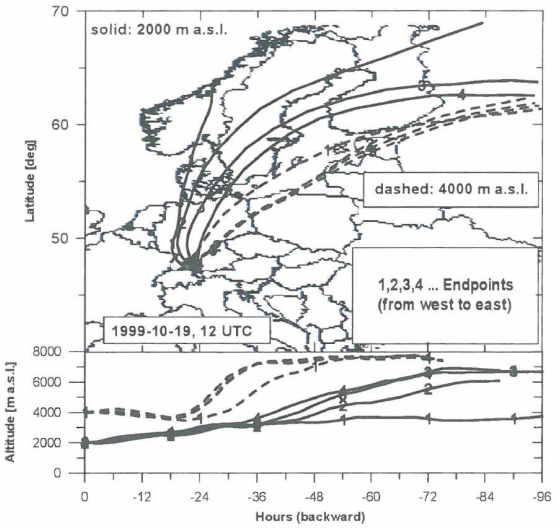

Fig. 7: Backward trajectories for 4 endpoints (locations shown in Fig. 1) at 2000 / 4000 m a.s.l. (top) and traveltime versus altitude (below)

Foehn case 20 October 1999

The trajectories arriving at 250 m, 500 m and 1 km above ground at Bregenz on October 20 18 UTC are depicted in Fig. 8.

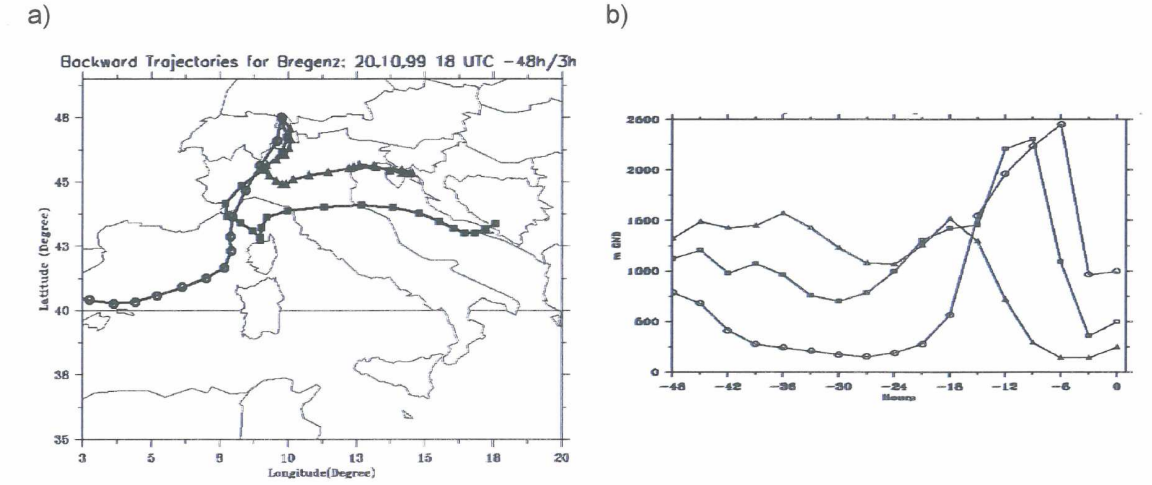

Fig. 8: Three-dimensional backward trajectories arriving at Bregenz on 20 October 1999 18 UTC at 250 m (triangles), 500 m (squares) and 1000 m gnd (circles) based on ECMWF analyses. Symbols mark trajectory position and height every 3 hours.

On October 20, the air arriving at 1 km height at Bregenz originates from the lower PBL above the Mediterranean Sea, while the air masses at lower levels spent the previous to days in 700 to 1500 m above ground (upper convective boundary layer during daytime and in the residual layer at night) at the Adriatic Sea and the Po Valley (Fig. 8 a,b).

Foehn case 24 October 1999

The trajectories arriving on October 24 at 12 UTC in 100 m, 500 m, 1000 m, 1500 m and 2000 m height at Bregenz were computed based on mesoscale model runs with MM5 and the Swiss Model. The MM5 trajectories are close to those calculated from the ECMWF analyses (not shown).

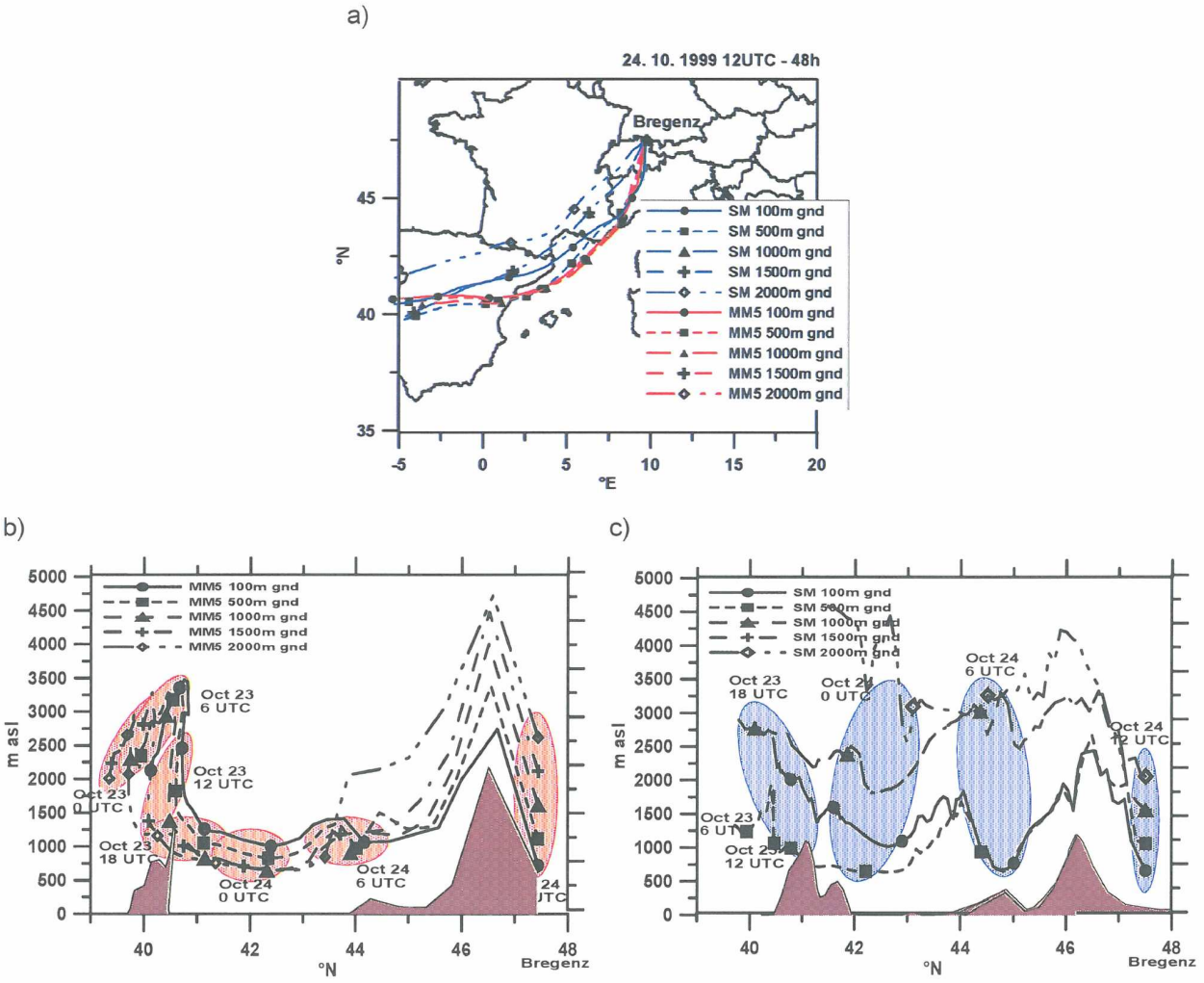

Fig. 9: Three-dimensional backward trajectories arriving at Bregenz on October 24 12 UTC based on MM5 and Swiss model (SM) simulations. a) horizontal tracks, symbols mark trajectory position and height every 6 hours. b) trajectory altitudes from MM5 run c) trajectory altitudes from SM run (shaded ellipses depict simultaneous trajectory positions).

The trajectories are much less spread than on the previous days (Fig. 9), but follow a similar track across the French Mediterranean coast and the western Po Valley. Differences between the MM5 and SM trajectories are due to a strong vertical wind shear which is found in the SM wind fields around 1500 m gnd above Bregenz. The MM5 trajectories arriving between 100 and 2000 m gnd at Bregenz all come from 500 to 1500 m above the Po Basin, while SM trajectories arriving above 1500 m gnd at Bregenz originate from altitudes above 2500 m gnd above the Po Basin. Considering ensemble trajectories based on the SM simulations (not shown), the differences between the two model runs are less pronounced, as most of these originate from lower levels above the Po Basin similar to the MM5 results.

The trajectories are confirmed by ozone profiles measured with a tethered balloon in the Piemont (Western Po Basin) on 23 October 1999. The ozone concentrations (40 to 50 ppb) observed close above an inversion around 1500 m gnd agree well with the ozone values found at the Alpine crest (at the mountain station Jungfraujoch) as well as within the Foehn air which arrived in the Rhine Valley. These findings are discussed in detail by Baumann et al. (2001).

Foehn case 5 November 1999

On 5 November 1999, an ARAT flight at a level of 5000 m asl. was performed under Foehn conditions.

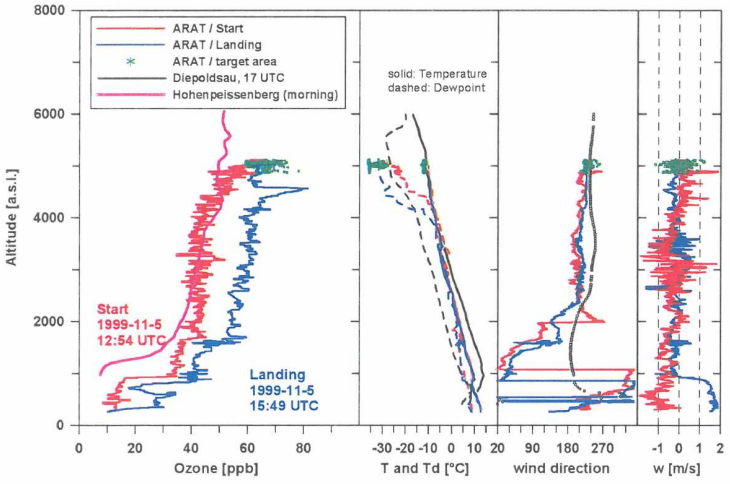

Fig. 10: Vertical soundings by the ARAT south of the Alps (red ... start, blue ... landing, green ... flight) and north of the Alps (Hohenpeissenberg, radiosonde at Diepoldsau). From left to right: ozone, temperature and dewpoint temperature, wind direction and vertical motion.

Horizontal cross-sections over Lake Constance and a flight leg along the Rhine valley reveal similarly to 19 October that ozone concentrations are lowest over the eastern part of the lake and the Rhine valley while nitrogen concentrations (not shown) are higher than in the western part of the area. Backward trajectories at lower levels arrive from the Mediterranean Sea, while the air at flight level has its origin over the Northern Atlantic Ocean (not depicted herein).

Ozone profiles south of the Alps are available from the start and landing flight of the ARAT (Fig. 10). Between start and landing at Milan, ozone has increased by almost 20 ppb between 1850 and 4500 m asl.

Cable car soundings undertaken at Bregenz (Fig. 11) indicate the downward mixing of air with higher ozone concentrations starting around 13 UTC.

At 1 km asl., ozone values up to 50 ppb were measured by the aircraft, similar values were found below 2 km south of the Alps. Ozone data from the regional Air Quality network indicate too that this Foehn event affected mainly the higher locations in the area south of Lake Constance.

Typical for most Foehn events in this area, the shallow layer of moist cool air at the ground was not removed entirely by the Foehn. The wind observations of the sodar at Lustenau (Fig. 12) reveal the wavy and changeable boundary between the weak southern (down-valley) flow in the morning and evening, the northern (up-valley) flow around noon and the much stronger south-eastern winds driven by the Foehn flow aloft.

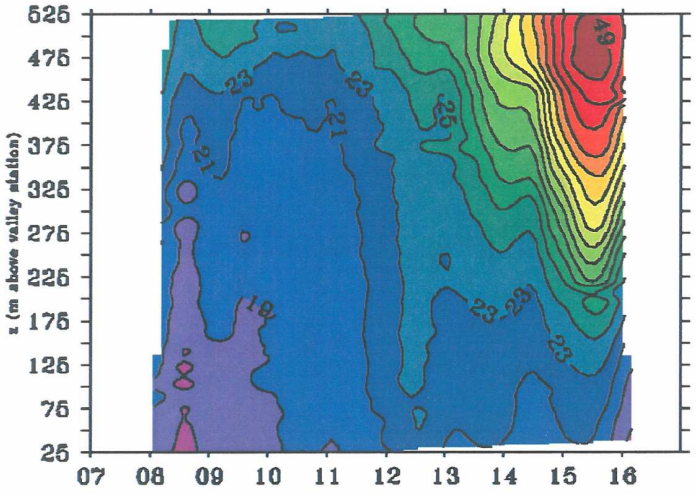

Fig. 11: Timeseries of cablecar ozone soundings at Bregenz on November 5, 1999 (time given in hours UTC).

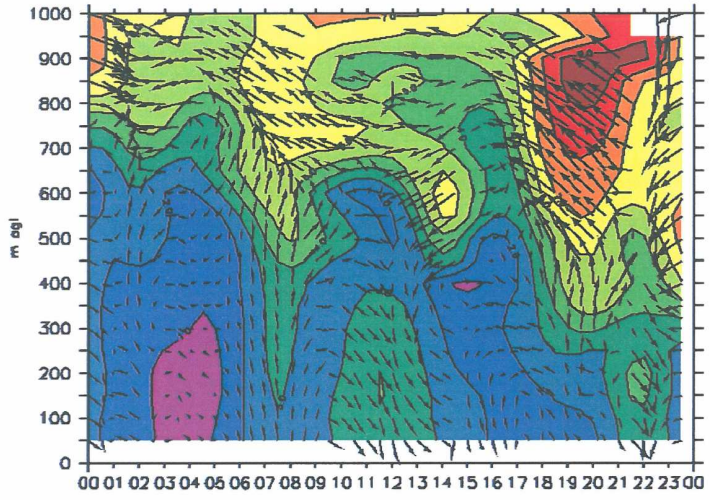

Fig. 12: Time-series of sodar wind soundings at Lustenau on 5 November 1999 (time given in hours UTC). Coloured contours show wind speed in 1 m/s intervals between less than 1 m/s (magenta) and more than 9 m/s (dark red). Overlying wind vectors show the horizontal wind in direction and length.

6 CONCLUSIONS

This paper gives an overview of the measurements, trajectory analyses and model runs undertaken in the frame of the project ROM, the Rhine valley ozone study within MAP, up to now.

One of the repeatedly occurring features of Foehn flow in the area just south of Lake Constance is the presence of a shallow ground-based cool and moist layer, usually preventing the Foehn flow from hitting the ground. Evidence for this pattern is found during several days during MAP. There are three different effects that might contribute to this northerly to easterly flow: the diurnal cycle of the valley wind system, a lake breeze from the Lake of Constance, and possibly advection due to a regional scale pressure gradient caused by the Foehn flow pattern. This result confirms previous findings by Baumann et al. (1998) achieved by MM5 model runs for a Foehn case. The special feature of the Foehn case on 24 October is the rare occurrence of the Foehn flow touching the ground also in the area just south of Lake Constance (section 3). Sensible heat flux can be a good indicator of Foehn air touching the ground (section 4). Measured and modelled sensible heat flux is in fairly good agreement under these circumstances. Trajectory analyses reveal the differences in the origins of Foehn- and non-Foehn air masses (sections 5). Thus, the combination of airborne and ground-based measurements gives a comprehensive picture of the often complex PBL vertical structure in the target area of the Rhine valley ozone study during Foehn. The additional analysis of high-resolution rawinsonde data collected during MAP will be addressed more closely in the future.

Acknowledgements

Project ROM was funded by the Austrian "Fonds zur Förderung der wissenschaftlichen Forschung (FWF)" under contract P13492-TEC. Franz Traher (ZAMG) is greatfully acknowledged for the installation and operation of the instruments used by ZAMG during the field experiment. Metair is thanked for the valuable Dimona aircraft data. The airborne measurements with ARAT, conducted by INSU/CNES, were made possible by the EU Programme STAAARTE. Pilgrim Kaufmann (MeteoSwiss) conducted the Swiss Model trajectory calculations.

References

Baumann K., H. Maurer, G. Rau, M. Piringer, U. Pechinger, A. Prévôt, M. Furger, B. Neininger, U. Pellegrini, 2001: The influence of south Foehn on the ozone distribution in the Alpine Rhine valley – results from the MAP field phase. Atmos. Environment 35, 6379-6390.

Baumann K., H. Maurer, G. Rau, M. Piringer, U. Pechinger, M. Furger, André S.H. Prévôt, B. Neininger, 2000: ROM project - Air mass analysis based on PBL soundings and trajectories. 26th intern. Conference on Alpine Meteorology, Österr. Beiträge zu Met. u. Geoph., Vol.23, No.392. (Ext. abstract CD-ROM)

Baumann, K., M. Langer, M. Piringer, 1998: Planning boundary layer measurements in the MAP foehn campaign (Rhine valley). Preprints 8th Conference on Mountain Meteorology, Flagstaff, Arizona, August 1998.

Berkowicz R. und L.P. Prahm, 1982a: Evaluation of the profile method for estimation of the surface fluxes of momentum and heat. Atmospheric Environment, 16, 2809-2819.

Berkowicz R. und L.P. Prahm, 1982b: Sensible Heat Flux Estimated from Routine Meteorological Data by the Resistance Method. J.Appl.Meteorol. 21, 1845-1864.

Duerr B., 2000: Föhn heute und gestern - ein interdisziplinärer Forschungsbericht. thesis. LAPETH.

Erbes G. and U. Pechinger, 1999: Comparison of synoptic-based preprocessor estimates. Agrictultural and Forest Meteorology 98-99, 509-519.

Holtslag A.A.M. und A.P. van Ulden, 1982: Simple Estimates of Night-time Surface Fluxes from routine Weather Data. KNMI Scientific Report, W.R. 82-4.

Holtslag A.A.M. und A.P. van Ulden, 1983: A simple scheme for daytime estimates of the surface fluxes from routine weather data. J. Clim. and Appl. Meteor. 22, 517-529.

Pechinger, U., K. Baumann, M. Piringer 2000a. MAP - Project ROM: Rhine Valley Ozone Study within FORM (Foehn Study in the Rhine Valley within MAP). Report, FWF Project No. P13492 - TEC, 16 pp.

Pechinger, U., K. Baumann, M. Piringer, G. Rau und H. Scheifinger, 2000b: ROM: The Rhine Valley ozone study within the MAP Foehn campaign FORM - Overview and selected results. 26th intern. Conference on Alpine Meteorology, Österr. Beiträge zu Meteorologie und Geophysik ., Vol.23, No.392. (Ext. abstract CD-ROM)

Piringer, M., K. Baumann, U. Pechinger, 2000: Project ROM: The vertical structure of the boundary layer in the Austrian Rhine valley during MAP IOPs. 26th intern. Conference on Alpine Meteorology, Österr. Beiträge zu Meteorologie und Geophysik ., Vol.23, No.392. (Ext. abstract CD-ROM)

Piringer, M., K. Baumann, U. Pechinger, S. Vogt, 2001: Meteorological and ozone sounding experience during a strong foehn event - a MAP case study. Meteorologische Zeitschrift, Vol. 10, No. 6, 445-455.

Rau G., K. Baumann, 2000a: Airborne Measurements with the ARAT (STAAARTE 99) over the Rhine Valley before deep Foehn (IOP 8). MAP Newsletter, Vol.13.

Rau G., K. Baumann, 2000b: Airborne Measurements with the ARAT (STAAARTE 99) over the Rhine Valley during deep Foehn (IOP 15). MAP Newsletter, Vol.13.

Rau G., K. Baumann, 2000c: Comparison of aircraft data (STAAARTE 99) and groundbased measurements of ozone (project ROM) before the onset of South Foehn. 26th intern. Conference on Alpine Meteorology, Österr. Beiträge zu Meteorologie und Geophysik ., Vol.23, No.392. (Ext. abstract CD-ROM)

Rau G., K. Baumann, 2000d: Aircraft measurements (STAAARTE 99) and Cable Car Soundings (project ROM) during a South Foehn Event. 26th intern. Conference on Alpine Meteorology, Österr. Beiträge zu Meteorologie und Geophysik ., Vol.23, No.392. (Ext. abstract CD-ROM)

GAP FLOW – AN OVERVIEW AND PRELIMINARY RESULTS

G.J. Mayr, I. Vergeiner, A. Gohm, J. Vergeiner, R. Mayr

Institute for Meteorology and Geophysics, University of Innsbruck

Abstract

GAP is one of the objectives of the Mesoscale Alpine Programme (MAP). It studies the effects of vertical and lateral topographical constrictions on atmospheric flow, i.e. flow through and over a pass. Detailed goals of GAP are given and the extensive observational network along the Brenner cross section for the MAP special observation period in fall of 1999 is described. It consisted of 70 surface stations, several radiosonde stations, remote sensors, and research airplanes. Nature contributed to the success of the measurement campaign by providing an above-average number of foehn cases.

While data processing and quality control of the huge data set are just being finished, several case studies have already been started. Preliminary results from three of them are in this article: the "Sandwich foehn" of October 18, 1999, foehn with high vertical velocities (October 20, 1999), and the deep foehn October 24-25, 1999.

Surface stations were deployed in lines along the valley slopes to continuously measure the mass field in the valley. They are compared with radiosoundings taken during intensive observation periods (IOPs) to judge their usability as sole providers of the vertical temperature profile for the gap flow cases outside the IOPs.

An analytical conceptual model has been developed to explain the salient flow features when foehn from the Wipp valley enters the Inn valley, which runs approximately perpendicular to the Wipp valley.

Zusammenfassung

GAP ist eines der Unterprogramme des Mesoskaligen Alpinen Programms (MAP). Es untersucht die Auswirkungen von seitlichen und vertikalen Verengungen auf die Luftströmungen, d.h. den Föhn über und durch einen Paß. Der Artikel beschreibt die genauen Zielsetzungen und das ausgedehnte Beobachtungsnetz entlang der Brennersenke während der MAP Feldphase im Herbst 1999. Das Messnetz bestand aus 70 automatischen Wetterstationen, mehreren Radiosondenstationen, Fernerkundungsgeräten und Forschungsflugzeugen. Mit einer überdurchschnittlich hohen Zahl von Föhnfällen trug die Natur das Ihre zum Erfolg der Messkampagne bei.

Obwohl die Verarbeitung und Qualitätskontrolle des riesigen Datensatzes gerade abgeschlossen wurde, sind schon mehrere Fallstudien begonnen worden. Erste Ergebnisse von drei Fällen werden in diesem Artikel beschrieben: der "Sandwichföhn" (18. Oktober 1999), ein Föhnfall mit hohen Vertikalgeschwindigkeiten (20. Oktober) und ein hochreichender Föhn (24.-25. Oktober).

Bodenstationen wurden linienförmig vom Talboden bis zu den Berggipfeln aufgestellt, um das Massenfeld der Strömung im Tal kontinuierlich zu messen. Diese Messungen werden mit Radiosondenaufstiegen während intensiver Messphasen (IOPs) verglichen, um ihre Brauchbarkeit für die Bestimmung von vertikalen Temperaturprofilen außerhalb der IOPs zu ermitteln.

Ein analytisches konzeptuelles Modell wird vorgestellt, das die wichtigsten Strömungsmerkmale bei der Einmündung des Föhns aus dem Wipp valley in das nahezu rechtwinklig dazu verlaufende Inntal beschreibt.

1 INTRODUCTION

In contrast to studies of airflow over 2-D and 3-D obstacles, the problem of airflow over mountain passes is a largely neglected area of atmospheric research. However, it represents an important issue, as the dynamics of gap flow controls the transport of airmasses, the generation of deep vertically propagating gravity waves, the occurrence of hazardous wind conditions for air traffic (e.g. for the Hong Kong International airport (Lau and Shun, 2000)), and the possible generation of PV banners. Specific to the Alps, passes control the flushing of polluted air from Alpine valleys and both shallow and deep foehn events downstream. All the famous Alpine foehn locations (Brenner cross section, Rhine and Reuss valleys) lie downstream of passes in valleys that run perpendicular to the main Alpine crest, whereas (at least to our knowledge) no foehn downstream of a ridge is reported in the literature.

A pass imposes a vertical and lateral constriction on the flow. The consequences of a vertical constriction, a mountain, have been extensively studied. Convenient overview papers are Smith (1979) and Smith (1989). More recent papers on flow over and around obstacles deal with the mechanisms that lead to wave-breaking aloft and vortex formation in the wake of an obstacle (eg. Smolarkiewicz and Rotunno (1989, 1990); Schär and Smith (1993a and b); Schär and Durran (1997)). The windstorms that can occur on the downstream side of a mountain have attracted numerous researchers and a variety of attempts to explain their mechanisms (Lyra (1940, 1943); Queney (1947, 1948); Long (1953, 1955); Durran (1986); Smith (1985)).

The consequences of a lateral constriction, a gap, on the flow have received much less attention. Among the few existing investigations of "gap flow" is the report by Scorer (1952) on an easterly low-level jet of 100 knots through the Strait of Gibraltar when cold air fills the western Mediterranean. Other observational and modeling studies refer primarily to "outflows" from fjords and canyons (e.g. Jackson and Steyn, 1994; Levinson and Banta, 1995).

Results from the combination of a vertical and lateral constriction, a pass, are even sparser. Colle and Mass (1998a, b) observed the effects of gap flow and mountain wave accelerations along the western side of the Washington Cascade mountains and simulated the flow numerically. Pan and Smith (1999) used hydraulic theory to study the effects of gaps of various depth and width between two idealized mountains and corroborated their conclusions from a satellite-based wind-field study of flow through a gap on an island.

The flow beneath a strong low-level inversion may, in a first approximation, be studied using single layer reduced gravity hydraulics. High winds develop when the flow undergoes a hydraulic transition from sub-critical to super-critical flow. Such a transition can be induced by a pure horizontal contraction as in the Strait of Gibraltar or a vertical contraction with almost identical effects on the flow. The third possibility is the combination of a horizontal contraction and a rise in the floor of the gap as in a mountain pass. When the flowing layer is continuously stratified, as is the more characteristic case for atmospheric flows through mountain passes, the problem is considerably more complex. It is a fluid mechanics problem that is particularly interesting because, unlike a single layer flow, this flow has an infinite number of characteristic wave speeds, each associated with a different vertical structure.

A series of experiments in a hydraulic channel and theoretical solutions discussed by Armi and Williams (1993) shed light on the mechanism of the continuously stratified hydraulic flow through a gap. Although the channel contains only a lateral contraction over level ground, the resulting flow has a striking similarity with that over a mountain ridge as derived, for example, by Smith (1985). A low-level jet of supercritical speed forms downstream of the narrowest section topped by a stagnant fluid mass overhead. For realistic flows over mountain passes the two models must be combined.

This background led to the incorporation of a gap flow program within the Mesoscale Alpine Programme (Binder and Schär, 1996; Bougeault et al, 2001). Its scientific questions are stated in Bougeault et al. (1998):

- to determine the relative importance of gap width versus terrain flow through realistic topography.
- A related question is to determine the relationship between the gap flow and the flow above mountain-top level; in particular, whether the gap flow is reinforced by flow aloft along the axis of the gap or by a mean-state critical level which caps the low-level cross-mountain flow.
- To study the vertical and cross-gap distribution of wind speed and thermodynamic properties. These are controlled by inviscid stratified dynamics together with surface friction along the valley floor and side walls. The frictional effects as well as dissipation and mixing of the low-level high speed flow need to be included in realistic models.

The region chosen for the field measurements was the Brenner cross section, an area with a more than one century long history of foehn research. The Brenner pass is the lowest in the Alpine crest. It lies in the central part of the Alps, where their meridional dimension is largest. For southerly flows, there is a larger basin upstream and a nearly straight valley downstream of the pass (Fig. 1). Several tributaries run perpendicular to the Wipp valley. At its exit, 30 km downstream from the Brenner pass, the Wipp valley merges with the Inn valley via a 100-200 m deep drop at an almost right angle. There its further way north is obstructed by the Northern Range (Nordkette), a W-E running ridge line of 2200-2600 m MSL. Air can then either flow eastwards out the Inn valley, which exits into the Bavarian foreland, flow over the Northern Range or through an opening in it 10 km west of Innsbruck.

The Brenner poses a vertical as well as lateral constriction for the flow. The lateral constriction is staggered in the vertical: the lower gap at approximately 1400 m with a width of few hundred meters is topped by another gap at approximately 2100 m with a width of roughly 15 km. On both sides the main Alpine crest continues with an average elevation of 3100 m MSL. The cross-sectional area of the lower gap is a mere fraction of the upper one. Most of the air reaching the downstream (northern) side of the Brenner will therefore have to come through the upper gap. The relatively minor role of the lower pass for the gap flow was only realized in the preparations for the MAP field phase.

Well known, on the other hand, are the consequences of the terrain drop at the merger of Wipp valley and Inn valley. During the night radiation-driven cooling of the air in the upper Inn valley, into which foehn does not reach, causes air to become potentially cooler than the foehn flow. Consequentially, this cooler air lifts the foehn air off the ground at the exit of the Wipp valley. The main mechanism to eliminate the difference in potential temperature between the two air masses is solar radiation, which explains the noon and afternoon maximum of foehn occurrence in Innsbruck. A secondary mechanism is the drainage of cooler air out the Inn valley due to lower pressure in the foreland caused by an approaching low/cold front or dynamically by large-scale flow over the Alps with the typical pressure dipole.

During south foehn an appropriately named "foehn inversion" frequently caps the flow below the main crest. Similarly, chinook along the Colorado Front Range is often accompanied by an inversion (Brinkman, 1971). Whether this inversion was sufficient to decouple the low-level flow from the one above the crest, was a main objective of GAP. It was hypothesized to be strong enough to be able to apply hydraulic theory to explain the salient flow features.

2 INSTRUMENTAL SETUP

To meet the project objectives, both mass and wind field had to be known with high spatial and temporal resolution. Crucial locations were the basin south of the Brenner for upstream conditions, the pass itself as a potential hydraulic control, and Innsbruck at the exit of the N-S valley. Since MAP had eight different objectives, competition for aircraft resources for intensive observation periods (IOP) was high. Therefore a high-density, continuously operating measurement network was set up to be able to put the few expected IOPs over the Brenner cross section in a longer-term context. Lines of automatic

surface stations were strung along the valley floor on both sides of the pass and in the Inn valley, and also up the sides to obtain vertical cross sections of the flow. Data were recorded every 30 seconds to 15 minutes. Four different types of surface stations were deployed.

Slope profiles up to a maximum altitude of 2800 m MSL consisted of a total of 35 temperature loggers (Whiteman et al., 2000). 35 automatic stations with additional wind, pressure, and humidity information were placed along the valley floor and on mountain peaks. With such a station at the bottom of a slope-temperature profile, pressure at the temperature loggers was computed hydrostatically. This allowed the computation of a conservative variable for the mostly non-precipitating gap flow: potential temperature. The inaccuracy of the temperature logger height (± 1 m) and a possible deviation from hydrostatic flow are negligible for the overall accuracy of the potential temperature since a pressure deviation of 1 hPa changes potential temperature by only 0.1 K. The difference between temperature above the valley axis and along the slope is small during gap flow episodes although it can be substantial during weak-wind situations (cf. section 4.5).

To make wind measurements less susceptible to peculiarities of the anemometer site, anemometer height was chosen to be the standard 10 m whenever possible. All 10 m winds bar one were mounted on power pylons of local electricity companies. This novel way saved cost and time.

Several automatic stations were equipped with microbarographs. Turbulent momentum flux was measured with sonic anemometers at three locations. Having 70 stations with heterogenous instrument components within approximately 50 km horizontal distance places high demands on their accuracy and intercomparability. Calibration of pressure, temperature, and humidity sensors against traceable standards and parallel measurements with several complete stations before and after SOP were performed. Only the factory calibration was used for wind sensors.

Remote sensors measured the wind field over large parts of the Brenner section. Doppler sodars were installed far upstream at the southern rim of the Alps near Verona, about 25 km upstream of the pass (mainly used for north-foehn), at the pass itself, and in Innsbruck. A very recently installed UHF wind profiler operated in Innsbruck. One of the central platforms was the NOAA ETL TEACO2 scanning Doppler lidar, which was positioned between Brenner pass and Innsbruck. It was available from October 1, 1999 on and provided radial velocities during selected periods. Due to the channeling of the valley, radial velocity closely approximates true velocity.

No remote sensors for temperature were available. Temperature information above the 600 - 2800 msl region covered by the surface stations could be measured only on a case-by-case-basis from radiosondes and aircraft in-situ measurements. Routine radiosonde stations in Milano and Udine (Fig. 1) provided vertical profiles upstream of the Alps. Soundings in Verona at the southern rim were made especially for the SOP. The immediate upstream profile was gathered at the first larger basin upstream of Brenner in Sterzing. Downstream of Brenner, radiosondes were launched from a site collocated with the Doppler lidar and from the routine station in Innsbruck.

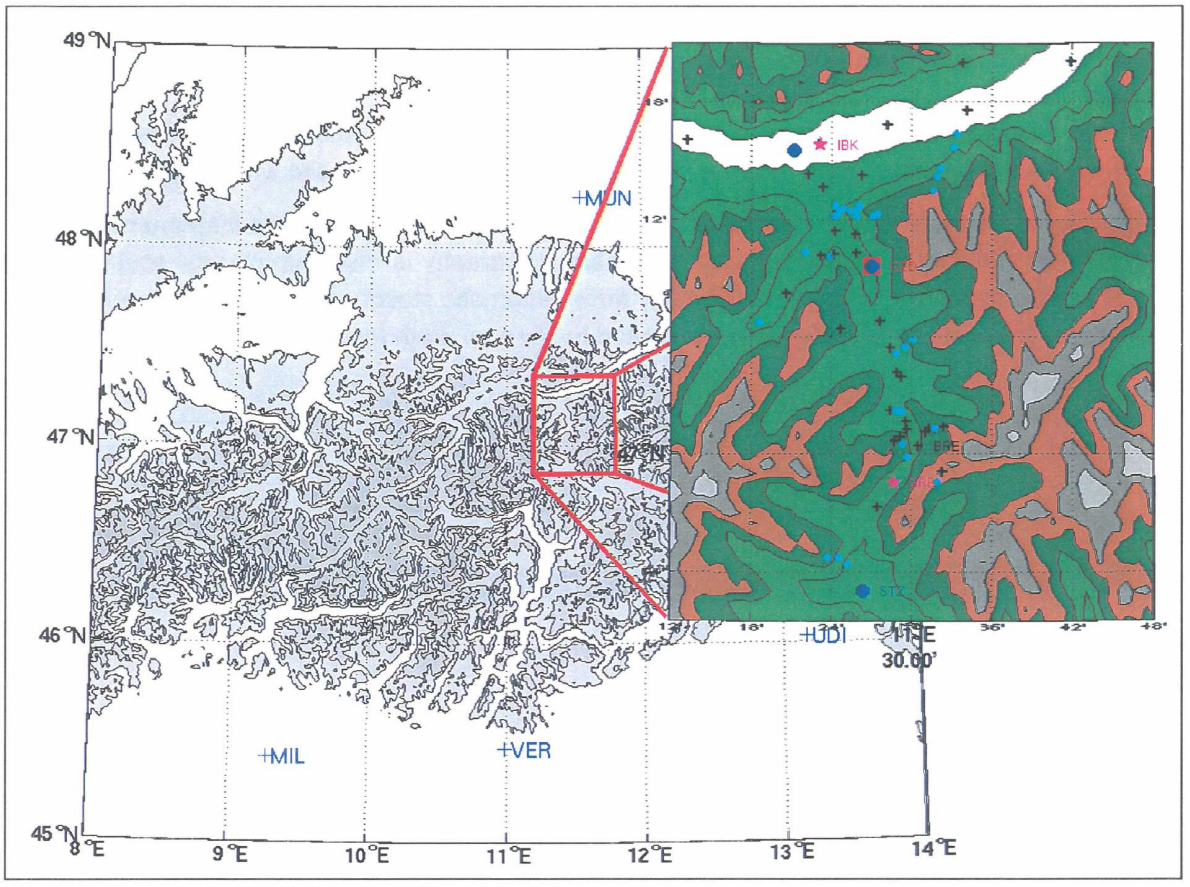

Fig. 1: Topography of the Alps with close-up of the Brenner target area. Radiosoundings (STZ .. Sterzing, GED .. Gedeir and Innsbruck) are marked with a blue circle, Sodars (BRB .. Brennerbad, IBK .. Innsbruck) with a pink pentagram, the lidar (GED) with a red square. Meteorological stations measuring at least temperature, humidity, pressure and wind are denoted by a black plus sign, temperature sensors with a tiny cyan circle. Isolines in the gray shaded picture: 600, 1300, 2000, 2700 and 3400 m MSL. In the zoomed area isolines every 400 m between 600 and 2600 m MSL.

Abb. 1: Topographie der Alpen plus herausgezoomte Brenner Target Area. Radiosondierungen (STZ .. Sterzing, GED .. Gedeir und Innsbruck) sind mit dem blauen Kreis markiert, die Sodars (BRB .. Brennerbad, IBK .. Innsbruck) mit einem pinken Pentagramm, das Lidar (GED) mit einem roten Quadrat. Meteorologische Stationen, die wenigstens die Parameter Temperatur, Feuchte, Druck und Wind messen, sind mit einem schwarzen Pluszeichen eingetragen, Temperatursensoren mit einem kleinen zyanfarbigen Punkt. Isolinien im grau schattierten Bild: 600, 1300, 2000, 2700 and 3400 m NN. Im herausgezoomten Bild: Isolinien alle 400 m zwischen 600 und 2600 m MSL.

After the Doppler lidar was in place, aircraft measurements augmented the dense surface network during IOPs (Fig. 2). The two main aircraft operated were the NOAA P3 and the NCAR Electra. If available, they flew joined missions. The P3 made in-situ measurements (Fig. 3) in the foehn layer below and immediately above the foehn inversion.

The advantage of the short horizontal distance of the cross section was that unprecedentedly dense stacks of tracks could be completed in a time during which the flow was quasi-stationary. The logistics of flights with a relatively big aircraft in a narrow and deep valley and the frequent presence of instrumented flight conditions upstream of the pass during south foehn posed challenges that had seemed unsurmountable before the beginning of SOP. Close cooperation between one of the PIs, the aircraft crew, and air traffic control in Innsbruck (the exit of the Wipp valley is the approach zone of the airport!) overcame these problems.

The Electra flew above the inversion to probe the layer below with the SABL aerosol lidar and drop sondes, and to make in-situ measurements. A primary goal of the Electra missions was to map the cross-flow variability of the flow. Dropping sondes over such complex terrain posed another challenge.

Practice was needed to get the sonde down over the desired location through a vertically strongly sheared wind field. The aircraft also had to maintain a line of sight connection till the sonde reached the ground.
On one day (October 30) the French Fokker Arat joined the measurements at altitudes above the inversion to use the on-board lidar, Leandre II, which measures reflectivity and water vapor content.

Although gap flow occurs in both directions along the Brenner cross section, the instrumentation was geared towards measuring south foehn. Downstream topography is much simpler for southerly flow and its likelihood is higher during the SOP. Only three automatic stations with microbarographs and a Doppler sodar (all south of Sterzing) were dedicated to observe north foehn.

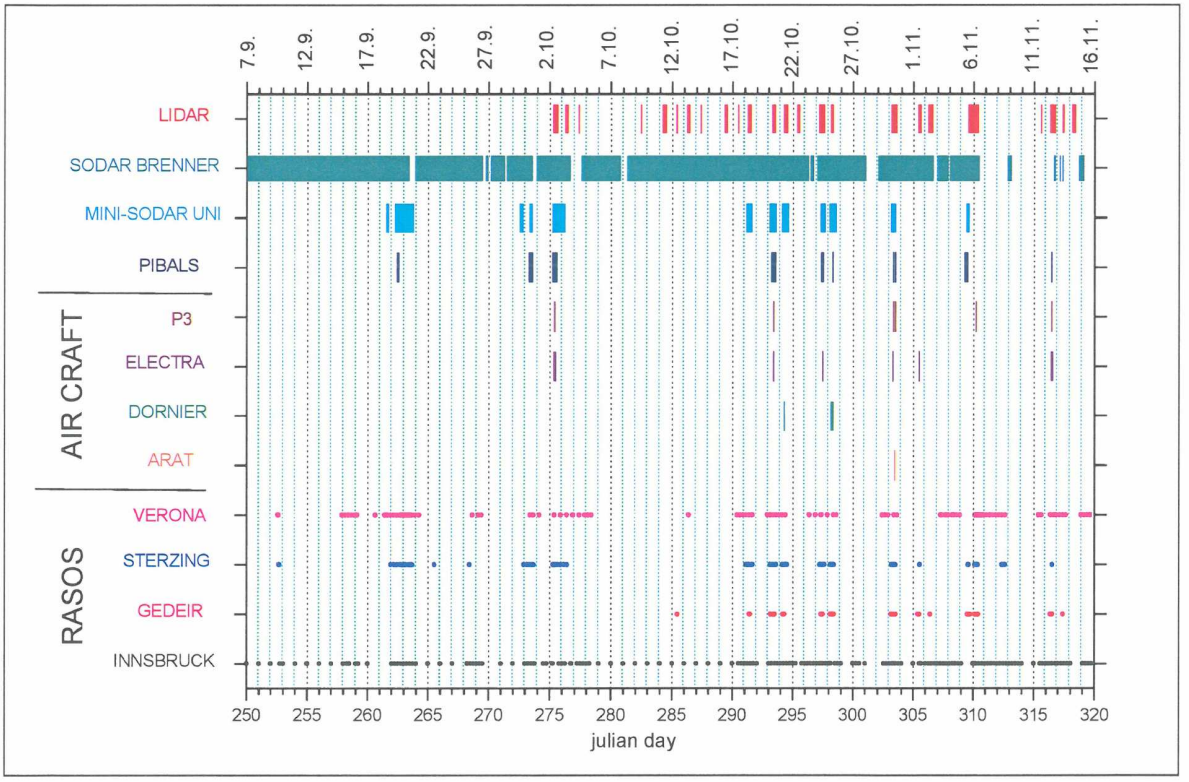

Fig. 2: Operation Periods of the most important instruments during the MAP-SOP 7 September – 15 November 1999

Abb. 2: Einsatzperioden der wichtigsten Instrumente während der MAP-SOP 7. September – 15. November 1999

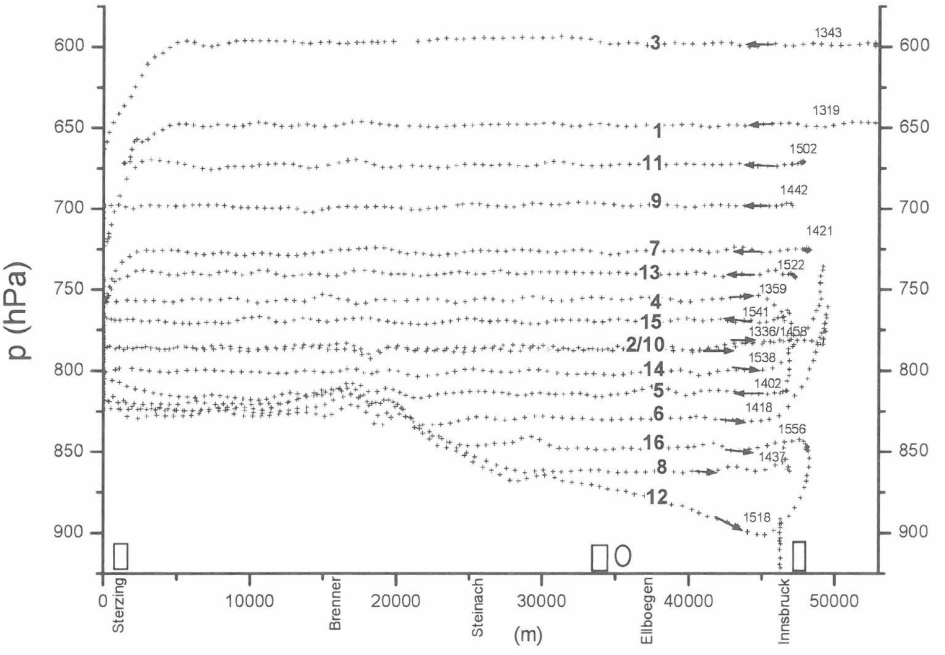

Fig. 3: P3-vertical tracks: Vertical cross-section of a P3-flight between Innsbruck and Sterzing, afternoon of 30 October, 1999.

Abb. 3: Vertikaler Querschnitt eines P3-Fluges zwischen Innsbruck und Sterzing, am Nachmittag des 30. Oktober 1999.

3 FOEHN CLIMATOLOGY DURING THE MESOSCALE ALPINE PROGRAMME

Seen from a climatological point of view, the autumn of 1999 was a good season to perform the MAP field program. During the 70 days of the Special Observing Period (SOP) 15 south foehn periods (29 days) in the Wipp valley were recorded. Innsbruck at the exit of the Wipp valley reported 16 days with foehn, which is well above the long term average 1906 – 1995 for the same period with 11 foehn days.

3.1 Foehn periods during the MAP-SOP

The 15 foehn periods cover a wide range between short "incidents" and persistent conditions over several days. Seven periods lasted 6 to 16 hours, the other eight periods longer than 24 hours; the longest one between 19 and 23 October lasted more than four days.

As can be seen from figure 4, most of the foehn periods are also connected to an IOP. This is quite natural since the study of foehn and gap flow in the Alps was one of the main goals of the MAP project. Not covered by an IOP were merely the shallow foehn on 22 September and the south flow on 27 September, which lasted only a few hours. The south-north orientation of the Wipp valley with the only 1370m high Brenner pass at the southern edge favors a high foehn frequency (compare chapter 3.2). Hence most foehn periods begin with a compensation flow caused by an already slightly higher pressure south of the Alpine crest before the actual gap flow is established.

3.2 Foehn and south wind frequencies and wind maxima during the MAP-SOP at three stations

The three stations listed below were chosen from the entire network due to their high quality sensors and the good exposition to south wind.

The mountain station Sattelberg (2120m MSL) measures the oncoming flow at the main Alpine crest. Most of the air during deep foehn conditions flows over the broad saddle between the very high mountain ranges Stubaier and Zillertaler Alps. Sattelberg is situated on this saddle and therefore experiences slightly channeled flow with quite high wind speeds compared to other mountain locations.

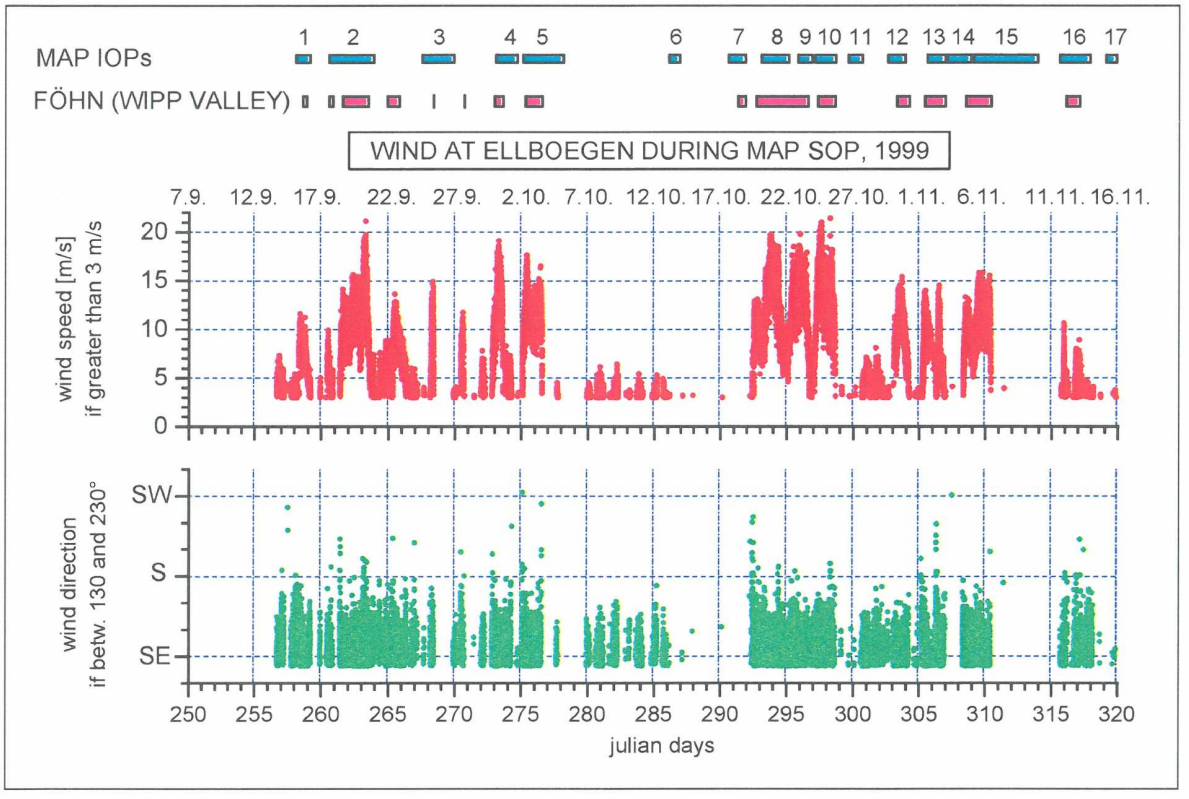

Fig. 4: MAP Intensive Observing Periods (IOPs), foehn periods in the lower Wipp valley, and wind speed and direction during south wind conditions at the station Ellbögen between 7 September and 15 November 1999

Abb. 4: MAP Intensive Beobachtungsperioden (IOPs), Föhnperioden im unteren Wipp valley und Windgeschwindigkeit sowie –richtung während Südwindlagen an der Station Ellbögen vom 7. September bis 15. November 1999

Ellbögen at 1071m MSL is situated in the lower third of the Wipp valley and is well exposed to the south.

At the station Innsbruck University at 580m MSL the Wipp valley and Inn valley merge. Here the foehn meets the Inn valley flow or has to deal with a cold air pool in the boundary layer.

At Sattelberg 876 hours with south wind were recorded. This corresponds to 52.14 % of the whole MAP-SOP.

Ellbögen had even 924 hours of south wind or 55 %. At first sight it may be surprising, that a station in the valley records more hours with southerly winds then a mountain station. But this is caused by a very regular thermally driven valley wind system in the Wipp valley during high pressure situations. At

Ellbögen about 50 % of all the hours with south wind are due to nocturnal outflow. A good example is the period 7 through 13 October (Fig. 4).

The station Innsbruck University accumulated 112 hours (6.7 %) of foehn. This relatively small number is mainly due to the fact, that the potentially colder air mass in the Inn valley can not easily be removed by the foehn flow. This air needs to be sucked out to the Alpine foreland or be warmed by diurnal sensible heating before it can give way to the southerly flow. Consequently the onset of foehn is usually a few hours later than in the Wipp valley and during short foehn periods the southerly wind may not reach the ground of the Inn valley at all.

The highest wind speed averaged over 1 minute at Sattelberg was recorded on 20 September with 35.4 m/s or 127 km/h. The strongest gust -on the same day- reached 43.2 m/s or 156 km/h.

At Ellbögen the highest 1 minute mean value was measured on 24 October with 22 m/s (79 km/h), the strongest gust reached 29.5 m/s or 106 km/h.

At Innsbruck University only 10 minute mean values were recorded, the highest value being 10 m/s or 36 km/h. The highest gust was 24.9 m/s (90 km/h) measured on 23 October.

4 CASE STUDIES

4.1 Lee Waves experienced by a Sounding Balloon on 20 September 1999

During the MAP field phase a radiosounding station based in a hangar of the local glider club in Sterzing just 13 km south of the Brenner pass was operated by the University of Innsbruck. The goal was to measure the upstream conditions of foehn flows during IOPs.

20 September was the last day of a three day foehn period. The cold front moved faster north of the Alps where it was not held back by higher orography and reached Innsbruck at the time of the launch. The deep southerly flow over the Alps was still strong with approximately 15 m/s at crest height, well confirmed by the station Sattelberg at 2120 m MSL. In Sterzing rain had started in the morning and was getting so heavy in the evening that the gliders had to be evacuated due to flooding of the hangar by a nearby small river. But, quite typically, the flow below 840 hPa (1400 m MSL), the height of a weak inversion, was nearly blocked all day and did not exceed 3 m/s.

Lee waves seemed to have been present at least since 09 UTC. Three launches prior to 18 UTC had been lost due to receiving problems because the balloons descended north of the main Alpine crest, which interrupted the line of sight to the base.

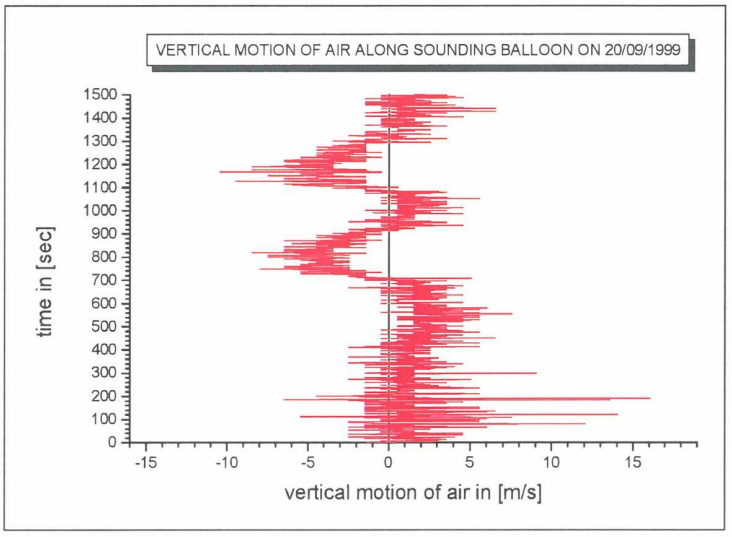

Fig. 5: Vertical motion of the air as a function of time along the flight track of the Sterzing sounding at 18 UTC on 20 September 1999. The vertical motion of the air was calculated as vertical motion of the balloon minus mean vertical motion up to 3000 m MSL

Abb. 5: Vertikale Luftbewegung als Funktion der Zeit entlang der Flugstrecke der Radiosonde Sterzing am 20. September 1999. Die Vertikalbewegung der Luft wurde gerechnet als Vertikalbewegung der Sonde minus mittlere Vertikalbewegung bis 3000 m NN.

When finally at 18 UTC the signal of the balloon could be followed until 4 km north of the main Alpine crest after the balloon had passed a second weak inversion at 755 hPa (2400 m MSL), it clearly flew through well established gravity waves with vertical motion of ±5 m/s (compare Fig. 5). The wave length was calculated with 6.6 km, the time between two maximum uplifts being 440 seconds and the mean speed 15 m/s. This value for the wave length matches the horizontal distance of the three mountain ridges mentioned below.

The starting point of the wave was a smaller ridge northwest of Sterzing (see Fig. 6). The balloon then descended 400 m into the Pflersch valley, then approached the main crest, was lifted to 3100 m MSL, passed the highest peak and descended into the Obernberg valley. Another updraft could be observed before losing the signal just upstream of the next northeast-southwest oriented ridge little west of Nößlachjoch.

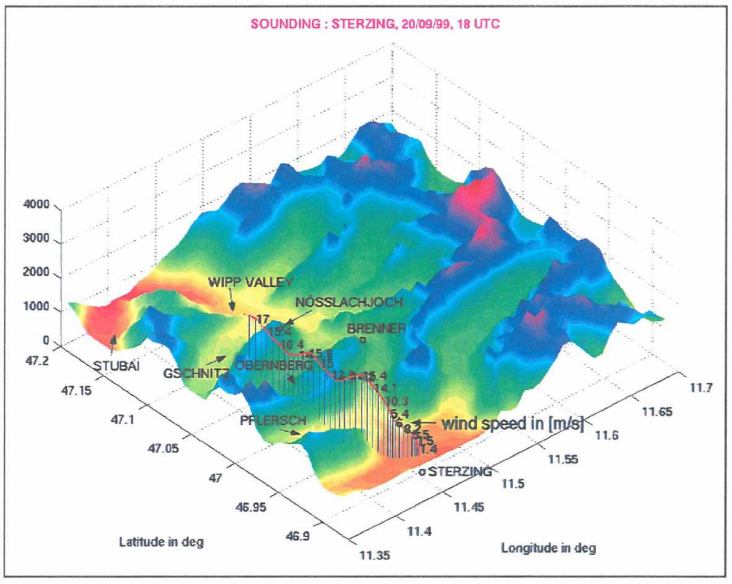

Fig. 6: Flight track of the 18 UTC sounding on 20 September 1999 and wind speed along the path

Abb. 6: Flugroute der 18 UTC Sondierung am 20. September 1999 sowie Windgeschwindigkeit entlang der Strecke

4.2 The MAP-IOP 7 "Sandwich" Foehn on 18 October 1999

A shallow south foehn event is defined by a pressure-driven south flow decoupled from a westerly or even northwesterly flow on top. Quite often a stable cold air surface pool remains underneath the southerly flow. This three layer structure is here referred to as "Sandwich" foehn.

During MAP-IOP 7 on 18 October such an event was recorded in the Wipp valley target area, with the additional feature that the lowest layer was not stagnant but actually flowing southward into the Wipp valley! There is a pressure low over northeastern Europe. It causes northwesterly flow in the Alpine region above crest height and below crest height it advects cold air into the Alpine foreland and around the Alps into Slovenia and Northern Italy (with easterly flow in the Udine and Milano soundings), thus producing higher pressure both north and south of the MAP target area Wipp valley. The pressure gradient from the Bavarian foreland towards Innsbruck drives the surface flow into the Inn valley and further towards Brenner, whereas the higher pressure south of the main Alpine crest is responsible for the south foehn flow in the middle layer.

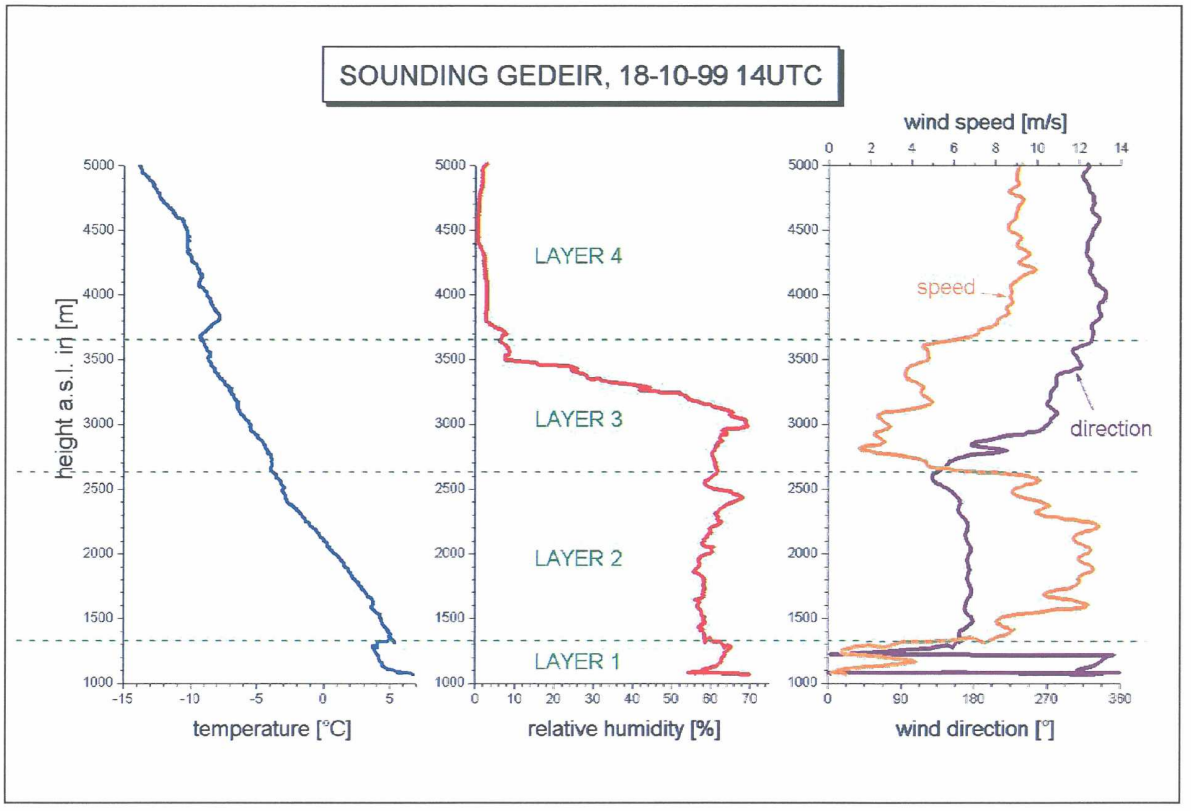

Fig. 7: Radiosounding from Gedeir (middle of the Wipp valley) during the Sandwich foehn on 18 October 1999, 14 UTC

Abb. 7: Radiosondenaufstieg Gedeir (im mittleren Wipp valley) während "Sandwich" föhn am 18. Oktober 1999, 14 UTC

This can clearly be seen in Fig. 7 presenting the Gedeir sounding in the middle of the Wipp valley at 14 UTC: A northerly surface flow up the Wipp valley with a vertical extent of approximately 300 m is present! The south foehn in a 1300 m thick layer above it is topped by a transition zone with winds turning from south over west to north accompanied by strong drying. A pronounced inversion marks the beginning of the very dry and strong NNW flow above 3600 m MSL.

The NOAA-lidar placed at Gedeir also reveals a wavy structure of the foehn flow (wave-length of approximately 10km) with descending air in the lee of the gap which is then ascending over the thickening cold air (not shown). The Brenner pass itself had always southerly flow in this period.

The comparison of upstream and downstream soundings in Fig. 8 exhibits a cold air pool in Sterzing, equally cold air also in the shallow northerly flow in the Wipp valley and pronounced warming in the foehn layer. Between 870 hPa (top of cold air) and 680 hPa (the inversion height) the horizontal difference in the potential temperature between the exit region of the Wipp valley and Sterzing is approximately 3K indicating a descent of the air in the lee of the main Alpine crest by 700-800 m.

The overall duration of this opposite flow structure is short. Prior to its onset there was weak (southerly) outflow at the valley bottom before the cold northerly flow penetrated the Wipp valley around 8 UTC. At that time the foehn flow was already established at higher altitudes. As shown in Fig. 9 the foehn managed to remove the cold air pool bit by bit during the day starting in the south of the Wipp valley (Zagl) with foehn break-through around 10:30 UTC. It finally reached the exit region (Zenzenhof) at about 17 UTC.

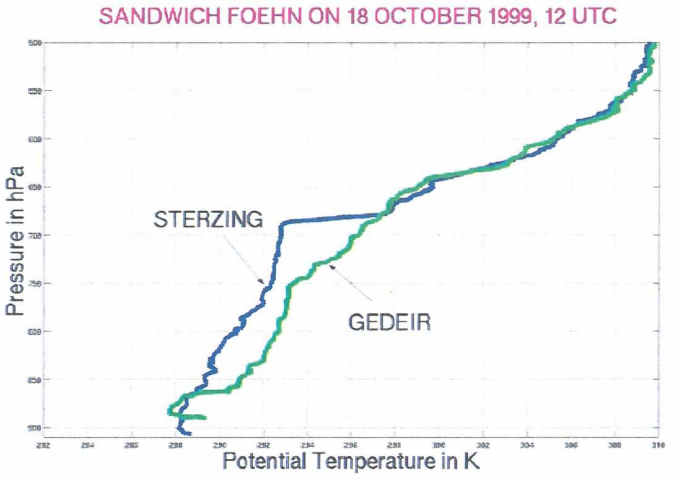

Fig. 8: Potential temperature profile of Sterzing and Gedeir sounding, 18 October 1999, 12 UTC

Abb. 8: Profil der potentiellen Temperatur der Radiosonden Sterzing und Gedeir, 18. Oktober 1999, 12 UTC

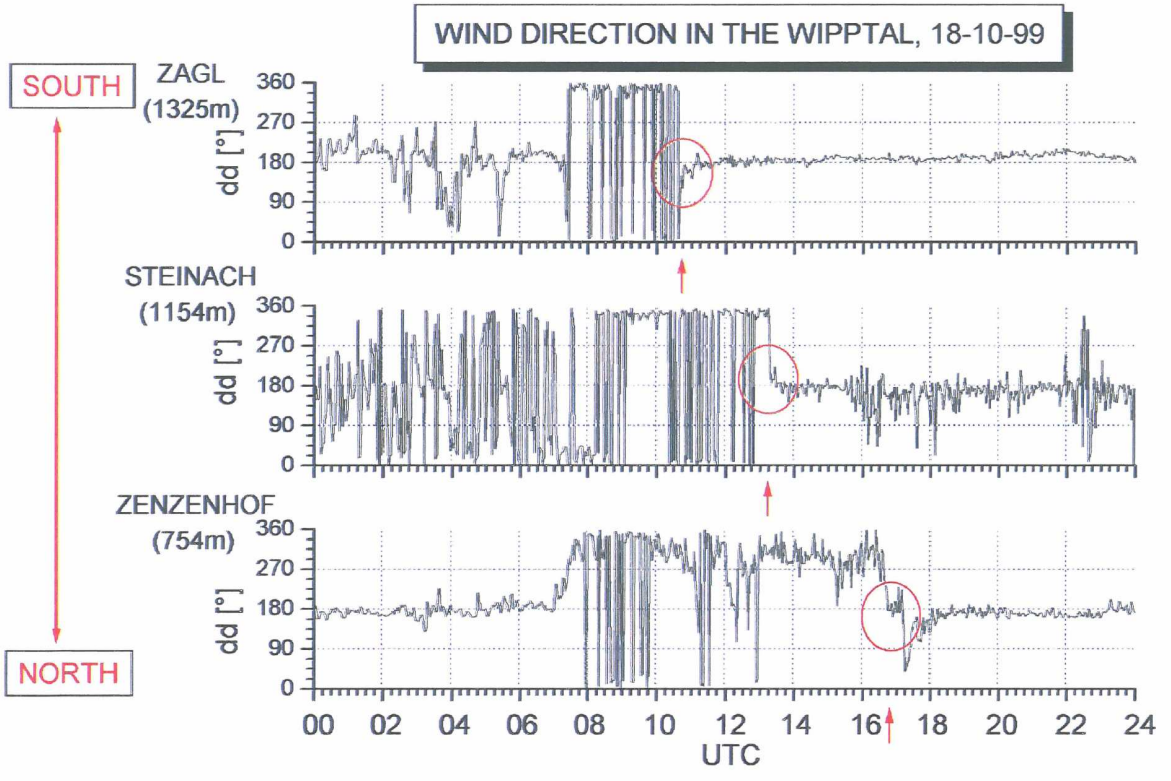

Fig. 9: Time-series of wind direction at three different stations in the Wipp valley on 18 October 1999

Abb. 9: Zeitreihe der Windrichtung an drei Stationen im Wipp valley am 18. Oktober 1999

4.3 Case Study of the 24 through 25 October 1999 Deep Foehn Event in the Wipp valley

4.3.1 Introduction

Between 24 and 25 October 1999 a deep foehn event occurred in the Wipp valley. Data from five weather stations located in the valley and on mountain peaks, from two atmospheric sounding systems north and south of the Brenner Pass, and from a Doppler lidar located in the middle of the Wipp valley were analysed to investigate the temporal evolution and spatial variability of this foehn case (Fig. 10).

Section 4.3.2 describes the synoptic-scale weather condition responsible for the occurrence of this phenomenon. In section 4.3.3 data from surface weather stations are presented. Section 4.3.4 shows atmospheric profiles of the foehn flow derived from rawinsonde data. The three-dimensional structure of foehn is investigated by analyzing Doppler lidar data, presented in section 4.3.5. A summary of this case study follows in section 4.3.6.

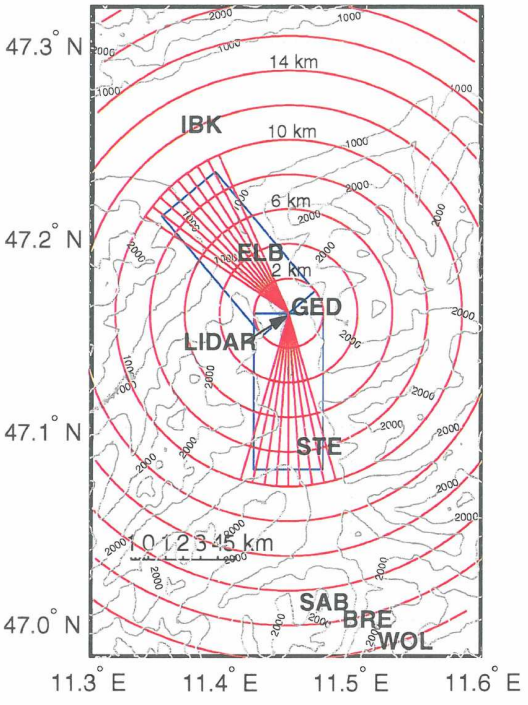

Fig. 10: Topographic map of the Wipp valley. Contour interval is 500 m. Doppler lidar site and location of balloon launch: Gedeir (GED, 1075 m MSL). Red circles are horizontal range rings drawn every 2 km around lidar site. Straight red lines mark two lidar scan sectors, up- and down-valley.

Abb. 10: Topographiekarte des Wipp valleys. Konturintervall: 500 m. Doppler Lidar und Radiosonden-standplatz: Gedeir (GED, 1075 m MSL). Rote Kreise bezeichnen den horizontalen Abstand vom Lidar alle 2 km. Gerade rote Linien markieren 2 Lidarsektoren talein- und talauswärts.

4.3.2 Synoptic overview

Foehn winds between 24 and 25 October 1999 in the Wipp valley and other Alpine valleys were caused by a classical weather condition of a pronounced mid-trophospheric pressure trough approaching central Europe and increasing southwesterly winds over the Alps. On 24 October 12 UTC the pressure trough at 500 hPa spread from Great Britain to the western shore of the Iberic peninsula. The associated surface cold front was located near western France with its surface pressure low over the British islands.

During the night form 23 to 24 October a pressure gradient pointing northward over the Alpine barrier was established near the surface (see Fig. 11). This pressure gradient was caused by the descent of the southerly flow over the northern Alpine foreland with the associated warming as well as the accumulation of cooler air masses in the Po Valley on the southern side of the Alps. The typical foehn feature of a "pressure nose" with high pressure on the southern side and low pressure on the northern side of the Alps was observed. On 24 October 12 UTC, the pressure difference was 11 hPa between Verona and Munich and 6 hPa between Verona and Innsbruck. The wind shift from WSW to SW above the Alps during 24 October characterizes the transition from an initially shallow to a deep foehn.

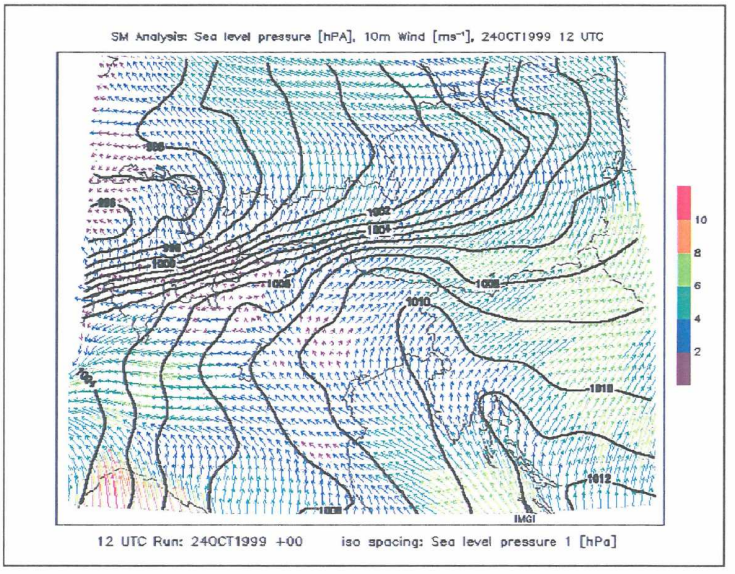

Fig. 11: 12 UTC SM model analysis of 24 October 1999: Sea level pressure in hPa (isolines) and winds at 10 m above topography in m s^{-1} (arrows).

Abb. 11: SM Modellanalyse vom 24. Oktober 1999: Auf Meeresniveau reduzierter Luftdruck in hPa (Isolinien) und 10 m-Wind in m s^{-1} (Pfeile).

4.3.3 Analysis of weather station data

The temporal evolution of foehn at five selected weather stations in the Wipp valley is shown in Fig. 12 and 13. The station Ellboegen, located approximately 9 km south of Innsbruck, is a good indicator for the occurrence of foehn in the lower third of the Wipp valley. There, winds are already turning to south on 23 October 21 UTC with wind speeds initially not exceeding a few m s^{-1}. The decrease of potential temperature at Ellboegen during that night and the prevailing northerly winds at the mountain station Sattelberg near the Brenner Pass indicate that the winds are not a foehn, but a thermally driven valley flow.

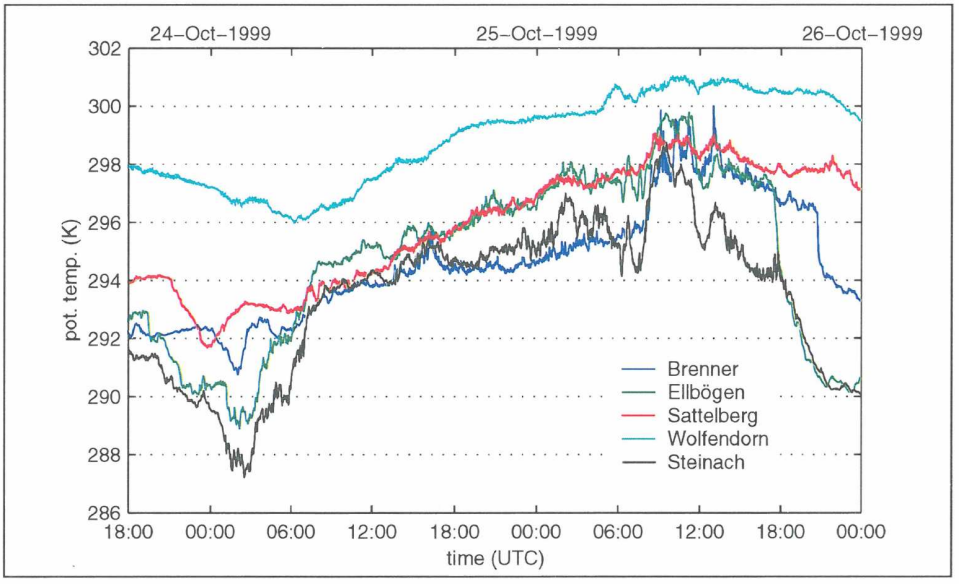

Fig. 12: Potential temperature at five weather stations located in the Wipp valley. From north to south: Ellboegen (green), Steinach (black), Sattelberg (red), Brenner (blue), and Wolfendorn (cyan).

Abb. 12: Zeitreihen der potentiellen Temperatur an fünf Wetterstationen im Wipp valley. Von Norden nach Süden: Ellbögen (grün), Steinach (schwarz), Sattelberg (rot), Brenner (blau) und Wolfendorn (zyan).

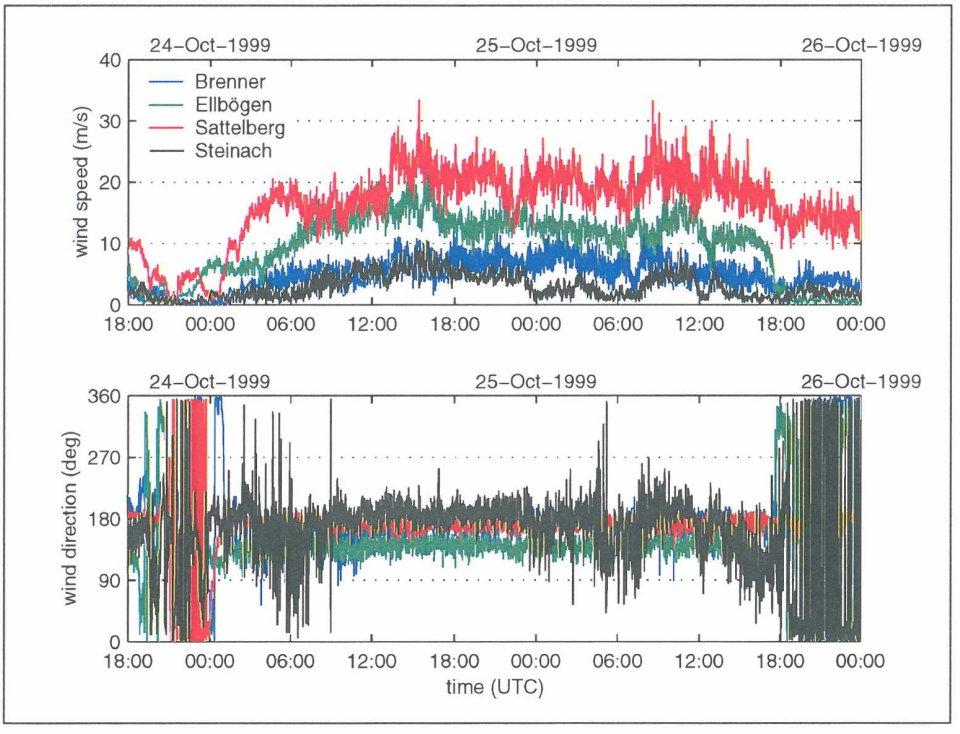

Fig. 13: Average wind speed (top) and wind direction (bottom) at the same weather stations as in Fig. 12, except station Wolfendorn, where no data are available due to freezing of the wind vane.

Abb. 13: Mittlere Windgeschwindigkeit (oben) und Windrichtung (unten) an den in Abb. 12 genannten Wetterstationen außer der Station Wolfendorn, an der wegen einer eingefrorenen Windfahne keine Daten verfügbar waren.

The onset of foehn in the Wipp valley is often observed as a gradual transition from a thermally driven valley flow to a dynamically driven flow over the mountain pass caused by the buildup of a pressure gradient pointing northward over the Alps. This gradual transition is observed at Ellboegen as a steady increase of the strength of the winds and of potential temperature. This is in contrast to the foehn onset in Innsbruck (on 24 October at 1045 UTC), where the penetration of the south foehn into the Inn Valley rapidly changes the west wind regime and often leads to a sudden increase in potential temperature, wind speed, and gustiness. Foehn in Ellboegen on 24 October is strongest during the afternoon with a maximum of the sustained wind speed of 22 m s^{-1} at about 16 UTC and with gusts up to 27 m s^{-1}. On 25 October winds at Ellboegen are slightly weaker.

During the night to 24 October, the air mass along the valley floor of the Wipp valley is not uniform. There seems to be a cold pool in the upper Wipp valley near Steinach. Potential temperatures at the weather station there are about 1 to 2 K lower than at Ellboegen and about 3 to 4 K lower than at the Brenner Pass. With the onset of foehn in the upper Wipp valley during the morning of 24 October these differences almost vanish. However, the foehn flow in the upper Wipp valley is always weaker than near Ellboegen. Sustained winds at Steinach do not exceed 11 m s^{-1} and gusts are below 16 m s^{-1}.

Winds at the Brenner Pass and at the mountain station Sattelberg are almost simultaneously turning to south on 24 October around 01 UTC. This time marks the transition from the pure thermally driven valley flow to the dynamically enhanced flow over the mountain pass. At Sattelberg the strongest winds are observed in the afternoon with up to 33 m s^{-1} mean winds and 37 m s^{-1} gusts. At the Brenner Pass winds do not exceed 13 m s^{-1}.

During the day of 24 October, potential temperatures at the three valley stations Ellboegen, Steinach, and Brenner differ only marginally from the ones at Sattelberg located at 2102 m MSL. Potential temperatures at the highest weather station Wolfendorn, located near the Brenner Pass at 2774 m MSL, are about 3 K higher. This indicates that the foehn air descends from near the Sattelberg level into the Wipp valley. However, during the following night and morning of 25 October the upper Wipp valley is 2 to 3 K potentially cooler than Ellboegen, which still has the same potential temperature as Sattelberg. Foehn winds at Steinach are distinctively weaker during that night with sustained winds below 5 m s^{-1}.

The general trend of an increase of potential temperature between 24 and 25 October at all five weather stations is caused by warm air advection along the eastern edge of the synoptic pressure trough. With the approach of the cold front, temperatures start to drop. The interruption of foehn by the cold front passage in the evening of 25 October causes a rapid decrease in potential temperatures and a pronounced wind shift to north – at Ellboegen at 1740 UTC and at the Brenner Pass at 2045 UTC, i.e. the front slowly progresses up the Wipp valley.

4.3.4 Analysis of rawinsonde data

4.3.4.1 Sounding on 24 October 1999

In Fig. 14, two soundings from Sterzing and Gedeir show the atmospheric structure up- and downwind of the Brenner Pass in the early afternoon of 24 October. Sterzing is located about 15 km south of Brenner in a basin formed by the Sarntaler Alpen south of Sterzing and the main Alpine ridge to the north near the Brenner Pass. Figure 14 shows that this basin is filled with cool air up to about 2 km MSL, whereas at Gedeir, located in the Wipp valley about 17 km north of Brenner, the air is up to 3 K warmer due to the penetration of the foehn into the valley. A stable isothermal layer between about 3.2 km and 4.2 km MSL characterizes the upstream sounding at Sterzing. Several shallow mixed layers below 2.4 km MSL are some indication of a descent of the southerly flow on the lee side of the Sarntaler Alpen. The stratiform cloud layer between 2.3 and 3.5 km MSL south of Brenner disappears

as the foehn descends into the Wipp valley. As seen from the Wipp valley, this cloud deck appears as a "foehn wall" near the Brenner Pass. A 200 m thick temperature inversion of 1.3 K above Gedeir separates an almost mixed layer between the surface and 2.4 km from a less stable layer which extends above the top of the main crest.

A comparison of the two potential temperature profiles in Fig. 14 indicates that two layers located upstream of Brenner Pass between 1.8 km and 2.1 km MSL and between 2.9 km and 3.3 km MSL descend by more than 500 m, i.e. up to 650 m, into the Wipp valley towards Gedeir. This is more than the drop of the valley bottom of approximately 300 m between Brenner and Gedeir. The strength of the foehn flow in the Wipp valley near Gedeir increases with height with a maximum of 29 m s^{-1} (56 knots) just below the temperature inversion at 2.3 km MSL. At the inversion the wind shifts from SSE to SW, indicating the transition from the low-level flow channeled by the valley to the flow above the Alpine crest. The flow below 3 km MSL is significantly weaker upstream of Brenner than on the leeside of the pass and does not exceed 13 m s^{-1}.

4.3.4.2 Sounding on 25 October 1999

Rawinsonde data of the 25 October show that the valley atmosphere downstream from Brenner is well mixed up to about 2 km MSL (Fig. 15). Foehn winds in the Wipp valley below the Alpine crest are slightly weaker than on the previous day and do not exceed 25 m s^{-1}. However, winds of the upstream sounding enhanced. Due to the approach of the mid-tropospheric pressure trough, the winds are more southerly then the day before.

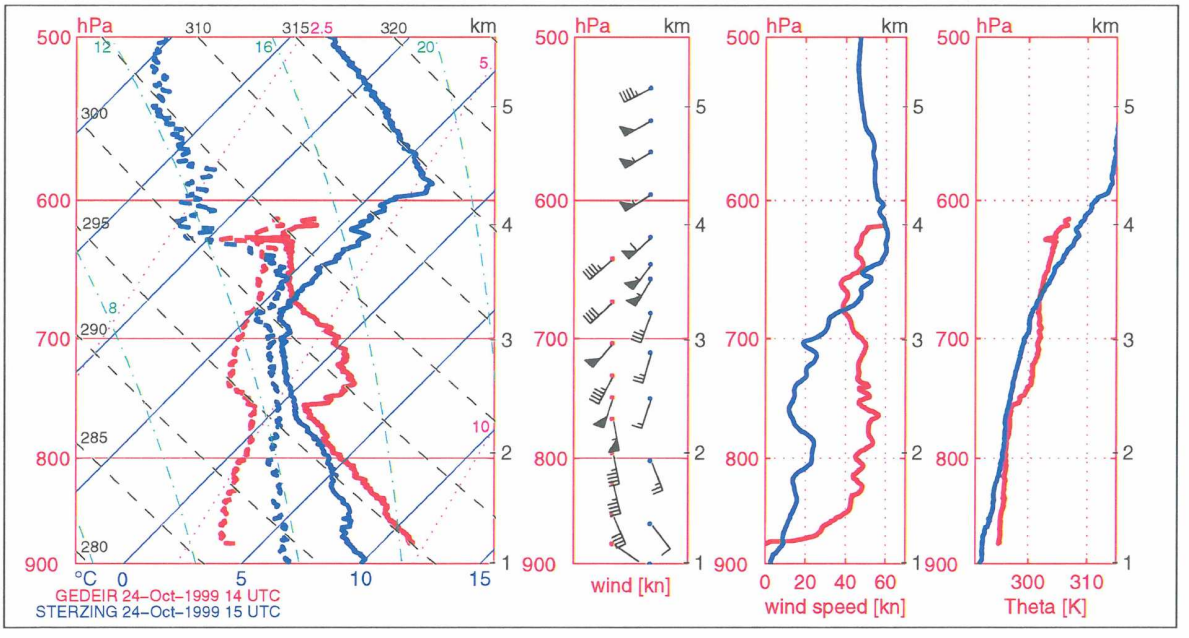

Fig. 14: Atmospheric sounding of a rawinsonde launch at Gedeir (red) in the Wipp valley and Sterzing (blue) south of the Brenner Pass on 24 October 1999 at 14 UTC and 15 UTC, respectively. From left to right: thermodynamic diagram with dry air temperature (solid) and dew point temperature (dashed), wind barbs in knots, wind speed in knots, and potential temperature in Kelvin.

Abb. 14: Sondierung von Gedeir (rot) im Wipp valley und Sterzing (blau) südlich des Brennerpasses am 24 Oktober 1999 um 14 UTC bzw, 15 UTC: Von links nach rechts: thermodynamisches Diagramm mit Lufttemperatur (durchgezogen) und Taupunktstemperatur (strichliert), Windfahnen in Knoten, Windgeschwindigkeit in Knoten und potentielle Temperatur in Kelvin.

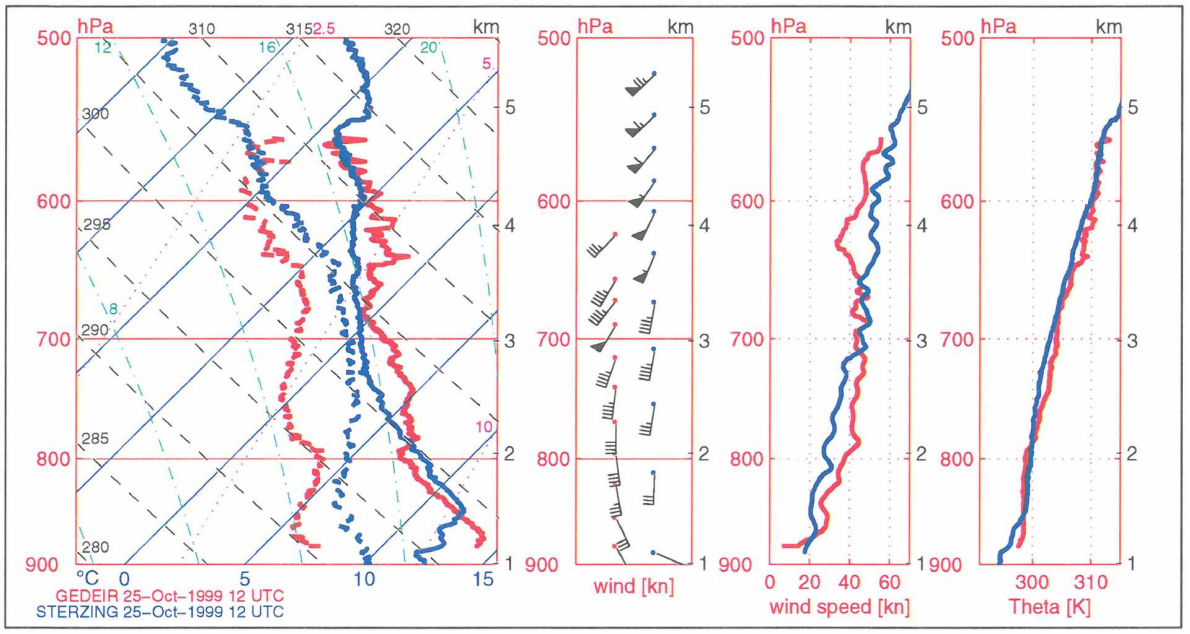

Fig. 15: As Fig. 14 but for 25 October 1999 12 UTC.

Abb. 15: Wie Abb. 14, jedoch für 25. Oktober 1999, 12 UTC.

The upstream sounding in the basin at Sterzing begins with an isothermal shallow cold pool followed by a weakly stable, almost mixed layer between about 1.5 km and 2.5 km MSL. Data from previous soundings between 6 UTC and 12 UTC show a continuous increase in the thickness of the mixed layer above the cold pool, which is supposed to be caused by the descent of air from the Sarntaler Alpen south of Sterzing.

4.3.5 Analysis of Doppler lidar data

4.3.5.1 NOAA/ETL Doppler lidar TEA CO_2

On 24 and 25 October 1999, the National Oceanic and Atmospheric Administration (NOAA) / Environmental Technology Laboratory (ETL) operated its Doppler lidar TEA CO_2 at Gedeir (1075 m MSL), located in the middle of the Wipp valley (see Fig. 10). TEA CO_2 emits light at 10.6 μm wavelength and measures the intensity and Doppler frequency shift of the signal, which is backscattered by aerosols distributed in the atmosphere and moving with the air flow. Radial (along-beam) velocities of the wind are derived from the frequency shift. The along-beam and across-beam resolution of this lidar is 300 m and 1 m, respectively. Depending on the amount and distribution of scatters in the atmosphere, the maximum range of TEA CO_2 can be up to 30 km. Liquid water clouds drastically decrease its range due to absorption of the emitted light by water. However, high Cirrus clouds increase the lidar range due to backscattering of the light by ice particles. Several different scan strategies were applied to measure the three-dimensional structure of the foehn flow in the Wipp valley. Scans on a vertical plane, where the azimuth angle is kept constant and the elevation angle varies, are called RHI's (range height indicator). Scans on a cone with constant elevation angle and varying azimuth angle are called PPI's (plan projection indicator). A VAD (velocity azimuth display) scan is a special PPI scan sweeping a complete circle between 0° and 360° (see section 4.3.5.1). Data from VAD scans are used to derive vertical profiles of the horizontal wind (see section 4.3.5.2). A sequence of RHI or PPI scans, where the constant angle of the scan is continuously changed by small increments, yields information of the flow structure of a whole air volume (see section 4.3.5.3). The present case study focuses on the analysis of lidar data collected during 24 October 1999.

4.3.5.2 The foehn flow in its early stage

Figure 16 shows a VAD scan with radial wind velocity of the early stage of the foehn flow in the morning of 24 October 1999. The lidar beam was swept on a cone with 25° elevation angle.

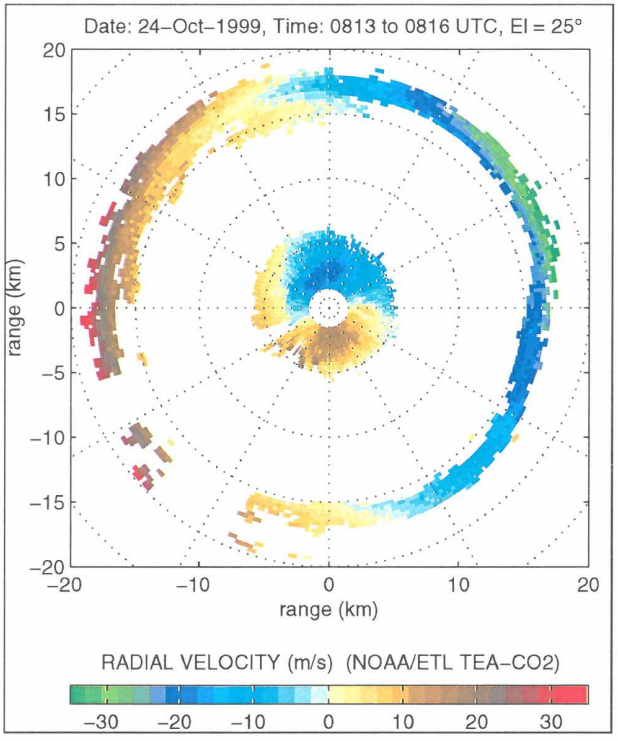

Fig. 16: Radial wind velocity in m s^{-1} on 24 October 1999 between 0813 and 0816 UTC measured with the NOAA/ETL Doppler lidar located at Gedeir. Shown is a conical PPI scan at a constant elevation angle of 25° with an azimuth angle varying from 0° to 360°. Axes and range rings show the along-beam distance from the lidar. The lidar location is at the center of the plot at (0,0). Blue and green colors (negative velocities) indicate flow away from the lidar; brown and red colors (positive velocities) are flow towards the lidar. Empty white areas are regions with no data due to the lack of back scatter signal (low content of aerosols) or ground clutter (hard target return). Such scans are used for deriving vertical profiles of the horizontal wind (see Fig. 17 to 20).

Abb. 16: Mit dem NOAA/ETL Doppler Lidar in Gedeir am 24. Oktober 1999 zwischen 0813 und 0816 UTC gemessene Radialgeschwindigkeit in m s^{-1}. Dargestellt ist ein konischer PPI-Scan mit konstantem Höhenwinkel von 25° und Azimuth zwischen 0° und 360°. Achsen und Abstandskreise zeigen die Distanz vom Lidar entlang des Strahles an. Das Lidar ist im Zentrum der Abbildung (0,0). Blaue und grüne Farben (negative Geschwindigkeiten) zeigen Strömung weg vom Lidar an, braune und rote Farben (positive Geschwindigkeiten) Strömung zum Lidar. Leere, weiße Gebiete sind Regionen ohne Daten wegen fehlendem Rückstreusignal (geringer Aerosolgehalt) oder Bodenechos. Solche Scans werden verwendet, um vertikale Profile des horizontalen Windes abzuleiten (siehe Abb. 17 bis 20).

Positive radial velocities (brown and red colors) indicate flow towards the lidar and negative values (blue and green colors) are flow away from the lidar. The flow direction at a certain height or range is normal to the line of zero radial velocity and points from the highest to the lowest values. In Fig. 16, a clockwise shift of the line of zero radial velocity with increasing range indicates a wind shift from S to SW with increasing altitude. Below mountain crests, the channeled foehn flow mainly follows the valley direction. Since the valley direction changes from S-N upstream to SE-NW downstream of the lidar site, winds within the valley, i.e. below the 5 km range or the 2.1 km height above ground level (AGL), are southerly upstream and southeasterly downstream of the lidar. In agreement with measurements of the weather stations (cf. section 4.3.3), low-level winds are slightly stronger downstream of the lidar, i.e. in the lower Wipp valley, but do not yet exceed 25 m s^{-1}. Above the Alpine crest, i.e. outside of the

5 km range ring, winds are from WSW, indicating that the early stage of this foehn event is a shallow foehn. In Fig. 16, a strong signal from high Cirrus clouds produces an outer ring of data points between the 15 km and 20 km range with winds from WSW and up to 35 m s^{-1}.

4.3.5.3 Temporal evolution of the foehn flow

Full VAD scans such as in Fig. 16 are normally used to derive vertical profiles of the horizontal wind speed and direction above the lidar by applying a least-square fit interpolation technique to the radial velocity data. This technique assumes that the wind field is horizontally homogeneous at a certain level above ground and that the vertical component of the wind is small compared to the horizontal component. The first assumption is hardly fulfilled in the complex terrain of the Wipp valley, where the upstream wind speed and direction differs form the downstream one. To take into account this asymmetry of the foehn flow within the valley, a full 360° VAD scan was split up in a northern (upstream) and southern (downstream) 180°-sector and then two separate wind profiles were derived from data of these two sectors representing the flow up- and downstream of the lidar. To eliminate small-scale features occurring in a single scan, the two profiles of a VAD scan at 20° and 25° elevation angle were averaged using a Cressman interpolation technique.

Figures 17 and 18 show the temporal evolution of the wind profile from the early morning to the late afternoon of 24 October 1999 upstream and downstream of the lidar site, respectively. In both Figures the first (left) profile shortly after 8 UTC was derived from data of Fig. 16.

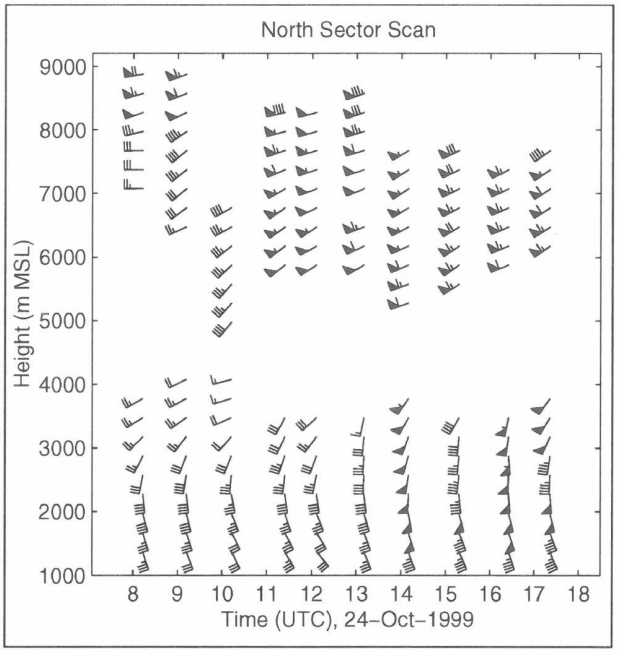

Fig. 17: Vertical profiles of the horizontal wind at Gedeir on 24 October 1999, derived from averaged Doppler lidar data of two north-sector scans at several times between 8 UTC and 18 UTC. The two scans were performed on a half cone between an azimuth angle of 270° and 90° at a constant elevation angle of 20° and 25°, respectively. The abscissa is time in UTC and the ordinate is height in meter above ground level. A half-barb is 2.5 m s^{-1}, a full barb is 5 m s^{-1}, and a triangle is 25 m s^{-1}.

Abb. 17: Vertikalprofile des horizontalen Windes in Gedeir am 24. Oktober 1999, abgeleitet aus gemittelten Nordsektorscans mit dem Doppler Lidar zwischen 8 UTC und 18 UTC. Die Scans umfassen einen Halbkreis von 90° bis 270° mit konstantem Höhenwinkel von 20° bzw. 25°. Die Abszisse gibt die Zeit in UTC an, die Ordinate ist Höhe über Grund in Metern. Kurzer Strich: 2.5 m s^{-1}, langer Strich: 5 m s^{-1}, Dreieck: 25 m s^{-1}.

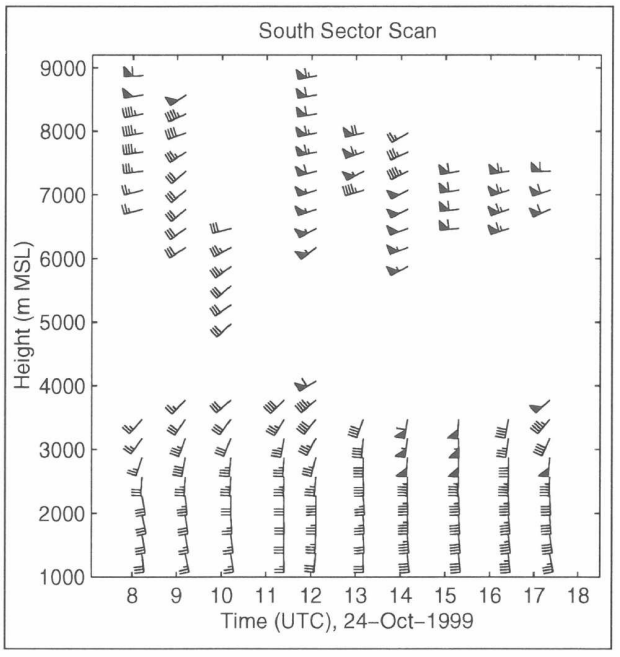

Fig. 18: As Fig. 17 but for south-sector scans with azimuth angle varying between 90° and 270°.

Abb. 18: Wie Abb. 17, jedoch für Südsektor-Scans mit Azimuthwinkel zwischen 90° und 270°.

The upper tropospheric winds above about 5 km MSL are basically the same in strength and direction in the northern and in the southern sector scan. This indicates that the flow between Brenner and Innsbruck at these levels is almost horizontally homogeneous. High-level winds continuously increase in strength during the day and reach a maximum of nearly 50 m s^{-1} at 8.5 km MSL in the early afternoon. A transition from a shallow to a deep foehn during 24 October is shown by a steady wind shift from SW to S and a increase of the strength of the flow above the main Alpine crest within the 3 km to 4 km MSL layer. The southerly flow within the Wipp valley below about 3 km MSL is generally stronger in the northern sector scan and has a pronounced easterly wind component.

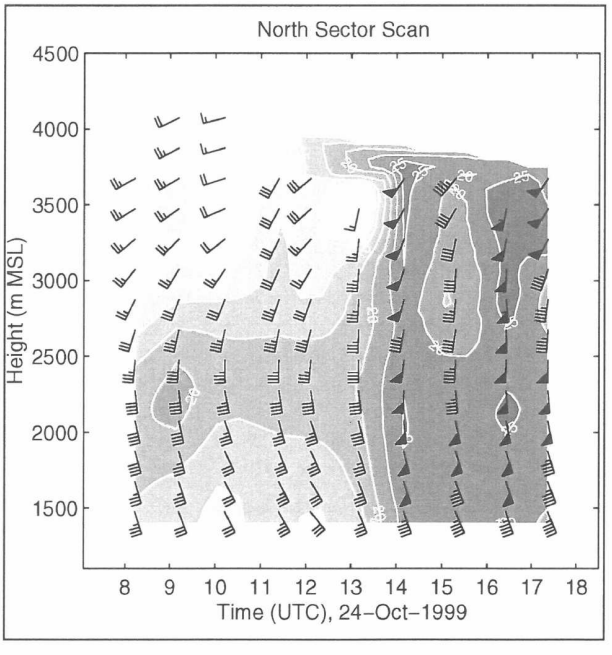

Fig. 19: As Fig. 17 but with contour lines of the horizontal wind speed (interval is 2.5 m s^{-1}).

Abb. 19: Wie Abb. 17, aber mit Konturlinien der horizontalen Windgeschwindigkeit (Intervall: 2.5 m s^{-1}).

Figure 19 and 20 are enlargements of the lower tropospheric flow of Fig. 17 and 18, respectively. During the first half of the day the downstream wind profile (Fig. 19) shows the strongest flow with 20 m s^{-1} at about 2.3 km MSL. Upstream of the lidar site this maximum is weaker but is located about 600 m higher (Fig. 20). This is an evidence for the descent and acceleration of the southerly foehn flow as it penetrates into the Wipp valley. In comparison to the descent of the flow, the average height of the valley bottom hardly changes over the horizontal distance between this up- and downstream wind maximum. In the afternoon the flow generally increase in strength with winds up to 25 m s^{-1}. The winds are more uniform in the vertical, especially in the downstream profile, since the foehn flow becomes deeper.

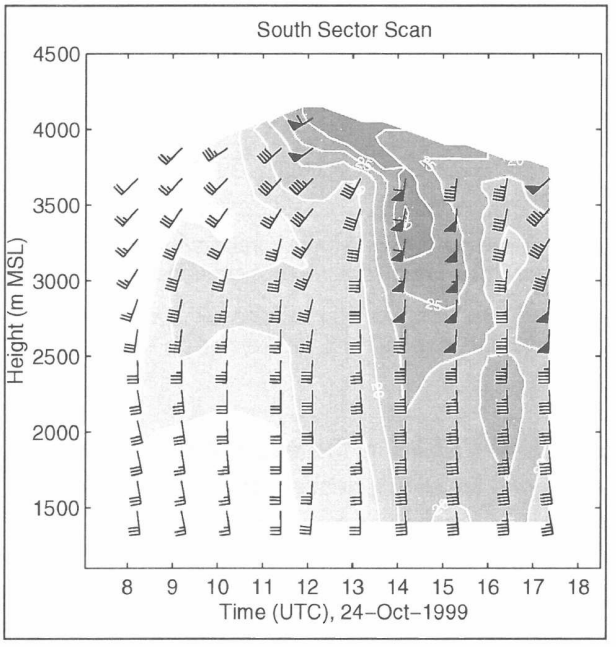

Fig. 20: As Fig. 18 but with contour lines of the horizontal wind speed (interval is 2.5 m s^{-1}).

Abb. 20: Wie Abb. 18, aber mit Konturlinien der horizontalen Windgeschwindigkeit (Intervall: 2.5 m s^{-1}).

4.3.5.4 Spatial variability the foehn flow

In order to investigate the spatial characteristics of foehn, several volume scans –sequences of PPI scans with changing elevation angle – were performed, where the lidar scanned within two narrow 32°-sectors up- and down-valley of the lidar site (see Fig. 10). Data of these scans where then interpolated with a Cressman method from spherical lidar coordinates to an up- and a down-valley Cartesian grid (see Fig. 21).

In Fig. 22 various horizontal and vertical cross-sections of radial wind velocities from the down-valley grid are presented. The data were collected on 24 October between 1325 UTC and 1330 UTC. The horizontal cross-sections show winds up to 35 m s^{-1}. Strongest winds near the surface occur approximately 7 to 8 km downstream of the lidar, i.e. 2-3 km south of weather station Ellboegen (see Fig. 10). The foehn flow does not follow the along-valley axis, but gravitates towards the eastern (right) slope of the valley as it moves downstream. Thus, foehn winds between Ellboegen and the northern exit of the Wipp valley are significantly stronger by almost 50 % in the eastern half of the valley.

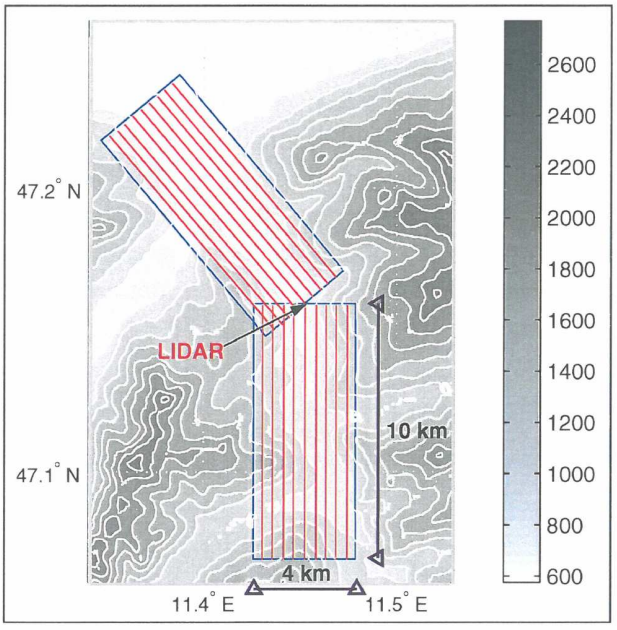

Fig. 21: Topographic map of the Wipp valley. Contour interval is 200 m. Heights are in m MSL. Indicated are location of horizontal (blue) and vertical (red) cross-sections shown in Fig. 22.

Abb. 21: Topographiekarte des Wipp valleyes. Konturintervall: 200 m. Höhen in m NN. Engezeichnet sind die Positionen der horizontalen (blau) und vertikalen (rot) Querschnitte von Abb. 22.

Accordingly, the strongest winds are found in the easternmost vertical cross-section shown, i.e. at x=1.6 km. Further, there is evidence for strong descent of the foehn flow into the valley, since the core of the flow with highest velocities descends by more then 1 km over a horizontal distance of approximately 6 km. The height of the valley bottom changes less then 100 m within this distance. The wavy velocity structure at the top of this core with strong horizontal gradients in wind speed, especially in the cross-sections of x=-0.4, 0, and 0.4 km, may be some indication for the existence of turbulent structures and hydraulic jumps.

The flow characteristics in the upper Wipp valley north of Gedeir are shown in Fig. 23. Wind maxima with about 30 m s^{-1} are generally lower than in the downstream grid of Fig. 22. The flow does not show any pronounced asymmetry across the valley axis. Downvalley, however, it continuously increases in strength, especially near the surface. The vertical cross-sections near the center of the valley (x~0 km) show again a general descent of the foehn flow into the valley as well as local ascents and descents associated with wave structures. The strong horizontal gradients in wind speed in the cross-sections x=-0.4 km and –0.8 km between 6 km and 8 km upstream of Gedeir and at about 1 km above the lidar site are related to strong descent of the foehn flow over the leeside of the eastern flank of the mountain Blaser west of Steinach (see Fig. 21).

4.3.6 Summary

A combination of several in-situ measuring devices and a remote sounding system were used to investigate the complex flow structure of foehn evolving in a valley – the Wipp valley. Weather stations, balloon soundings, and Doppler lidar, all indicate a significant acceleration of the foehn flow as it flows over the Brenner Pass, penetrates into the valley, and progresses northward. The upstream thermodynamic structure south of Brenner shows a cold pool below the pass, whereas the atmosphere downstream of the pass is warmer due to vertical mixing caused by the descent of foehn. Lidar data indicate, that this flow follows the along-valley axis especially in the upper part of the Wipp valley where the valley is rather narrow, but gravitates towards the eastern slopes of the Wipp valley, where the valley widens. The wind maximum is approximately 2 km north of the weather station

Ellboegen. Lidar measurements also show the existence of small-scale wave structures probably associated with turbulent regions and hydraulic jumps. Some of these structures are related to the flow over local topography within the valley.

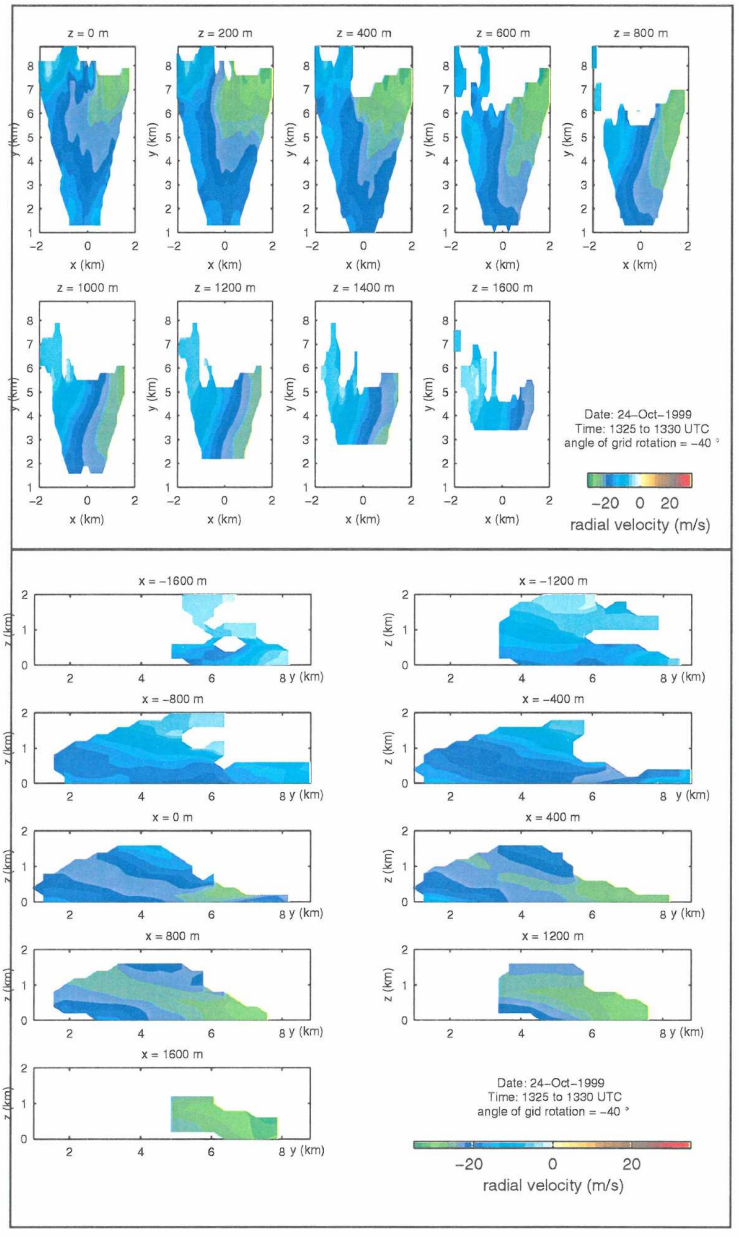

Fig. 22: Radial wind velocities on 24 October 1999 1325-1330 UTC. Data are displayed on a Cartesian grid located down-valley (north) of Gedeir. The flow is away from the lidar, which is at x,y,z=0,0,0. Y-axis is aligned parallel to the valley axis at an azimuth angle of -40° (see Fig. 10). X-axis increases northeastward; y-axis increases northwestward. Altitudes are heights above the lidar site. Horizontal cross-sections between z=0 km and 1.6 km AGL (top) and vertical cross-sections between x =-1.6 km and +1.6 km (bottom). Color scale ranges from -35 m s^{-1} to +35 m s^{-1} with increments of 2.2 m s^{-1}. Blue and green colors indicate flow away from the lidar; brown and red colors are flow towards the lidar.

Abb. 22: Radialgeschwindigkeiten am 24. Oktober 1999 1325 – 1330 UTC. Die Daten sind auf einem kartesischen Gitter talauswärts (nördlich) von Gedeir dargestellt. Die Strömung ist vom Lidar an der Position x,y,z = 0,0,0 weggerichtet. Die y- Achse ist parallel zur Talachse ausgerichtet im Azimuthwinkel –40° (siehe Abb. 10). Die x-Achse nimmt nach Nordosten hin zu; die y-Achse nach Nordwesten. Höhen sind über Grund an der Lidarposition. Horizontale Querschnitte zwischen z=0 km und 1.6 km ü.G. (oben) und vertikale Querschnitte zwischen x =-1.6 km und +1.6 km (unten). Die Farbskala geht von -35 m s^{-1} bis +35 m s^{-1} mit Intervallen von 2.2 m s^{-1}. Blaue und grüne Farben zeigen Strömung weg vom Lidar an; braune und rote Farben Strömung zum Lidar.

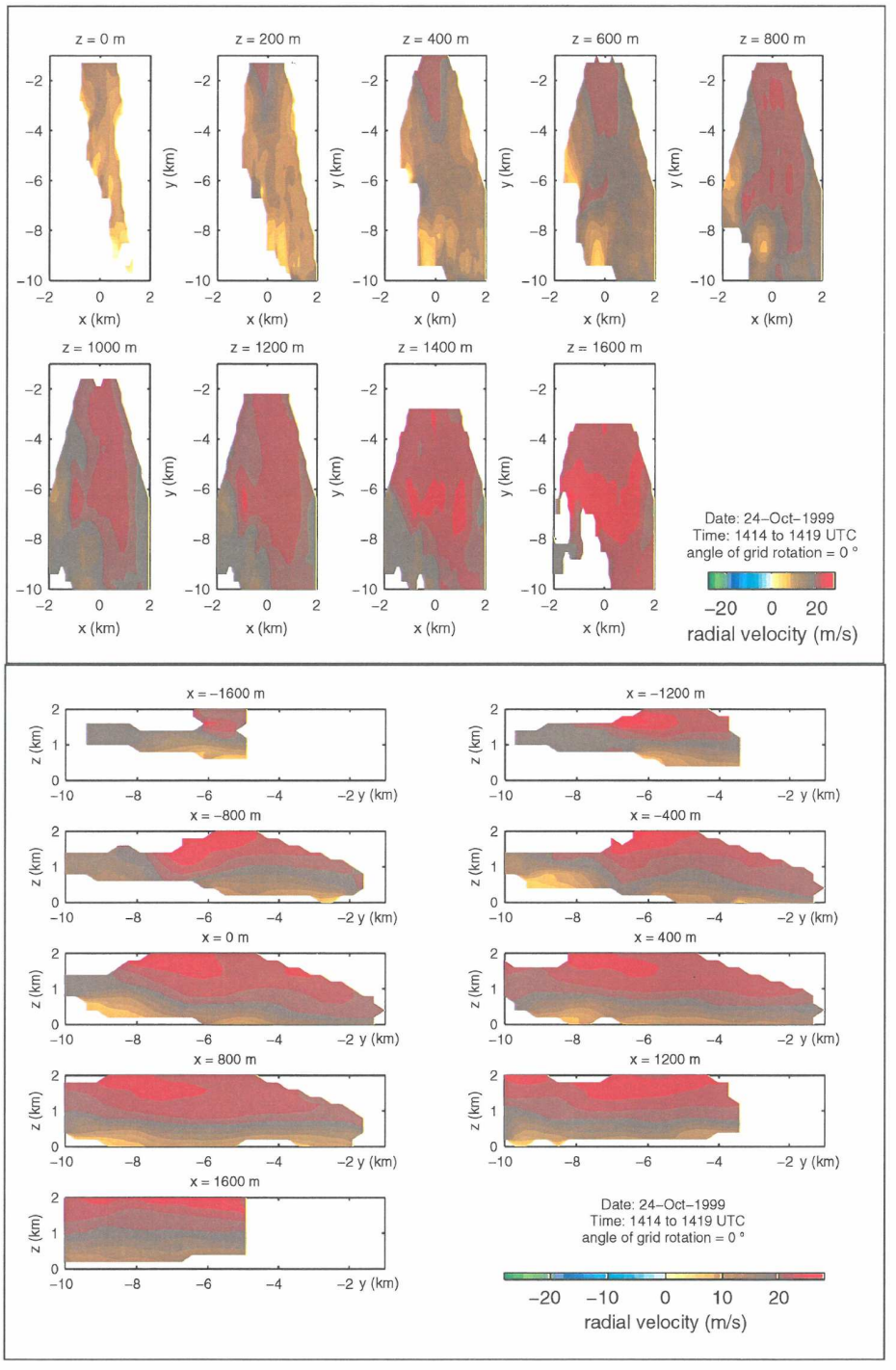

Fig. 23: As Fig. 22 but on 24 October 1999 1414-1419 UTC. Cartesian grid is located up-valley (south) of Gedeir; the flow is towards the lidar. Y-axis is aligned parallel to the valley axis at an azimuth angle of 0°. X-axis increases eastward; y-axis increases northward. Color scale ranges from -28 to +28 m s^{-1} with increments of 1.75 m s^{-1}.

Abb. 23: Wie Abb. 22, aber am 24. Oktober 1999 1414-1419 UTC. Kartesisches Gitter liegt taleinwärts (südlich) von Gedeir, die Strömung geht zum Lidar. Die y-Achse ist parallel zur Talachse mit einem Azimuthwinkel von 0°. Die x-Achse nimmt nach Osten hin zu, die y-Achse nach Norden hin. Die Farbskala reicht von –28 bis +28 m s^{-1} mit Intervallen von 1.75 m s^{-1}.

4.4 Conceptual modelling of the linking up between Wipp valley and Inn valley

The unique MAP data set invites some conceptual considerations on how the foehn flow from the Wipp valley might behave at the junction with the Inn valley around Innsbruck. For some time yet, numerical modelling may not be the most convenient way to obtain a fundamental understanding of possible flow regimes.

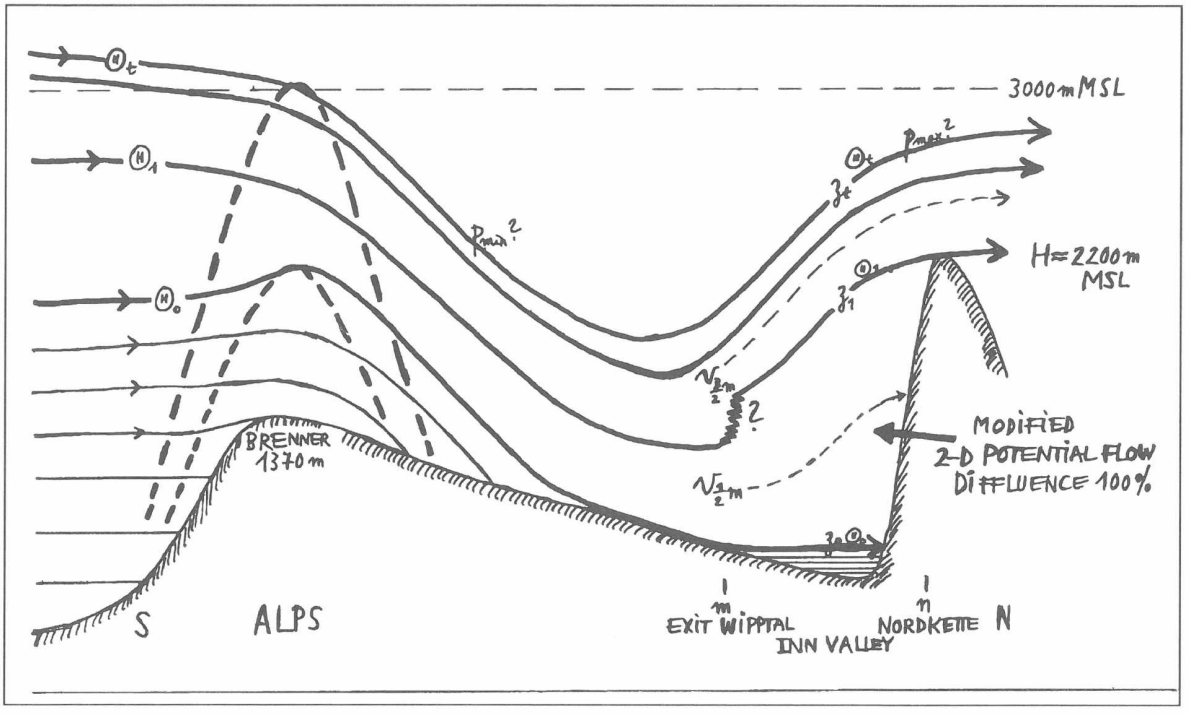

Fig. 24: Schematic cross-section from the southern to the northern side of the Alps; see text for further explanation.

Abb. 24: Schematischer S-N-Querschnitt über den Alpenhauptkamm; für nähere Erläuterungen siehe Text.

Fig. 24 is a schematic cross section from the southern to the northern (lee) side of the Alps, along the Wipp valley and across the Inn valley. The Figure shows a deep foehn with a southerly wind component at the Alpine summit level and consequent wave motion. In order to save an extra Figure, the case of a shallow foehn may be imagined by letting the upper most isentrope Θ_t be horizontal, with vanishing horizontal pressure gradient along it. Each deep foehn contains important elements of shallow foehn at the lower levels. To the extent that the flow at lower levels may be considered hydraulic, it joins two different atmospheric „reservoirs", the northern, warmer one being the Inn valley. If, for example, warmer air across the Bavarian forelands has not been able to flush out the cooler air remaining in the Inn valley, downvalley winds from higher to lower pressure will ensue, and the corresponding forced subsidence within the interior basins will gradually warm the cooler air. This is the process that H. v. Ficker (1931) must have had in mind when he talked about the „sucking out" of the cool air into the Bavarian low-pressure area. The foehn air from the south with $\Theta < \Theta_t$ replaces the air in the northern „reservoir" locally along the Wipp valley and the diffluent region west and east of Innsbruck, but eventually it must join up with the atmospheric state in the leeside „reservoir", whether that be stationary or changing with time. In hydraulic terms, the „Nordkette" north of Innsbruck, whose height almost exactly equals the height of the shoulder of Sattelberg = effective height of the Brenner pass (G. Mayr, private communication), must be an important „downstream control" (L. Armi, private communication).

Fig. 24 implies a regime in which the lower layer $\Theta \leq \Theta_1$ is completely blocked at the Nordkette. It is hard to imagine how such a flow should not bear qualitative similarities with two-dimensional potential flow. Figs. 25a and 25b show the two possible cases of such a flow:

Let $\bar{v} \cdot B \cdot \Delta z$ be the volume flux of the foehn air from the south entering the Inn valley as shown, and $u_0 \cdot D \cdot \Delta z$ be the volume flux of the Inn valley wind. Then if $\frac{1}{2}\bar{v}B > u_0 D$, the foehn air penetrates to the Nordkette, being diffluent to both sides away from the stagnation point, where the pressure $p = const - \frac{1}{2}\rho \cdot \left(u^2 + v^2\right)$ attains a local maximum, frequently documented in earlier field traverses by P. Seibert and R. Steinacker.

If $\frac{1}{2}\bar{v}B < u_0 D$, the foehn air does not reach the Nordkette, but is carried off by the valley wind.

a) b)

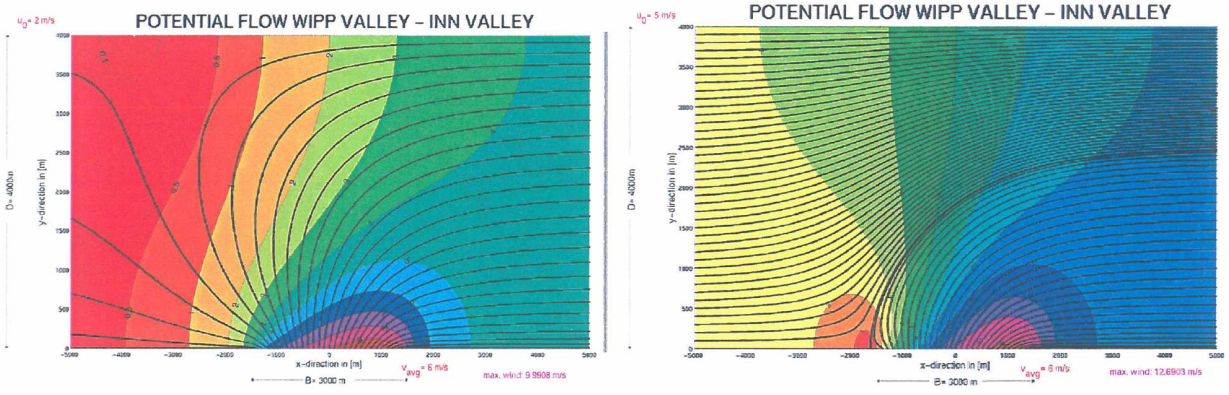

Fig. 25: Two dimensional potential flow with flow in the Inn valley coming from the left and flow from the Wipp valley from the bottom center. Black lines are streamlines, colored areas give the strength of the flow. D denotes the width of the Inn valley, u_0 the strength of the oncoming westerly wind, B the width of the Wipp valley in the exit region and v_{avg} the strength of the oncoming south (foehn) wind. (a) with stagnation on the northern wall and flow splitting with part of the foehn flow going towards the upper Inn valley due to the weak westerlies;(b) stagnation on the south wall and all the foehn flow being deflected to the east.

Abb. 25: Zweidimensionale Potentialströmung mit der Strömung im Inntal (von links) und aus dem Wipp valley (aus der unteren Mitte der Abbildung). Die schwarzen Linien stellen Stromlinien dar, die farbigen Flächen die Strömungsgeschwindigkeit. D ist die Breite des Inntales, u_0 die Windgeschwindigkeit der ankommenden Westströmung, B die Breite des Wipp valleyes im Mündungsbereich und v_{avg} die Stärke der Südströmung (Föhn). (a) mit Stagnationspunkt an der Nordseite und Strömungsaufspaltung, wodurch ein Teil der Föhnströmung wegen der schwachen Westwindkomponente ins Oberinntal geht; (b) Stagnation auf der Südseite, die gesamte Föhnströmung wird nach Osten abgelenkt.

Surface wind patterns with foehn in the Innsbruck area are reminiscent of the flows shown in Fig. 25, although their systematic classification might be worthwile. The deviations from strictly 2-D horizontal nondivergent and irrotational potential flow are not pursued here in detail, but should be appreciated: Real flow is along isentropic surfaces, with the foehn air possibly gliding over wedges of cold air in the Inn valley away from the immediate influence of the Wipp valley, and different isentropic surfaces are not equidistant. The relation between foehn speed and valley wind speed will, in general, change with height, and the pressure pattern imposed at the top will not match the Bernoulli-type potential flow pressure pattern.

Can the general character of this flow regime be investigated without full-scale numerical simulations? For a first attempt, let us consider the two isentropic layers between Θ_0, Θ_1 and Θ_t, and between

„m" (mouth or exit of Wipp valley) and „n" (Nordkette). Perturbations of Montgomery potential and height of isentropes are M' and z'. The hydrostatic relation is

$$-\frac{\partial M'}{\partial \Theta} = \frac{g}{\Theta_{00}} z' \qquad (1)$$

As an upper boundary condition for the equivalent of $\frac{pressure}{mean\ density} M'$ we tentatively use $M'_t = \gamma N_u \cdot \overline{V}_u \cdot z'_t$, where N_u and $\overline{V}_u$ are Brunt-Vaisala frequency and southerly wind component of the upper wave flow and γ is a nondimensional constant. With γ positive, this makes the pressure on top increase in proportion as the isentrope Θ_t rises over the Nordkette. Whereas such a correlation is vaguely plausible, we need to remind ourselves that the upper pressure field along the isentrope Θ_t depends on the complete shape of that isentropic surface, 2D or 3D, and on the wave propagation further up, such that entirely different relations are also feasible. The „shallow foehn" situation with a lid on top $\left(M'_t = 0\right)$ may be recovered as a special case. Working downward hydrostatically, we compute M'_1 and M'_0, and further by interpolation for the middle of each layer

$$M'_{\frac{3}{2}} = \gamma N_u \cdot \overline{V}_u \cdot z'_t + \Delta_{\frac{3}{2}} \cdot \frac{1}{4}\left(z'_t + z'_1\right) \qquad (2)$$

$$M'_{\frac{1}{2}} = \gamma N_u \cdot \overline{V}_u \cdot z'_t + \Delta_{\frac{3}{2}} \cdot \frac{1}{2}\left(z'_t + z'_1\right) + \Delta_{\frac{1}{2}} \cdot \frac{1}{4}\left(z'_1 + z'_0\right) \qquad (3)$$

Here

$$\Delta_{\frac{3}{2}} \equiv \frac{g}{\Theta_{00}}\left(\Theta_t - \Theta_1\right) \qquad (4)$$

and

$$\Delta_{\frac{1}{2}} \equiv \frac{g}{\Theta_{00}}\left(\Theta_1 - \Theta_0\right) \qquad (5)$$

We set $z'_0 = 0$ (see Fig. 24).

We now assume the foehn flow to cross the Inn valley, as it usually does, and apply the Bernoulli equation

$$\left(M' + \frac{1}{2}v^2\right)_m = \left(M' + \frac{1}{2}v^2\right)_n \qquad (6)$$

to each of the two layers. The foehn speeds $v_{\frac{1}{2}m}$ and $v_{\frac{3}{2}m}$ are taken to be known, more or less. The lower layer is assumed to be completely blocked, therefore along that particular streamline $v_{\frac{1}{2}n} = 0$.

For the upper layer we try some forced diffluence, let's say $\frac{1}{2}v^2_{\frac{3}{2}n} \approx \frac{1}{2}v^2_{\frac{3}{2}m}\left(1-\varepsilon\right)$ with $\varepsilon \approx 0{,}3$ or so.

For the lower layer, eqn. (6) could be modified to include some Bernoulli loss. If that is proportional to the kinetic energy, an analogous, but different coefficient e would apply to that energy of the lower layer.

The two Bernoulli equations may now be solved for the two height differences $\left(z_n' - z_m'\right)_t$ and $\left(z_n' - z_m'\right)_1$, for example

$$\left(z_n' - z_m'\right)_1 = \frac{\left(4\gamma N_u \bar{V}_u + \Delta_{\frac{3}{2}}\right) \cdot \frac{1}{2} v_{\frac{1}{2}m}^2 - \left(4\gamma N_u \bar{V}_u + 2\Delta_{\frac{3}{2}}\right) \cdot \frac{1}{2} v_{\frac{3}{2}m}^2 \cdot \varepsilon}{\gamma N_u \bar{V}_u \cdot \left(\Delta_{\frac{3}{2}} + \Delta_{\frac{1}{2}}\right) + \frac{1}{4}\Delta_{\frac{3}{2}} \cdot \Delta_{\frac{1}{2}}} \qquad (7)$$

These algebraic expressions can be interpreted and checked for consistency in various ways. For example, if the height difference in eqn. (7) is non-negative, the (modified) kinetic energy of the lower layer at *m* must be larger than that of the upper layer. Furthermore, the postulated quasi 2-D blocked flow regime in the lower layer requires that that height difference be less than the effective height of the Nordkette (H - z_0). This condition clearly puts a limit on some mean foehn speed $\bar{V}_m$. As long as γ remains small, the pertinent criterion (see eqn. (7)) will qualitatively come out to be $\frac{\bar{V}_m}{N(H - z_0)} < O(1)$ where Δ has been converted to buoyancy frequency N.

It is tempting to speculate how far such an analysis could be carried in more complicated cases, including not only forced foehn flow across the Nordkette from the valley bottom, but possibly also rotor flows.

4.5 Temperature profiles along mountain slopes and their relationship to vertical profiles in the mid-valley atmosphere

4.5.1 Introduction

During the field experiment phase of MAP thirty-five temperature data loggers were distributed along seven lines that ran up the sidewalls of the Wipp valley. These data loggers sampled and recorded 2-m air temperatures at 5-minute intervals during the entire 11 September to 15 November 1999 MAP SOP, providing quasi-continuous information on the stratification of the valley atmosphere and supplementing measurements from rawinsondes that were launched from the lower part of the Wipp valley during MAP IOPs. Case studies will be presented in which the pseudo-vertical temperature profiles obtained from the data logger lines on the valley sidewalls are compared with rawinsonde temperature profiles from the adjacent "free" valley atmosphere.

4.5.2 Earlier Research

There is a long history in the meteorological literature of atmospheric temperature structure investigations that have used observations taken from valley sidewalls. Early investigations were reported by von Hann (1913), von Ficker (1913) and Suering (1916). Temperatures along mountain slopes were generally found to be colder than the free air (on average) although surface temperatures on days with calm winds and clear skies were found to be several degrees Celsius higher than in the free atmosphere. Fergusson (1934) and Schell (1935) compared aircraft data with observations on Mt. Washington and found a greater lapse rate within 10 to 20 m of the slope than in the free atmosphere on windy days, but with the opposite effect on calm days. Samson (1962) collected temperature and humidity data in Colorado by holding a psychrometer out the window of an automobile while driving up the road to Pikes Peak (4150 m MSL). He compared these data with radiosonde data from Denver, Colorado, located 100 km NNE of Pike's Peak, documenting the strong influence of air mass differences, winds, cloudiness, precipitation and surface radiation characteristics. A more recent paper by Dreiseitl (1987) developed a method to convert observed screen temperatures from six stations on

the sidewalls of the Inn Valley near Innsbruck, Austria, into temperatures of the "free" valley atmosphere. A general summary of the scientific literature on temperature differences between mountain-slopes and the free atmosphere is given by Barry (1992).

4.5.3 Sites

The map of the experimental area in Fig. 26 shows seven numbered lines that represent the surface temperature profiles. The main observations (line 2) were taken on the Patscherkofel, a 2250 m MSL peak located 8 km SSE of Innsbruck.

There, temperature data were obtained at 5-min intervals from a line of 12 data loggers extending from the valley floor at 700 m up to 2100 m MSL along the west face of the Patscherkofel. The rawinsondes were launched at Gedeir, a station located on the lower part of the west-facing sidewall of the Wipp valley about 5 km south of the Patscherkofel profile, at an altitude of 1075 m MSL, 300 m above the valley floor.

4.5.4 Instruments

A large number of surface instruments is necessary to obtain detailed vertical temperature structure information on the stratification of the valley atmosphere. The recent development of inexpensive temperature data loggers makes this possible. We used Hobo H8 Pro data loggers produced by Onset Computer of Bourne, Massachusetts. These loggers used epoxy-potted thermistors with a time constant of 122 s exposed at 2-m heights in 6-plate unaspirated radiation shields. A recent article (Whiteman et al. 2000) reports the operating characteristics and performance of these loggers.

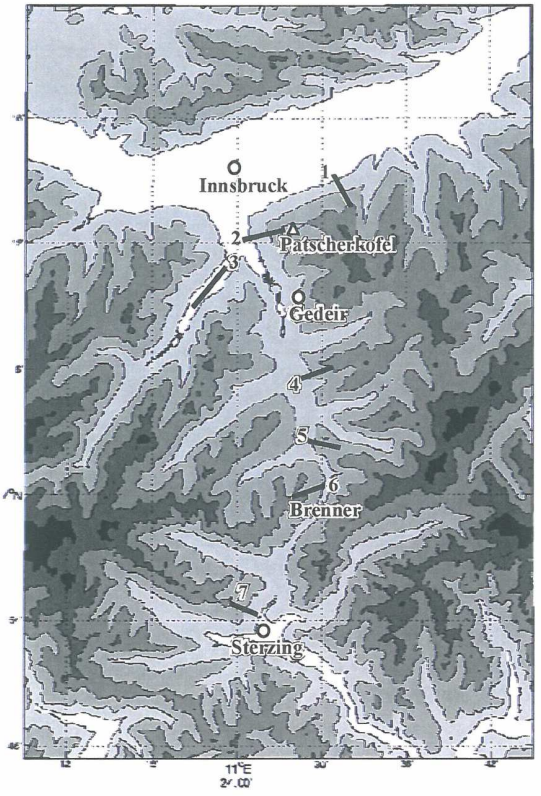

Fig. 26: Map of the Innsbruck-Brenner Pass area showing topography and measurement sites. The numbered heavy lines represent the profiles of surface temperature data loggers.

Abb. 26: Topographie und Meßstellen entlang der Brennersenke. Die numerierten dicken Linien repräsentieren die Profile der Temperaturdatenlogger.

4.5.5 Surface Temperatures For Different Atmospheric Conditions

For the part of the MAP experiment which happened around the Wipp valley the main interest was gap wind, so rawinsondes were launched only during pre-foehn, shallow foehn or deep foehn situations. The present article is restricted to these weather situations. Fig. 27 compares pseudo-vertical temperature profiles obtained from the Patscherkofel surface stations based on a single 5-minute sample with vertical profiles obtained from rawinsondes launched at Gedeir.

Fig. 27a shows the stratification in the Wipp valley on 18 October at noon when an overcast cloud layer was present with a base at 1200 m MSL in the first part of the day and rime at the surface in the lowest, shallow part of the valley.

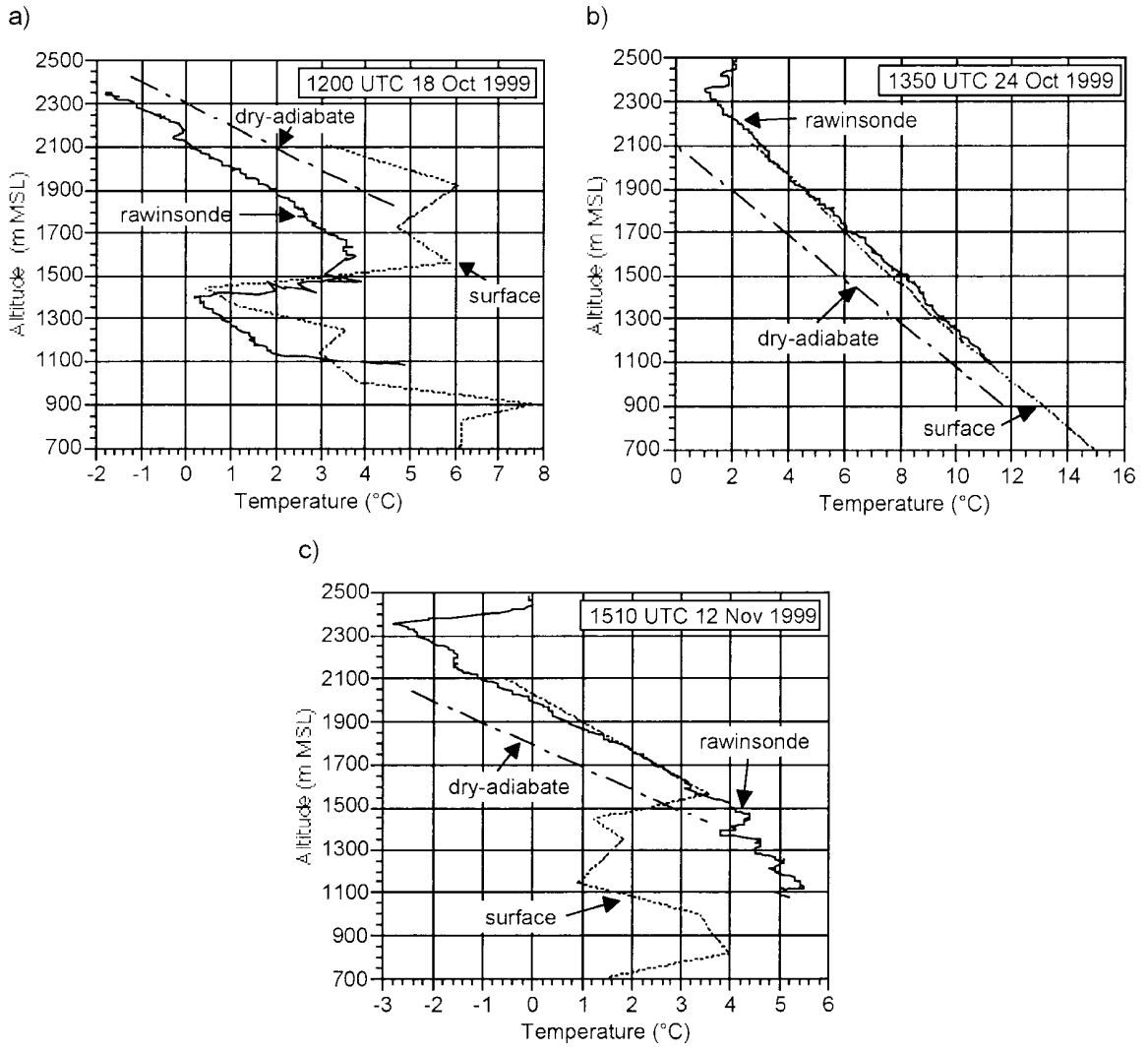

Fig. 27: Vertical temperature profiles measured with rawinsondes at Gedeir and with surface data loggers on the Patscherkofel west face for a) 1200 UTC 18 October 1999, b) 1350 UTC 24 October 1999, and c) 1510 UTC 12 November 1999.

Abb. 27: Vertikale Temperaturprofile von den Radiosonden Gedeir bzw. den Temperaturdatenloggern an der Westseite des Patscherkofels für a) 1200 UTC 18 October 1999, b) 1350 UTC 24 October 1999, und c) 1510 UTC 12 November 1999.

There is a strong inversion between 1400 and 1500 m MSL which corresponds with the overcast cloud layer above 1200 m MSL. Rawinsonde and surface temperature profiles show similar inversion depths and temperature gradients, the sidewall temperatures above the inversion are about 2 °C higher than in the free atmosphere. This difference is thought to be heating at the sidewall due to incoming solar

radiation. Temperatures below the inversion on the sidewall are also up to 2 °C higher than in the adjacent free atmosphere. Wind direction and speed measured with the rawinsonde at 1350 UTC (not shown) indicate wind from 170° with more than 8 m/s above the upper border of the inversion at 1500 m MSL and weak winds with directions around 310° below 1400 m MSL. Fig. 27b shows rawinsonde and surface temperature profiles on 24 October, a day with wind speeds higher than 20 m/s from 160°, between the surface at the valley floor and ridge height (2300 m MSL for the northern part of the Wipp valley). Above 2300 m MSL the wind speed exceeds 25 m/s, but from 230°. Observations indicate an overcast cloud layer above ridge height which should correspond with the shift in wind direction at 2300 m MSL. For this type of weather condition the temperature profile along the surface is very close to the free atmosphere, because of the good vertical mixing caused by the Foehn and the reduction of insolation caused by the overcast.

Fig. 27c represents temperatures in the afternoon of 12 November, a cloudless day with surface snow-cover. The wind speed is continuosly increasing with altitude from 6 m/s at 1100 m MSL to 15 m/s at 2300 m MSL. Directions are fluctuating between 140 and 180°. Surface temperatures at the lowest altitudes are up to 5 °C colder than the rawinsounding, and the strong inversion at 1500 m MSL is seen only from the surface observations, indicating the effect of snow-cover on the Patscherkofel. A well-mixed layer descends into the valley, first over the valley center and then, with a delay, to the adjacent sidewalls.

As long as wind speed exceeds 10 m/s (Fig. 30b and c) temperatures from surface observations are close to rawinsounding temperatures. For wind speeds below 10 m/s (Fig. 30a) there can be several degrees between surface temperatures and "free" valley temperatures.

The following case study gives an example how the temperature information from the pseudo profiles can be used to identify different air- masses.

4.5.6 Case Study of 30 October 1999

30 October provides one of the best data sets available from the Wipp valley part of the MAP experiment, containing lidar and research aircraft data that supplement the data obtained from the routinely operated surface-based instrument networks in the Brenner Pass area. Further, the lidar data are of high quality because of good scattering from Saharan dust advected over the Mediterranean Sea by a strong southerly wind component. The MAP IOP began on the morning of 30 October at 0600 UTC. The availability of the Hobo data before this time provides further details on the evolution of the stratification that culminated in the foehn event.

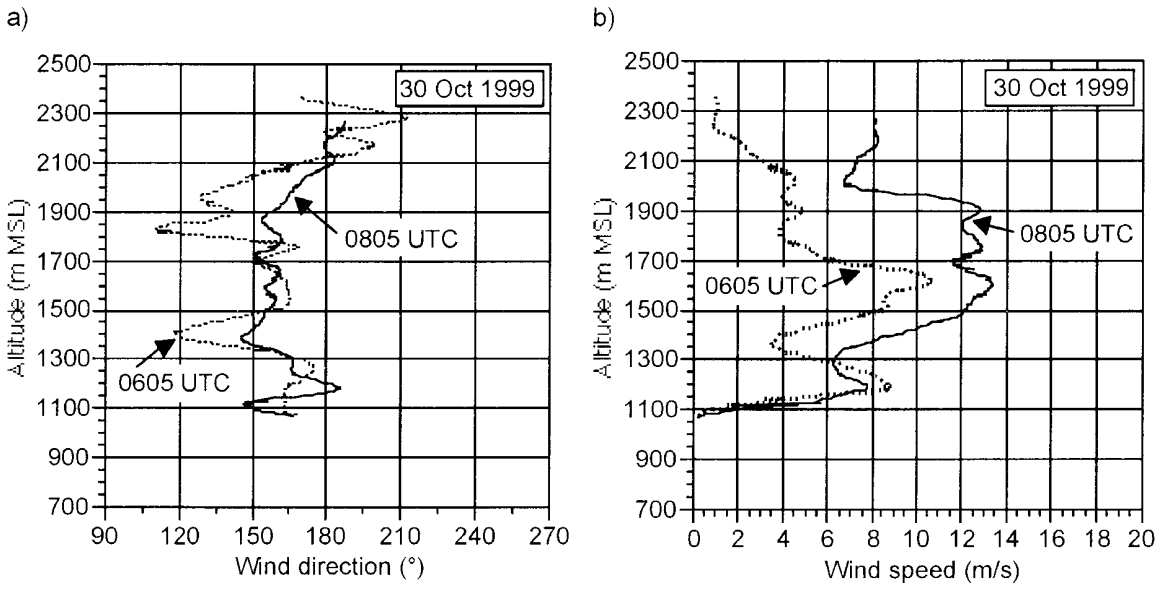

Fig. 28: Wind direction and wind speed on 30 October as measured from rawinsondes launched at 0606 and 0807 UTC at Gedeir.

Abb. 28: Windrichtung und –geschwindigkeit aus den um 0606 und 0807 UTC am 30. Oktober in Gedeir gestarteten Radiosonden.

Fig. 28 shows rawinsonde wind speeds and directions for 30 October. At 0605 UTC, there are two accelerated layers with southerly directions and wind speeds exceeding 8 m/s, one around 1200 m MSL and one from 1500 to 1700 m MSL, with directions around 170°. By 0805 UTC, the upper accelerated layer grew significantly in both depth (to 1400 - 1900 m MSL) and speed (to 12-13 m/s).

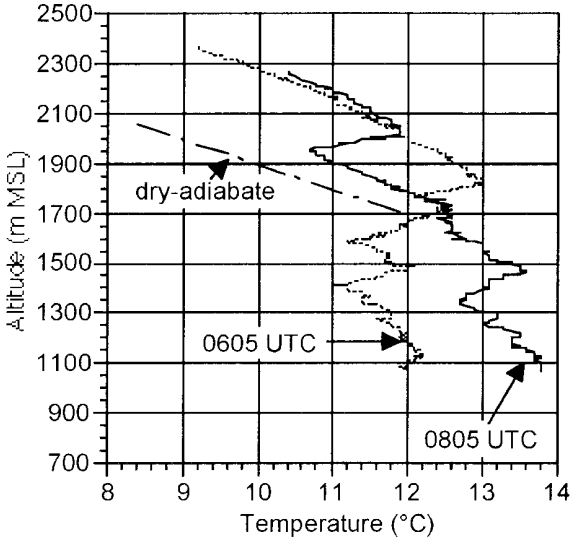

Fig. 29: Vertical temperature profiles measured with rawinsondes at 0605 and 0805 UTC on 30 October 1999 at Gedeir.

Abb. 29: Vertikales Temperaturprofil aus den um 0605 und 0805 UTC am 30. Oktober 1999 in Gedeir gestarteten Sonden.

Rawinsonde temperatures at 0605 UTC (Fig. 29) indicate a strong inversion at 1800 m MSL which separates the accelerated mixed layer below 1800 m MSL (Fig. 28) from the air above. In the period between 0605 and 0805 UTC this inversion layer moved upwards to 2000 m MSL indicating a significant growth of the accelerated mixed layer below the inversion. The air below 1600 m MSL is now about 1.5 °C warmer. The inversion between 1600 and 1700 m MSL in the 0605 UTC sounding has evolved into an isothermal layer at 0805 UTC. A comparison of rawinsonde and surface temperatures (Fig. 30a) shows that - due to its limited vertical resolution - the slope temperature profile is unable to capture the complex structure of the atmosphere at 0605 UTC. At 0805 UTC, when the atmospheric structure is less complex, the pseudo-vertical temperature profile is closer to the rawinsonde profile (Fig. 30b).

The rawinsonde and the pseudo-vertical temperature profile at 1200 and 1450 UTC (Fig. 30c, d), show a well-mixed atmosphere with a dry adiabatic temperature gradient.

Data from the surface temperature loggers (Fig. 31) give a temporally finer resolved evolution of the atmosphere than the rawinsonde launches provide.

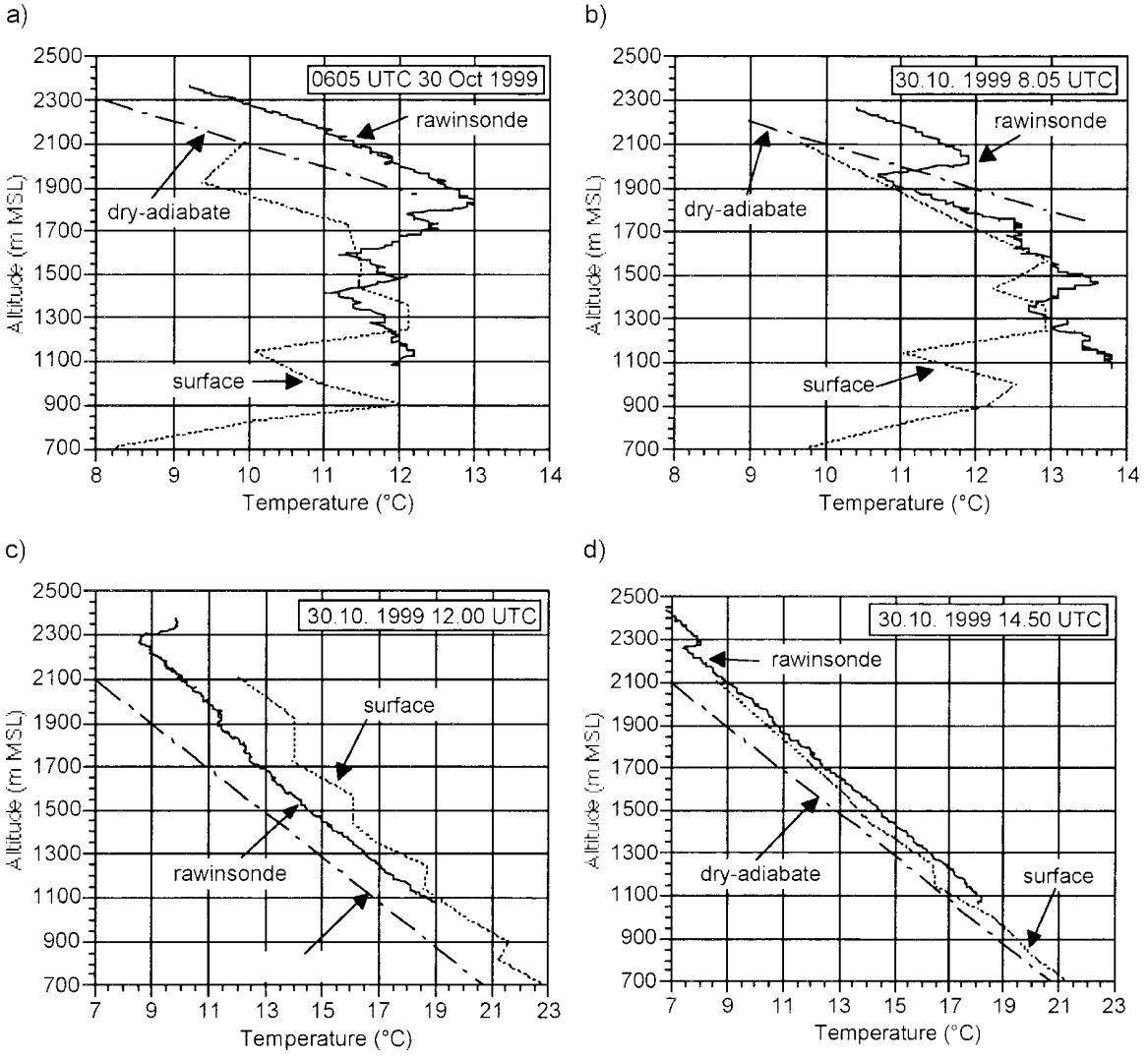

Fig. 30: Vertical temperature profiles measured with rawinsondes at Gedeir and with temperature data loggers on the west face of the Patscherkofel on 30 October 1999.

Abb. 30: Vertikale Temperaturprofile vom 30. Oktober 1999 gemessen von der Radiosonde Gedeir und von den Temperaturdatenloggern auf der Westseite des Patscherkofels.

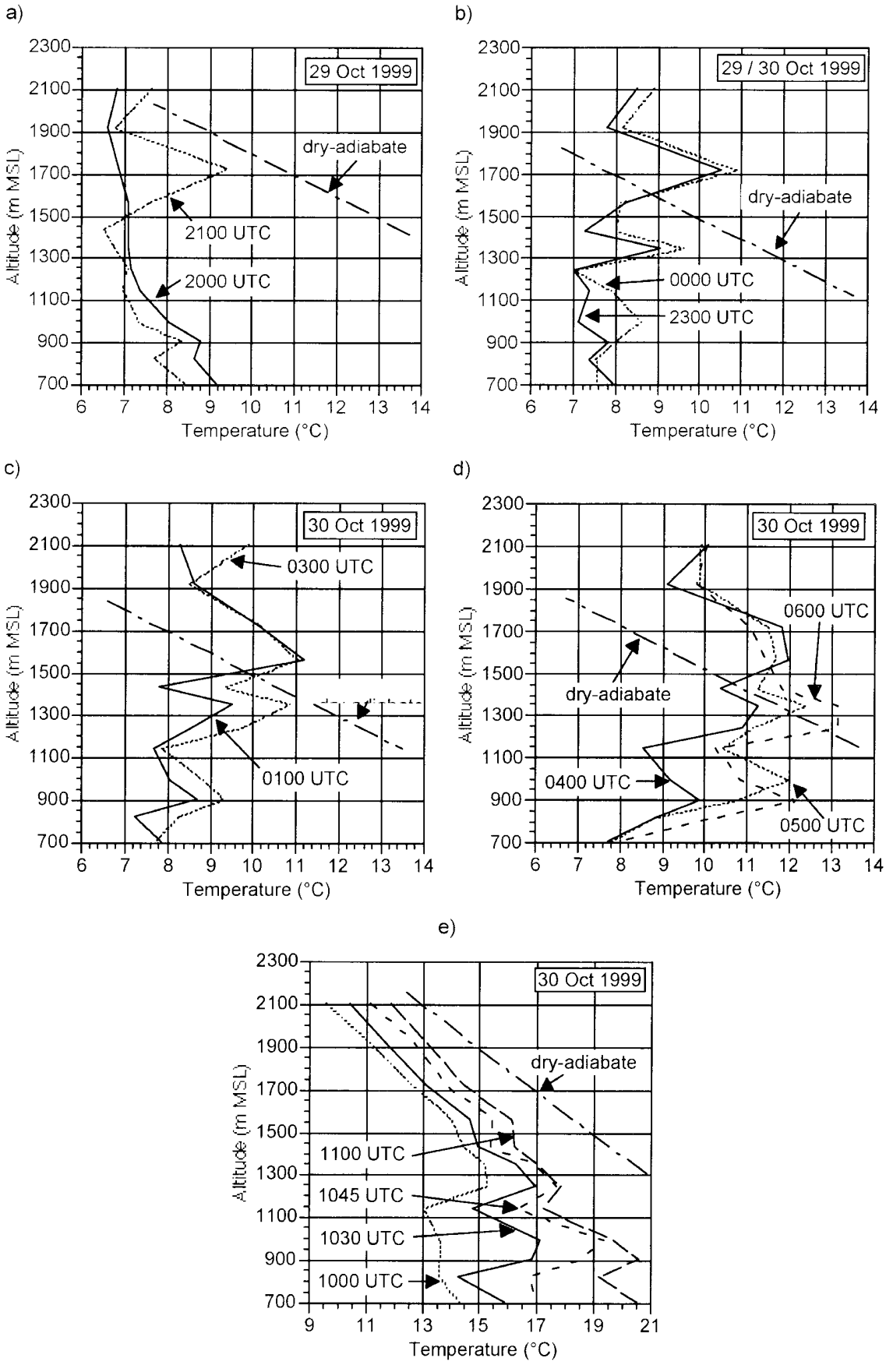

Fig. 31: Vertical temperature profiles measured with surface stations on the west face of the Patscherkofel on 29 and 30 October 1999.

Abb. 31: Vertikales Temperaturprofile vom 29. und 30. Oktober 1999 aus Messungen von Bodenstationen auf der Westseite des Patscherkofels.

Between 2000 and 2100 UTC of the previous day (Fig. 31a) the temperature at 1720 m MSL warmed from 6.8 to 9.4 °C, indicating advection of a different air mass at this altitude. The lowest part of the profile was still cooling by radiation processes. By 2300 UTC (Fig. 31b) the temperature at 1350 m had risen from 7.1 °C to 9.1 °C. Between 2300 and 0000 UTC a third warm air break-in happens at 1000 m and 1150 m, resulting in an almost dry adiabatic temperature gradient between 1000 and 1225 m MSL, represented by three data-loggers. Further development of this three layer structure is documented in Fig. 31c. Between 0000 UTC and 0100 UTC the station at 1550 m MSL warms from 8.1 °C to 11 °C, resulting in a layer with a vertical temperature gradient of 0.7 °C / 100 m above and a sharp inversion below 1550 m MSL.

The nearly dry-adiabatic layer progresses downward with time. At 0100 UTC it is between 900 and 1150 m MSL. During the remainder of the night (Fig. 31d), the inversion at 1500 m MSL disappears. At 1100 UTC (Fig. 31e) the inversions at 1200 and 850 m MSL are almost destroyed. Rawinsonde and surface temperature profiles at 1200 UTC (Fig. 30c) show one nearly mixed layer in the valley.

The Foehn break-in on 30 October 1999 started with warm air advection at three different layers separated by shallow inversions. While the two upper layers grew and merged during nighttime the lowest inversion was destroyed only by heating after sunrise.

4.5.7 Conclusions

A comprehensive comparison between the rawinsonde soundings at Gedeir and Sterzing and the surface temperatures at nearby slope profiles for the entire MAP period shows that slope temperatures on days with strong radiation and weak winds depend very much on the local microclimates at the individual data loggers. In particular, the forest clearing sites have a very different microclimate from the more open hillsides or meadows. On the other hand, slope and free air temperatures agree well on days with strong winds when the atmosphere becomes well mixed. The given vertical resolution of the surface temperature profile undersamples finely structured temperature profiles of the valley atmosphere. The advantage of the surface temperature pseudo profiles is their high temporal resolution Thus the evolution and propagation of different air masses can be studied This makes the slope temperature profiles a powerful tool for the observation of air mass changes produced by Foehn break-ins or frontal passages.

The present article deals only with one of the six surface temperature pseudo profiles. Future research will deal with all profiles along the Wipp valley that offers the opportunity to see the horizontal propagation of different air masses along the Wipp valley.

5 OVERALL CONCLUSIONS AND OUTLOOK

GAP has been the most comprehensive research effort so far in studying the effects of lateral and vertical constrictions on atmospheric flow. Since it is embedded within MAP it mustered an impressive array of basic and sophisticated instrumentation provided by an international community of research institutions along the lowest pass of the Alpine crest, the Brenner. Even though this region has been a playground for foehn researchers for about 130 years, GAP has already provided and is going to provide substantial new insights to the mechanisms and details of the foehn there.

The biggest surprise so far has been the extent to which the gap flow is decoupled from the flow aloft. This allows the use of a relatively easy-to-handle theoretical framework – hydraulic theory (or reduced-gravity shallow water theory as meteorologists might prefer calling it) – to describe the salient features and mechanisms of the flow. Whether this conclusion will still hold when all gap flow cases of the 70 days of MAP SOP have been examined is one of the big questions for the continuing work.

The quality control and data processing of the huge data set with a multitude of different sensors has proved to be a time consuming process that is just now coming to its end. With the complete data set, more details of the case studies undertaken for this article will be available. And more cases will be examined to study various foehn flow features: e.g. the horizontal variation of the flow within the Wipp valley, foehn in the Stubaital, which is the main tributary to the Wipp valley, and the temporal evolution of the gap flow and its link to mesoscale (e.g. cold air upstream of the pass) and synoptic scale (e.g. position of upper-level trough and front; upper-level flow directions) features.

The data set will be used extensively to validate current and future operational and research numerical models. Studies are already under way to compare observations with forecasts by the operational Swiss model (14 km grid distance) and the Canadian MC2 model, which provided special forecasts for the MAP SOP with a horizontal grid distance of 3 km.

A main goal of MAP was the improvement of forecasts of mountain-related and mountain-modified weather features. Since the weather services have been directly involved with MAP and an international working group of bench forecasters has been founded for dedicated SOP forecasts and ongoing education of the forecasters, the findings from GAP will directly go into everyday forecast practices.

Airplanes using the airport in Innsbruck face difficult flow patterns during foehn, particularly during the transition phases of foehn break-through into the Inn valley and of foehn cessation. Two joint studies with the aviation weather service (Austrocontrol) have been initiated.

These are just a few topics and applications for the use of the rich GAP data set by the international community of researchers that have been involved in the data gathering.

Acknowledgments

The measurement campaign would never have been possible or become such a success without the strong support from many people and institutions.

Thanks for the financial support goes to the Austrian Fonds zur Förderung wissenschaftlicher Forschung (science fund, project P13489-TEC), and the Südtiroler Landesregierung (government of the province Südtirol, Italy).

Local and international partners from the meteorological and hydrological community joined us with their expertise, instrumentation, and personnel: Hydrographisches Amt Bozen, Zentralanstalt für Meteorologie und Geodynamik (Wien und Innsbruck), AustroControl Innsbruck, University of Modena, University Trento, University Munich, University Leeds, DLR Oberpfaffenhofen, Service d`Aeronomie CNRS/UPMC, ETL NOAA Boulder, Scripps Institute La Jolla, Pacific Northwest Laboratories Richland, University of Washington Seattle, University of Northern British Columbia Canada, and NCAR Boulder.

The following institutions along the Brenner cross section gave us logistical support: Hydrographisches Amt Bozen, Segelfliegerclub Sterzing, Italienische Eisenbahn, TIWAG, Österreichische Bundesbahnen, Österreichisches Bundesheer, Gemeinden Gries am Brenner, Trins und Fulpmes, Agrargemeinschaften along the Austrian part of the Wipp valley and Inn valley.

A big thank you is sent to the many land owners who permitted us to set up our stations on their property.

And finally, there are the people who made the organizational, logistical, and scientific setup come alive. Thank you very much!

References

Armi, L., and R. Williams, 1993: The hydraulics of a stratified fluid flowing through a contraction. J. Fluid Mech., 251, 355-375.

Binder, P., and C. Schär, 1996: MAP-Mesoscale Alpine Programme Design Proposal, December 1996. Available from SMA, Krähbühlstr. 58, CH-8044 Zürich, and http://www.map.ethz.ch/proposal.html.

Bougeault, P., P. Binder, A. Buzzi, R. Dirks, R. Houze, J. Kuettner, R.B. Smith, R. Steinacker, and H. Volkert, 2001: The MAP special observing period. Bull. Amer. Meteor. Soc., 82, 433-462.

Brinkmann, W. A. R., 1971: What is a foehn? Weather, 26, 230-239.

Colle, A. B., C. F. Mass, 1998a: Windstorms along the western side of the Washington Cascade Mountains. Part I: A High-resolution observational and modelling study of the 12 February 1995 Event. Mon. Wea. Rev., 126, 28-52.

Colle, A. B., C. F. Mass, 1998b: Windstorms along the western side of the Washington Cascade Mountains. Part II: Characteristics of past events and three-dimensional idealized simulations. Mon. Wea. Rev., 126, 53-71.

Dreiseitl, E., 1988: Slope and free air temperatures in the Inn valley, Met. Atmos. Phys., 39, 25-41.

Durran, D. R., 1986: Another look at downslope windstorms. Part I: The development of analogs to supercritical flow in an infinitely deep, continuously stratified fluid. J. Atmos. Sci., 43, 2527-2543.

Fergusson, S. P., 1934: Aerological studies on Mount Washington, Transactions, American Geophysical Union, Pt. 1, 114-117.

Ficker, H., 1913: Temperatur Differenz zwischen freier Atmosphaere und Berggipfeln, Met. Z., 30, 278-289.

Ficker, H., 1931: Kleinere Mitteilungen. Warum steigt der Föhn in die Täler herab? Met. Z., 66, 227-229.

Hann, J., 1913: Die Berge kaelter als die Atmosphaere, ein meteorologisches Paradoxon, Met. Z., 30, 304-306.

Jackson, P. L., and D. G. Steyn, 1994a: Gap winds in a fjord. Part I: Observations and numerical simulation. Mon. Wea. Rev., 122, 2645-2665.

Jackson, P. L., and D. G. Steyn, 1994b: Gap winds in a fjord. Part II: Hydraulic analog. Mon. Wea. Rev., 122, 2666-2676.

Lau, S. Y., and C. M. Shun, 2000: Observation of terrain-induced windshear around Hong Kong International Airport under stably stratified conditions. AMS, Ninth Conference on Mountain Meteorology, Aspen, Colorado, 93-98.

Levinson, D. H., and R. M. Banta, 1995: Observations of a terrain-forced mesoscale vortex and canyon drainage flows along the front range of Colorado. Mon. Wea. Rev., 123, 2029-2050.

Long, R. R., 1953: Some aspects of the flow of stratified fluids. I. A theoretical investigation. Tellus, 5, 42-58.

Long, R. R., 1955: Some aspects of the flow of stratified fluids. III. Continuous density gradients. Tellus, 7, 341-357.

Lyra G., 1940: Über den Einfluß von Bodenerhebungen auf die Strömung einer stabil geschichteten Atmosphäre. Beitr. Phys. frei. Atmos., 26, 197-206.

Lyra, G., 1943: Theorie der stationären Leewellenströmung in freier Atmosphäre. Z. angew. Math. Mech., 23, 1-28.

Pan, F., and R. B. Smith, 1999: Gap Winds and Wakes: SAR observations and Numerical Simulations. J. Atmos. Sci., 56, 905-923.

Queney, P. 1947: Theory of perturbations in stratified currents with applications to airflow over mountain barriers. Dept. of Meteorology, Univ. of Chicago, Misc. Report No. 23.

Queney, P. 1948: The problem of airflow over mountains: A summary of theoretical studies. Bull. Am. Meteorol. Soc. 29, 16-26.

Samson, C. A., 1965: A comparison of mountain slope and radiosonde observations, Mon. Wea. Rev. 93 No. 5, 327-330.

Schär, C., and D. R. Durran, 1997: Vortex formation and vortex shedding in continuously stratified flows past isolated topography. J. Atmos. Sci., 54, 534-554.

Schär, C., and R. B. Smith, 1993a: Shallow-water flow past isolated topography. Part I: Vorticity production and wake formation. J. Atmos. Sci., 50, 1373-1400.

Schär, C., and R. B. Smith, 1993b: Shallow-water flow past isolated topography. Part II: Transition to vortex shedding. J. Atmos. Sci., 50, 1401-1412.

Scorer, R. S., 1952: Mountain-gap winds; a study of surface wind at Gibraltar. Quart. J. Roy Met. Soc., 78, 53-61.

Smith, R. B., 1979: The influence of mountains on the atmosphere. Adv. Geophys., 21, 87-230.

Smith, R. B., 1985: On severe downslope winds. J. Atmos. Sci., 42, 2597-2603.

Smith, R. B., 1989a: Mountain-induced stagnation points in hydrostatic flow. Tellus, 41A, 270-274.

Smith, R. B., 1989b: Comment on "Low Froude number flow past three-dimensional obstacle. Part I: Baroclinically generated lee vortices". Tellus, 46, 3611-3613.

Smolarkiewicz, P. K., and R. Rotunno, 1989: Low Froude number flow past three-dimensional obstacles. Part I: Baroclinically generated lee vortices. J. Atmos. Sci., 46, 1154-1164.

Smolarkiewicz, P. K., and R. Rotunno, 1990: Low Froude number flow past three-dimensional obstacles. Part II: Upwind flow reversal zone. J. Atmos. Sci., 47, 1498-1511.

Suering, R., 1916: Absteigende Luftstroemungen auf Bergen, Das Wetter, Assman Issue, 33, 26-29.

Wagner, A., 1930: Uber die Feinstruktur des Temperaturgradienten laengs Berghangen, Zeit. Geophys. 6, 310-318.

SELECTED RESULTS OF THE FORMAT FIELD MEASUREMENTS

Reinhold Steinacker, Manfred Spatzierer, Manfred Dorninger, Christian Häberli

Institute of Meteorology and Geophysics, University of Vienna, Austria

Abstract

Selected results of the field campaign of the research project FORMAT (Foehn research in the Rhine valley during MAP in Austria) are being shown and discussed. The series of surface and upper air stations, operated during MAP-SOP, have been carefully quality controlled and processed to give for the first time such a picture of the foehn flow in the Alpine Rhine valley and its tributaries, which is necessary to resolve the temporal and spatial evolution and cessation of foehn at very small scales and to compare these data with high resolution numerical models. A surprise was the observation that in the Brandner Tal, far downstream of the main Alpine crest line, the foehn flow may be strongly decelerated due to its direction towards higher pressure.

1 INTRODUCTION

In the frame of the Mesoscale Alpine Programme (MAP), a field experiment took place in the area of the Alpine Rhine valley to investigate "unstationary aspects of foehn in a large valley" (Bougeault et al, 1998). This was a specific project (P5) of MAP, where research groups of Austria, Switzerland, Germany and France took part (Steinacker, 2000a). Our Department concentrated its measurements in the Brandner valley, a small north south oriented side valley of the Vorarlberg Walgau (Bludenz – Feldkirch) and a portion of the Rhine valley between Bad Ragaz and Feldkirch within the project FORMAT sponsored by the Austrian Science Foundation. A dense array of surface stations with a high temporal resolution, one radiosonde and one SODAR station were set up, furthermore pilot balloons were released and car traverses were conducted. One of the mayor interest for our group was the investigation of the temporal evolution of foehn flows and the difference in characteristics and behavior in the main valley and in side valleys. A description of the overall instrumental setup is given in Richner, H, et al, 2002

Due to an unexpected high number of foehn cases during the MAP Special Observing Period (SOP, 7 September – 15. November 1999, see Bougeault et al, 2001), the data collected by us (see also Chimani, 2002 and Spatzierer, 2002) and the other groups (see e. g. Baumann et al, 2000a,b,c,d, Drobinski et al, 2001a,b, Dürr, 2000, Haeberli et al, 2000, Pechinger et al, 2000, Piringer et al, a,b,c,d,e, Poli et al, 2000, Rau et al, 2000a,b,c,d, Seiz et al, 2000a,b, Spatzierer et al, 2000, Steinacker et al, 2000b,c) represent a unique opportunity to investigate phenomena related to foehn with an accuracy, never achieved before. The present paper wants to give an overview of the measurements and first results.

2 DATA PROCESSING

The data collected during MAP-SOP have been processed immediately after the experiment (November 1999) to transmit the data set to the international MAP Data Centre (MDC) in Zurich. From there every participant of MAP should have the opportunity to access the whole wealth of data collected by the different research teams. Before transferring the data a quality control and correction of erroneous data had to be conducted (6 sets with 52500 data just for the 6 surface stations in the Brandner Tal) and mean values (10 minute means of wind derived from original 2 minute data) had to be calculated to meet the rules of the international MAP data format. Early February 2000 they have been transferred to the MDC in Switzerland. During this period data of further 6 surface stations which

have been set up in the Rhine valley were quality controlled and synchronized. In addition we got access to data series of surface stations of the Vorarlberger Illwerke, which were also included in the quality control and evaluation procedure. For an easier comparison of the series, the data have been treated by an averaging procedure (10 minutes arithmetic means), eventually filling shorter data gaps

3 DATA EVALUATION

In the beginning, a statistics of the wind direction distribution of the stations in the Brandner Tal has been carried out. A 10 degree resolution (36 direction classes plus calm) has been chosen. To focus on a situation with a pronounced flow in the valley, only the 10 minute mean values of the speed exceeding a certain threshold (see Fig. 1) have been counted and a relative frequency distribution has been plotted as a wind rose. For the location of the stations see Fig. 12. The stations in the Brandner Tal in an up-valley array are (see Figs 1 – 6): Bürserberg, Brand-Nesler, Innerdorf, Schattenlagant, Talstation and Lünersee at an elevation between 950 m msl (Bürserberg) and 2000 m msl (Lünersee) and with a horizontal distance between the stations ranging from 1 to 3 km.

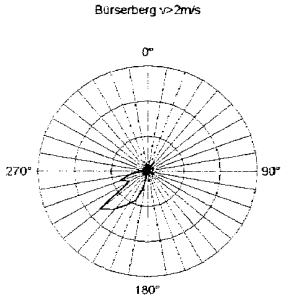

Fig. 1: Frequency distribution of wind direction for speeds above 2 m/s Bürserberg (1 circle=10%)

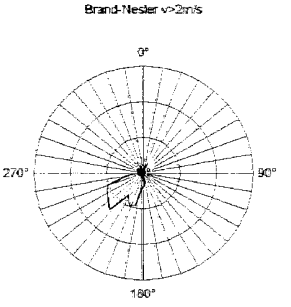

Fig. 2: same as Fig. 1 but for Brand-Nesler

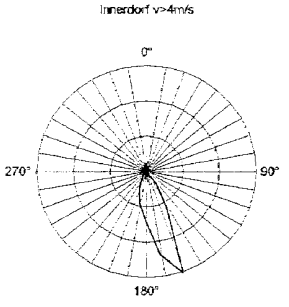

Fig. 3: same as Fig. 1 but for Innerdorf

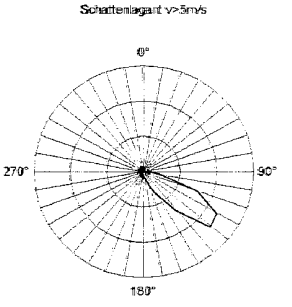

Fig. 4: Same as Fig. 1 but for Schattenlagant

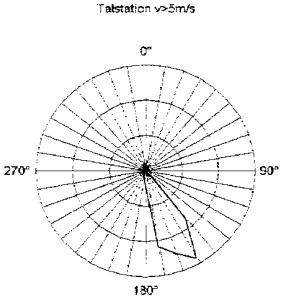

Fig. 5: same as Fig. 1 but for Talstation

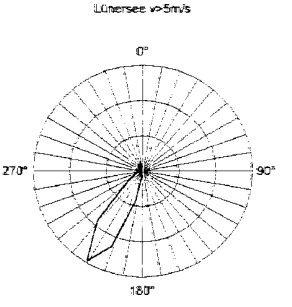

Fig. 6: same as Fig. 1 but for Lünersee

One can clearly see that the wind direction with higher speeds is exclusively oriented down-valley during the whole period (10 weeks) which means that foehn flows were dominating the wind field in the Brandner Tal. There were virtually no stronger up valley winds, despite some fair weather periods. This means that the valley wind circulation does not reach wind speeds above the chosen threshold.

4 CHARACTERISTICS OF THE FOEHN IN THE BRANDNER TAL

The longest foehn period with some interruptions occurred between October 20 and 25. Several penetrations of the foehn flow down the valley and retreats can be clearly seen in the time series of parameters like temperature, potential temperature, humidity and wind speed (see Figs 7 – 10). In general the foehn (high potential temperature, low humidity and high wind speed) occurs first at the highest station and considerably (some hours) later, at the lowest station, whereas the cessation of foehn always starts at the lowest station with a more rapid progress up valley. To make the comparison easier, in Figs 7, 9 and 10 a shift of the scale as indicated by the number in brackets has been carried out.

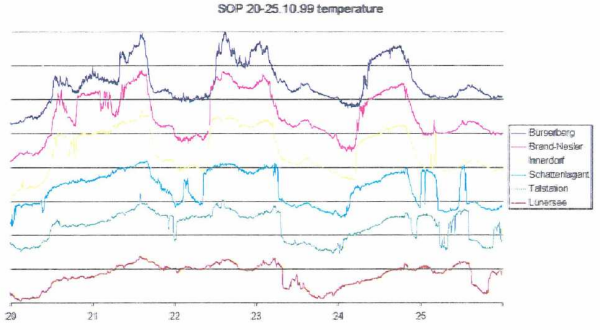

Fig. 7: Temperature 20-25.10 [7 K]

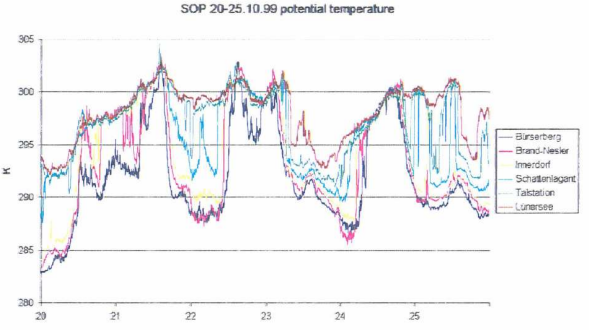

Fig. 8: Potential temperature in K

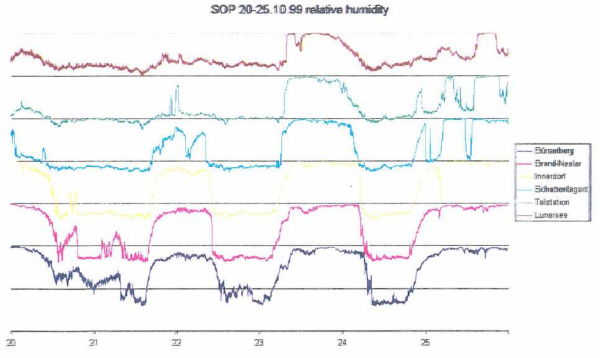

Fig. 9: Relative humidity [50%]

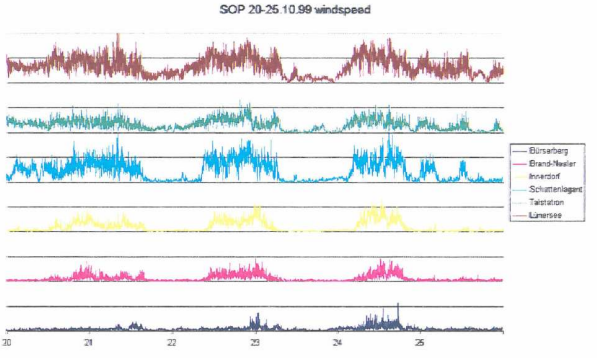

Fig. 10: Wind speed [15m/s]

The spatio-temporal behavior of the different parameters can be visualized in an optimal way by the use of computer animations. In a first step only an array of 6 stations in the Brandner Tal has been treated in a way as shown in Fig. 11. The valley axis, where the stations were located, is slightly S-shaped. The location of stations are plotted at their actual position by wind arrows, whereas the temperature is plotted as a continuous 2D colored area. The animation was produced to run on a standard PC. It was put to the home page of our University Department to make it generally accessible via an internet browser.

In a second step the loops have been extended towards a larger domain and number of stations. Furthermore, instead of color coded areas, the wind arrows have been color coded. In addition a high resolution topography has been introduced to see more accurately the valley orientation and

characteristics. An example for a single plot of the loop, which consist of increments with 10 minute temporal resolution is given in Fig. 12. The production of these loops was rather time consuming due to the fact, that data from different data providers with different formats and temporal resolution had to be merged.

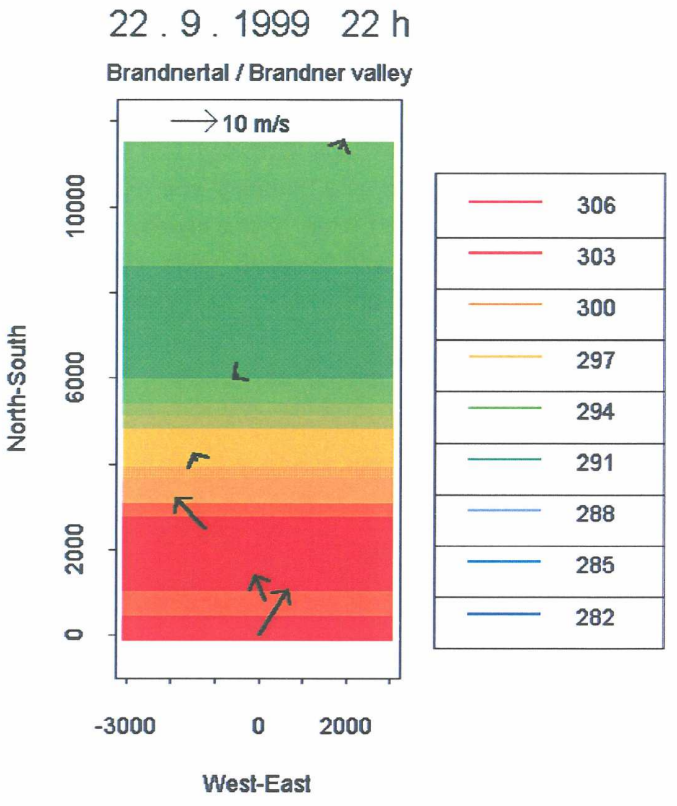

Fig. 11: An example of a single picture of the loop with time increments of 1 hour and a time period of 6 days (October 20, 00 UTC – October 26, 1999, 00 UTC

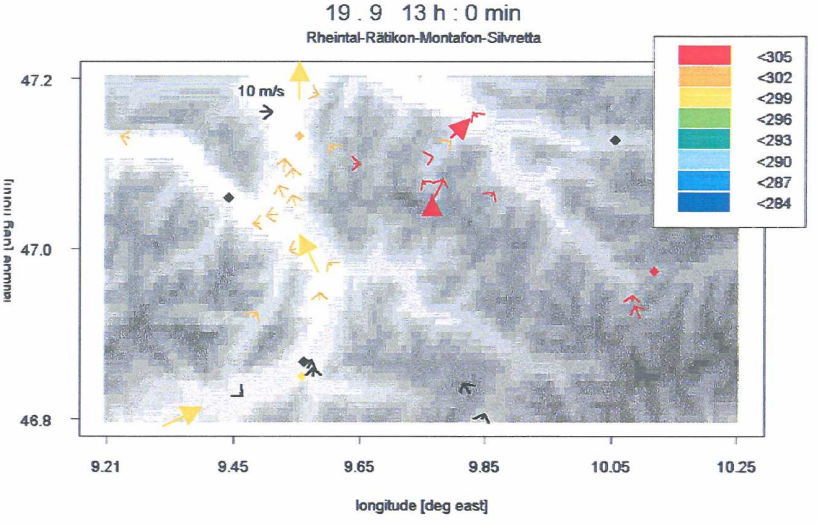

Fig. 12: An example of the loop covering the Rhine valley and tributary valleys. The winds are plotted as arrows, the color code indicates potential tem-perature. The Rhine valley is indicated by yellow arrows, the Brandner Tal by red arrows.

An interesting question was to investigate the relation between the foehn winds at the different stations with respect to along valley pressure gradients. As the exact station elevation was not known with sufficient accuracy, the determination of along valley pressure gradients were done by a hydrostatic evaluation of the observed pressure of adjacent stations. The variation of the height difference may be interpreted as variation of the inclination of pressure surfaces which touches the higher one of the stations. Two examples for these height differences are shown in Figs 13 and 14.

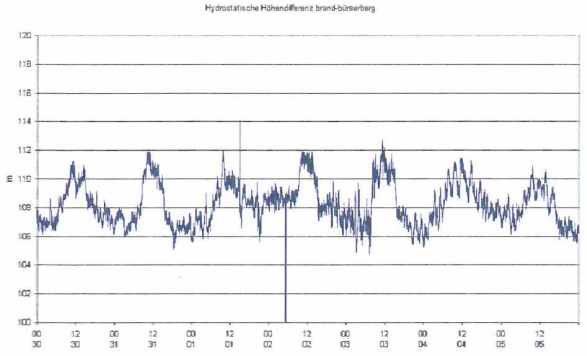

Fig. 13: Hydrostatic height difference Bürserberg-Brand, August 30 – September 6, 1999, a week with well pronounced valley winds

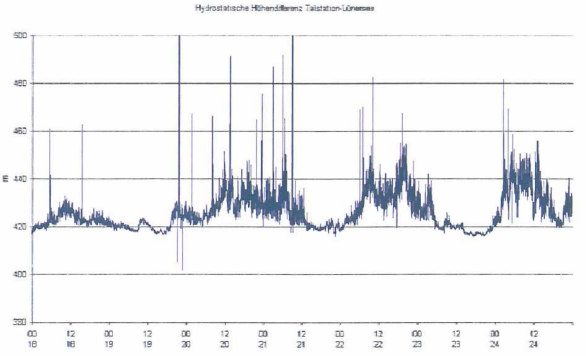

Fig. 14: Same as Fig. 13 but for Talstation-Lünersee, October 18 – 24, 1999, a week with several foehn episodes

Whereas during fair weather conditions (Fig. 13), the maximum of the height difference (strongest inclination of the pressure surface into the valley) is found during the day, combined with up valley winds, the opposite is true for the night. During foehn wind storms (Fig. 14), the diurnal range is disturbed and a correlation between wind speed and height difference is evident. An investigation of the Bernoulli effect (dynamic pressure) showed that for some stations the peak values of the height difference actually could be explained by wind gusts. It was furthermore found that the specific location of the station and especially the orientation of the solar panel at the station tripod influenced the results quite considerably, see e. g. Fig. 15.

Fig. 15: Station Schattenlagant. The pressure sensor is situated in the tube at the upper part of the tripod. Depending the orientation of the solar panel with regard to the foehn wind direction, the sensor may be in the lee of the solar panel or hardly influenced.

The Bernoulli corrected height differences show a substantial reduction of fluctuations which might be explained by the non-hydrostatic pressure fluctuations (see Figs. 16 and 17). Here, the height differences are plotted together with the temperature records. It can be clearly seen, that during weak gradient situations (Fig. 16), the diurnal fluctuations of the height difference are driven by the thermal forcing, whereas during foehn episodes (Fig. 17), the correlation between pressure and temperature is hardly present. Between the two stations shown, the foehn winds are blowing against higher pressure, leading to a deceleration. Hence the general weakening of the wind speed down valley cannot be explained by frictional effects solely.

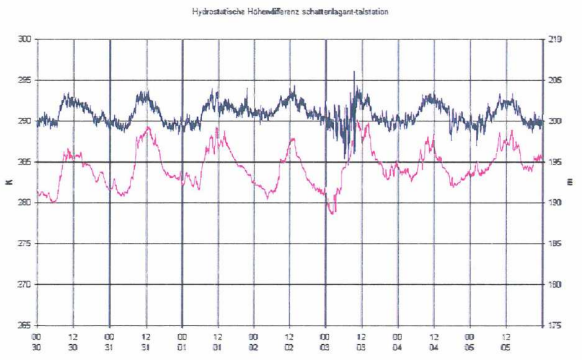

Fig. 16: Hydrostatic height difference between Schattenlagant and Talststation on August 30 until September 5, 1999.

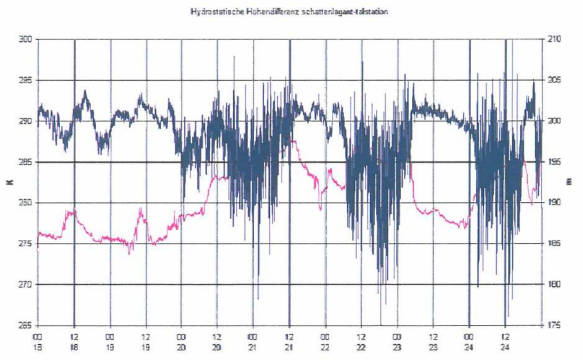

Fig. 17: Same as Fig. 16 but on October 18 – 24, 1999

Finally, an interesting comparison is shown in Figs. 18 and 19., where the (relative) hydrostatic height differences between two pairs of stations in the Brandner Tal and the Rhine valley are shown. During fair weather situations the amplitude in the narrow and steep Brandner Tal due to high frictional effects is much more pronounced as compared to the wide and nearly horizontal less frictional Rhine valley. Furthermore there is a considerable time shift of the phases evident. This is the well known retardation time of the valley wind circulation in large valleys (e. g. Barry, 1992). During foehn episodes the along flow pressure is increasing in the Brandner Tal but decreasing – as one would expect – in the Rhine valley.

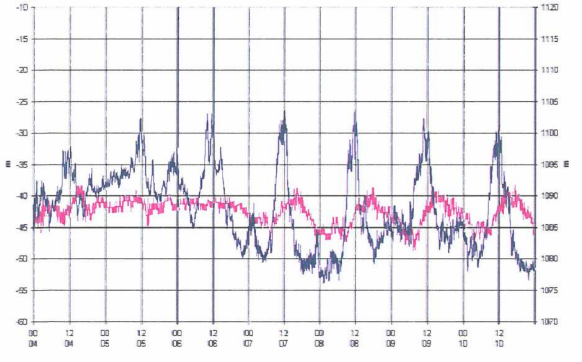

Fig. 18: Hydrostatic height difference between Lünersee and Bürserberg in the Brandner Tal (blue) and between Vilters and Weite in the Rhine valley (purple), from October 4 until October 10, 1999

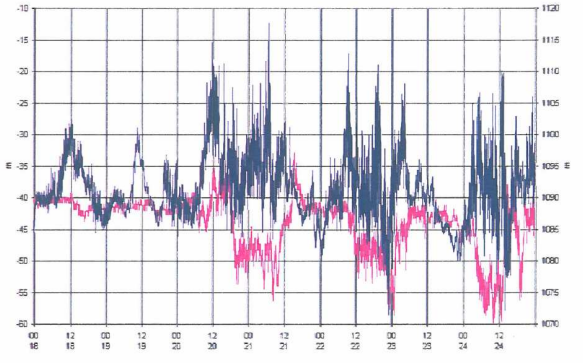

Fig. 19: Same as Fig. 18 but for October 18 – 24, 1999

5 CAR TRAVERSES

In the frame of FORMAT, several car traverses in the Brandner Tal and the Rhine valley have been conducted. The car was equipped with a thermometer, hygrometer, barometer and anemometer with a 1 minute sampling rate, which were stored in a data logger. Driving with a speed of 60 km/h this sampling rate means a distance between data points of 1 km. On winding mountain roads like in the Brandner Tal the speed is generally low, so that the horizontal increments were rather 500 m. To evaluate the data set, the geographic coordinates of roads and the corresponding elevation had to be digitized at significant locations from a high resolution map.

Knowing the elevation of the start point - and eventually the end point - of the car traverse, the pressure record was transformed hydrostatically into elevations and a fit between the elevations from the digitized map and the data from the traverse had to be carried out. From the wind record of the anemometer, mounted roughly 1 m above the top of the car, a distance was computed and compared with the height-distance profile of the digitized road map. Two examples of the profiles are shown, one up-way (Fig. 20) and one down-way the Brandner Tal (Fig. 21). Whereas the profile from the map shows the actual relation of the horizontal versus the vertical distances of the road, the profile from the car is influenced by the speed of the car plus the actual head or tail wind speed similar to the true air speed of airplanes. If the inclination of the car traverse profile is less than the actual inclination of the road, there is head wind and vice versa. By this relation the mean wind speed between two way points can be obtained. If stops are held during the traverse, the calculated distance divided by the duration of the stop gives the mean wind speed at the location during the stop.

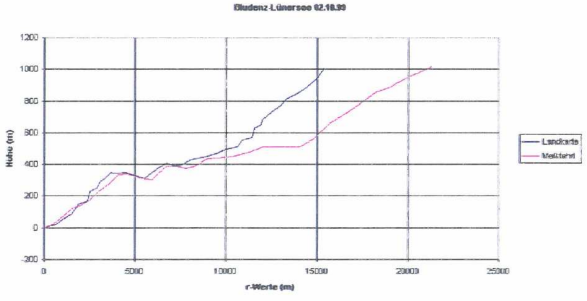

Fig. 20: Example of an up-valley car traverse in the Brandner Tal on October 2, 1999. Heights are relative to Bludenz (560 m msl). Note the stop at a height of 500 m above Bludenz.

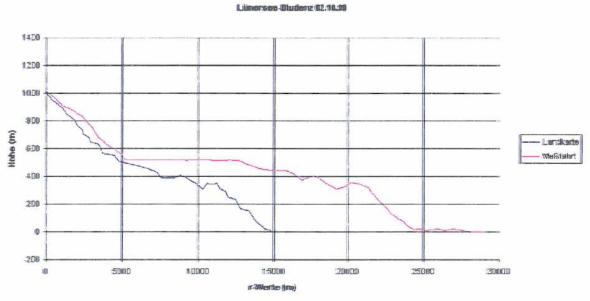

Fig. 21: Same as Fig. 20, but down-valley. Note the long stop at 520 m above Bludenz

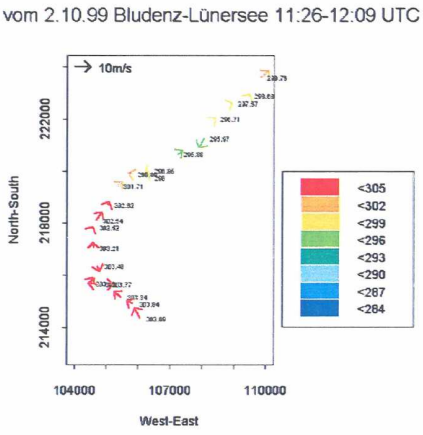

Fig. 22: Plots of wind speed (wind component parallel to the road direction) and potential temperature, color coded, in the Brandner Tal, derived from an up-valley car traverse on October 2, 1999, around noon.

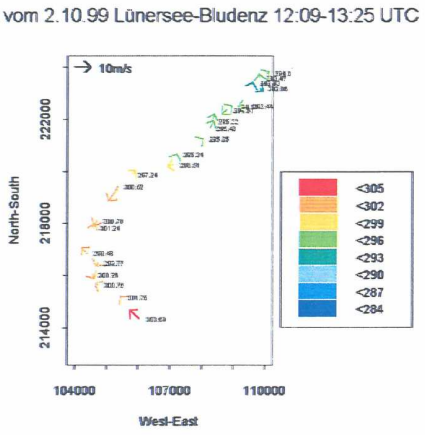

Fig. 23: Same as Fig. 22 but for the down-valley traverse, early afternoon.

The mean wind speed at the way points was then plotted together with potential temperatures, see Figs. 22 and 23. During the up-valley traverse (Fig. 22) at mid levels of the valley a stable stratification may bee seen in connection with a convergence. This means that the foehn flow was well established in the upper part of the valley at that time. The down-valley traverse (Fig. 23), roughly one hour later shows a cooling of the air in most parts of the valley, which means that a cessation of the foehn was caused by an inflow of colder air masses from the North. The wind speeds vary considerably, which may be explained by the fact that the road is winding up the valley, so that the foehn winds may be sometimes perpendicular to the driving direction. The variability of the wind direction indicates the change of the mean orientation of the road segments.

Also in the Rhine valley some car traverses have been evaluated which allow to distinct between areas of foehn touching the ground and cold air pools. The enterprise of using instrumented cars as observing platform has proven to work out well, although the evaluation procedure is rather time consuming.

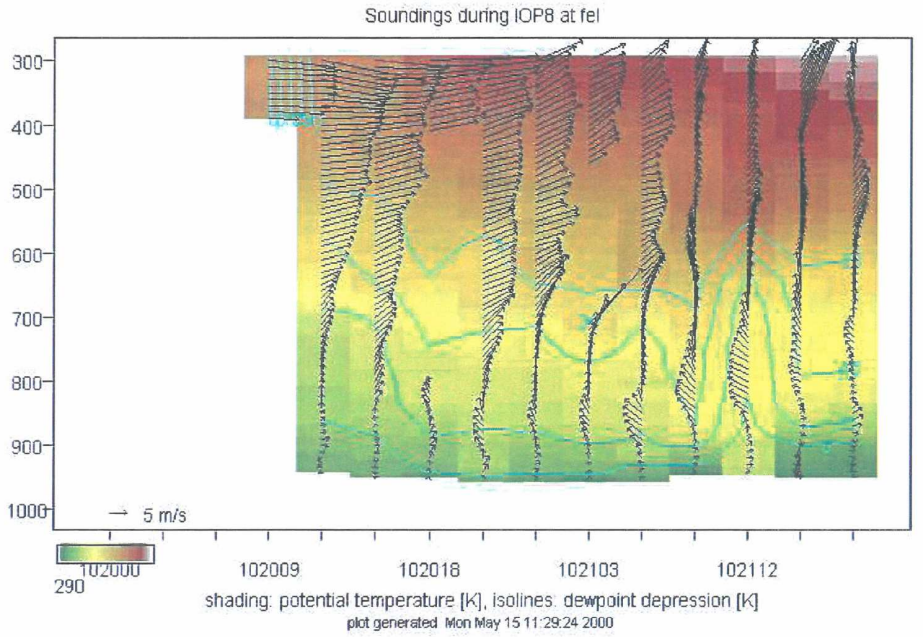

Fig. 24: Time series of the soundings at Feldkirch from October 20 – 21, 1999. The foehn flow in the Rhine valley (below approx. 700 hPa) with direction from SE is clearly separated from the upper level SW gradient wind flow. The stable shallow cold air pool is mostly just a few 100 meters thick.

6 RADIOSONDE AT FELDKIRCH

During selected foehn episodes 3-hourly radiosondes were released in Feldkirch. This sounding was one of an array of 6 similar stations in the Rhine valley, operated by Swiss colleagues. An example of a time section of the Feldkirch radiosonde is shown in Fig. 24. Together with the other soundings an extremely dense resolution of upper level winds temperature and humidity data has been collected, which is certainly unique worldwide.

7 PILOT BALLOONS IN THE BRANDNER TAL

During selected foehn periods pilot balloon measurements have been conducted in the Brandner Tal and in the Walgau. Due to technical problems, most of the evaluations could be evaluated only with a single theodolite. This means that the data have to be interpreted concerning the vertical velocity. Assuming a constant vertical velocity of the balloon during the whole ascent the data may be filtered with respect to wave motions. Even with respect to these uncertainties, most of the wind profiles clearly show a distinct boundary between the foehn flow within the valley (roughly southerly flow) and the flow aloft (mostly westerly to southwesterly), see Fig. 25. These wind profiles will be very important to compute the 3D flow field in the Brandner Tal, using mass continuity, in future calculations.

8 SODAR IN THE WALGAU

The Doppler SODAR of our Department was set up during the MAP SOP at a military camp in the Walgau (Walgaukaserne, Bludesch). Despite a rather remote location, the instrument could not be operated with full intensity due to noise sensitivity of neighboring residents. Therefor the quality of the data was rather disappointing. Only during short periods the full range of data could be evaluated. Nevertheless, for these periods especially the derived wind profiles will serve as input data for a 3D flow analysis planned in future. One example of the time height profile of the wind speed and wind direction is plotted in Fig. 26 and one single vertical wind profile, including vertical velocity and its variance is shown in Fig. 27.

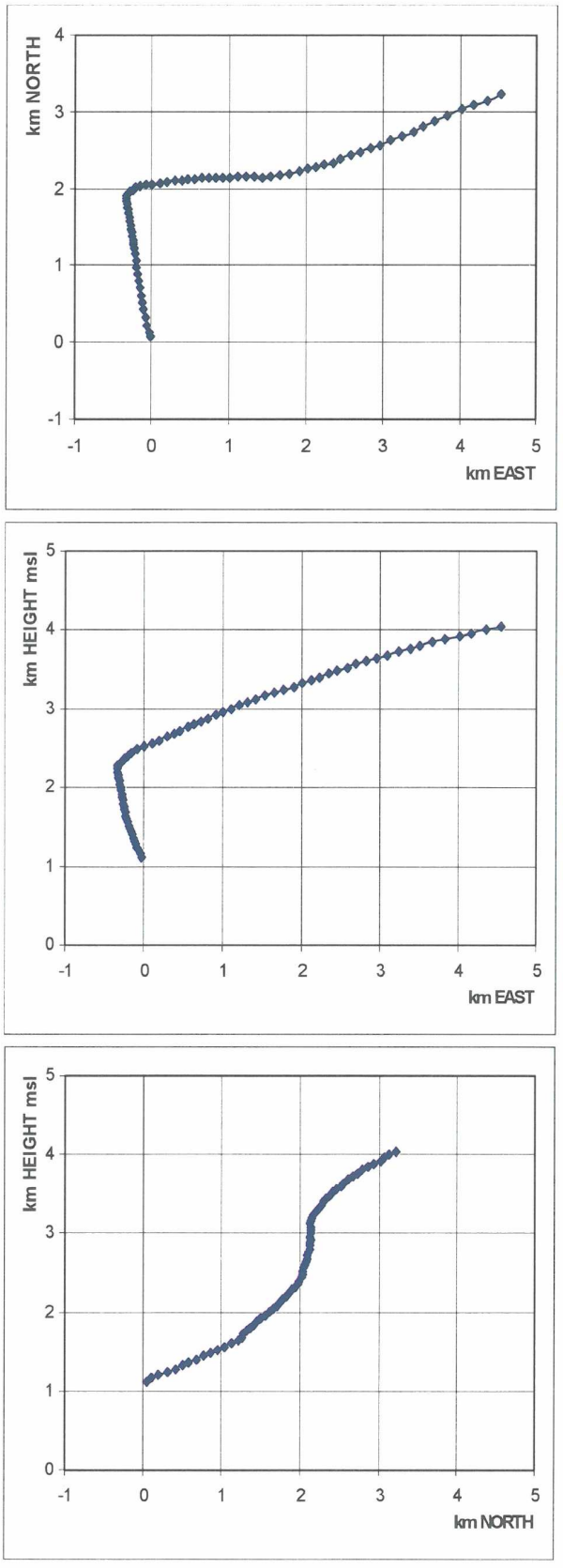

Fig. 25: Example of pilot balloon trajectories during a foehn event (October 12, 1999) in the Brandner Tal. Plotted are the horizontal projection (top), the projection to the East- height plane (center) and the North- height plane (bottom). The dots are plotted every 15 sec.

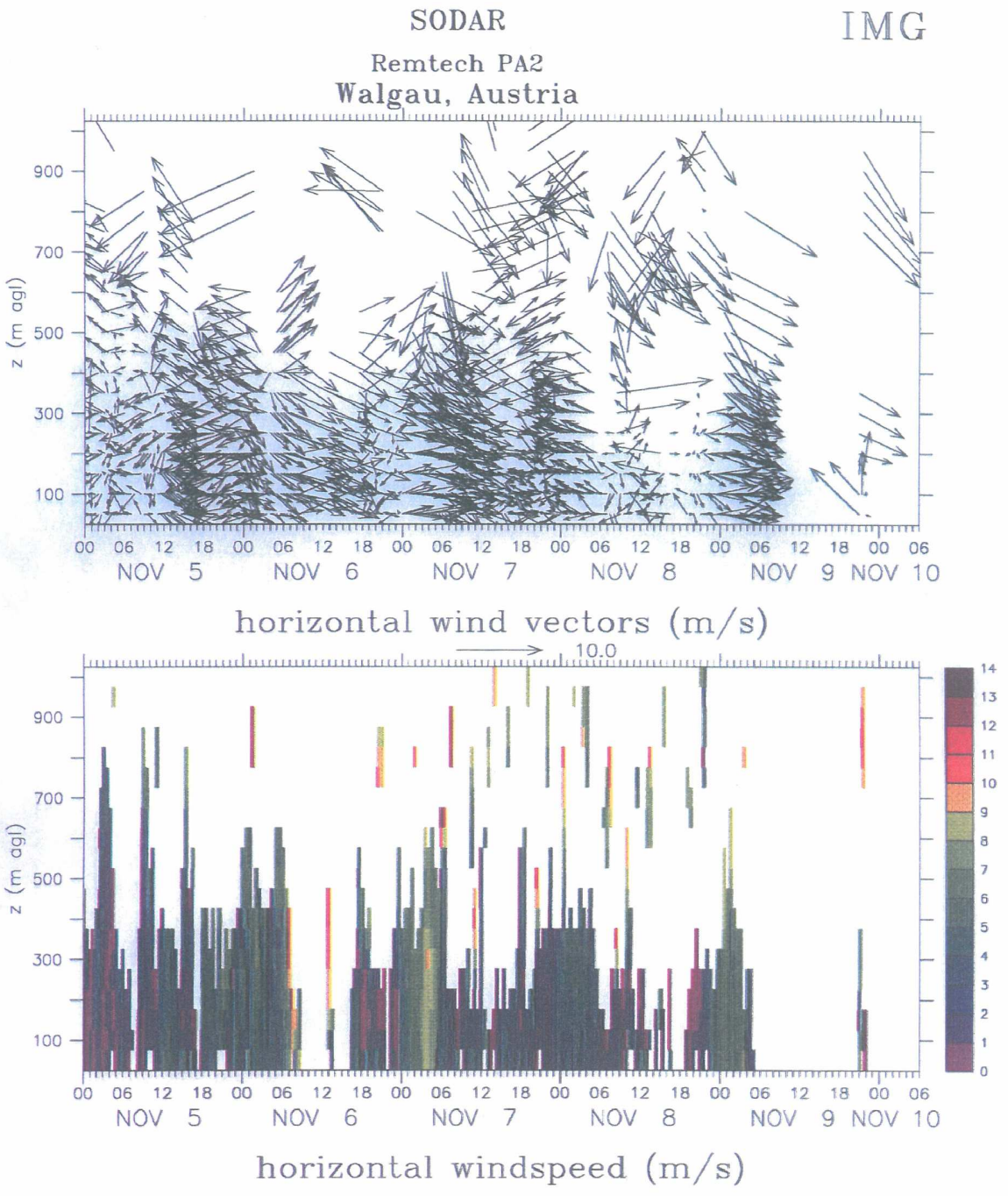

Fig. 26: Example of Doppler SODAR measurements in the Walgau. In the upper panel the horizontal winds are plotted in a vector representation, in the lower panel the horizontal wind speed is shown for the period November 5 – 10, 1999.

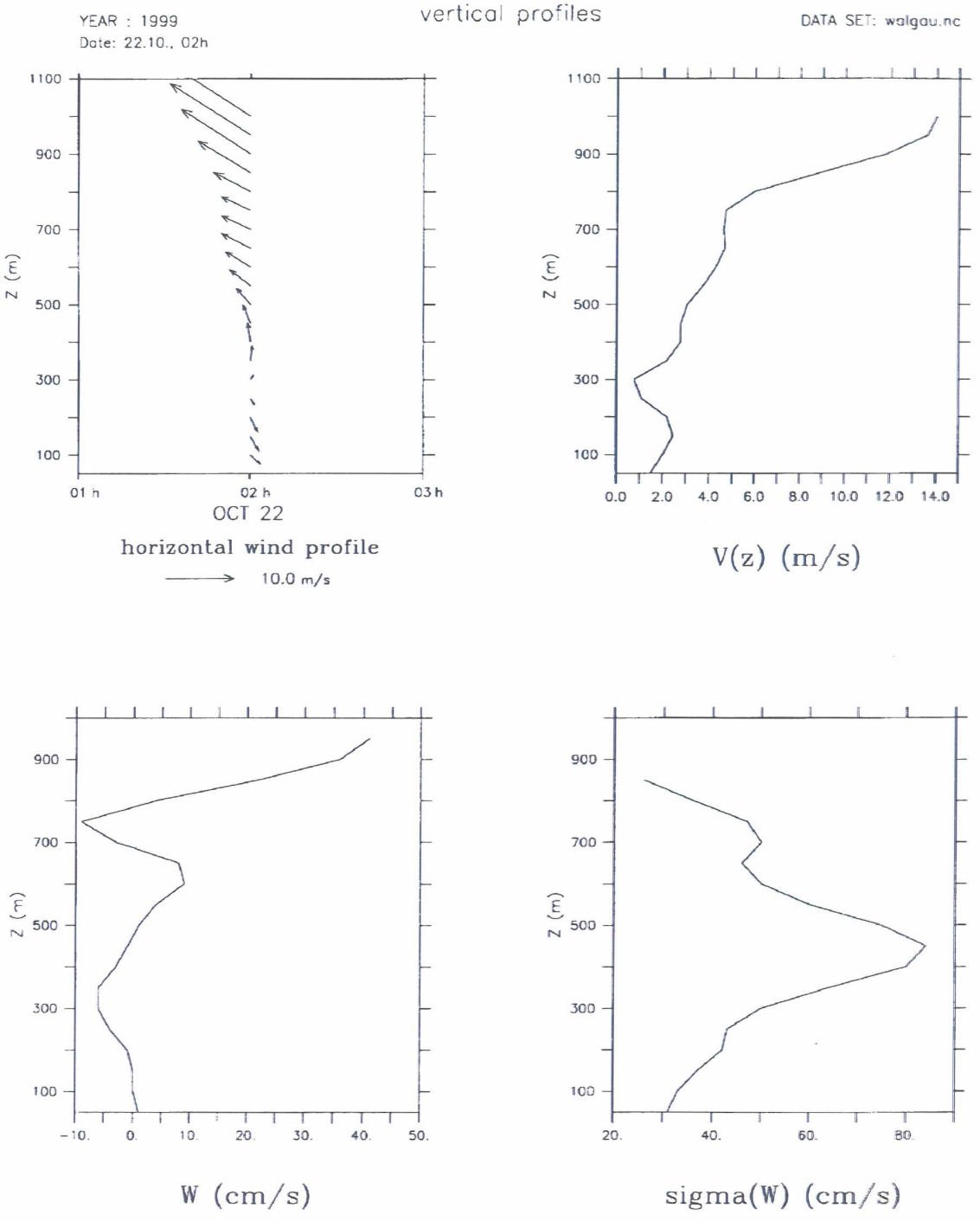

Fig. 27: Example of vertical profiles of the horizontal wind vectors (top left), the horizontal wind speed (top right), the vertical wind (bottom left) and the RMS of the vertical wind (bottom right) derived from the SODAR in Bludesch on October 22, 1999, 0200UTC.

9 MOTOR GLIDER PROFILES

During several foehn episods in October 1999 the motor glider Dimona of METAIR was carrying out research flights, observing temperature, pressure, humidity, winds and chemical tracers at different levels. Most flights were carried out along the Rhine valley, some went also into or above the Walgau and the Brandner Tal. An example of an evaluation of a flight along the Rhine valley is shown in Fig. 28.

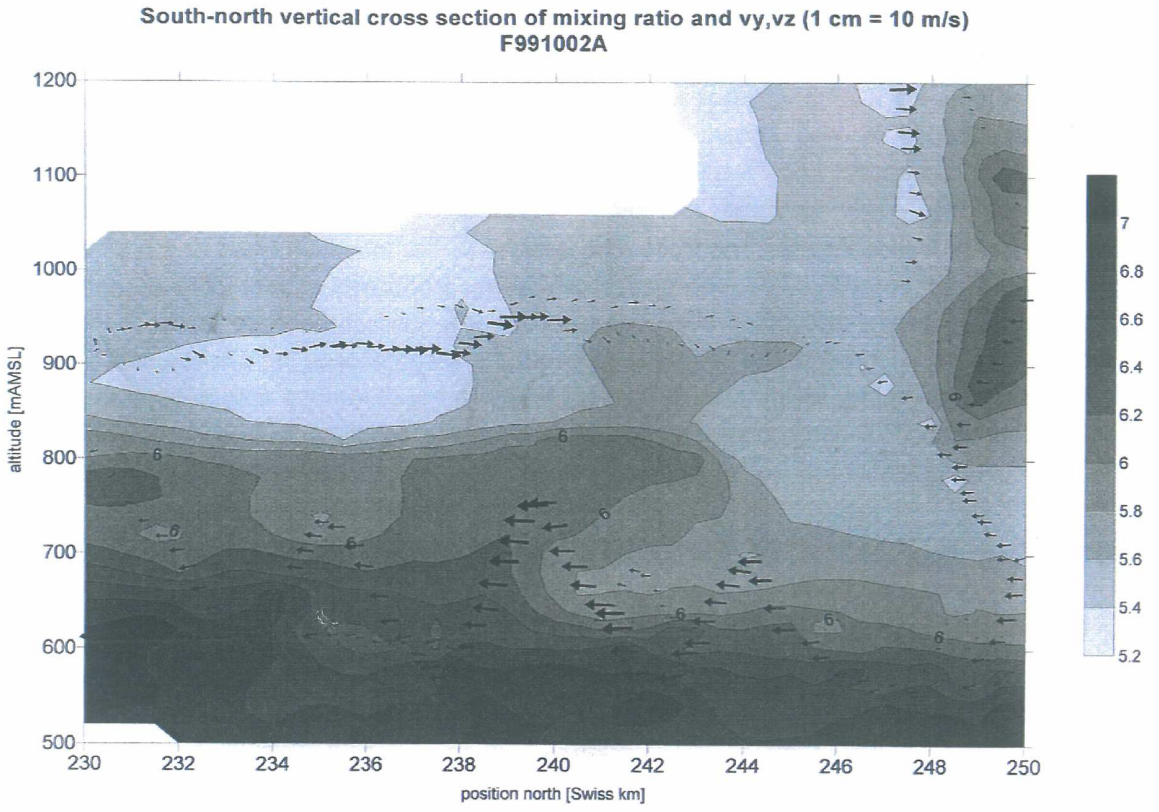

Fig. 28: Example of an evaluation of a flight with the METAIR Dimona along the Rhine valley. Shown are the vectors of the north south component plus the vertical wind component and the water vapour mixing ratio. Note the moist low level air with northerly flow components, i. e. flowing into the Rhine valley and the dry upper level (foehn) air with southerly flow components.

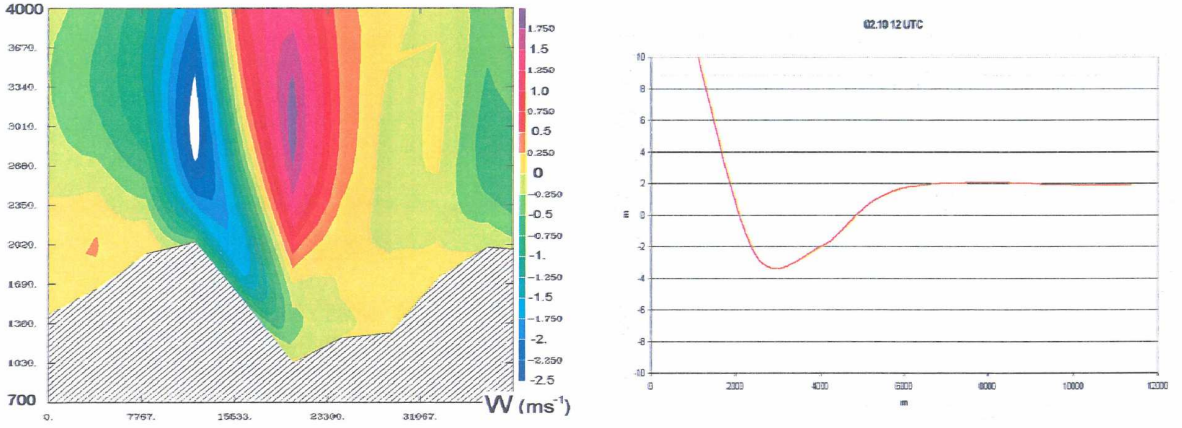

Fig. 29: Model simulation of the Mountain wave (vertical motion field) in the lee of the Raetikon massif left (Meso NH, courtesy of M. Lothon, Lannemezan) and the horizontal pressure distribution along the Brandner valley righ, showing the footprint of the wave. The red curve of the right figure is corresponding to the length of the arrows in the left figure.

10 MODEL COMPARISONS WITH OBSERVATIONS

One mesoscale feature of special interest was the observation that the foehn flow in the Brandner valley usually affects the Oberdorf, but rarely the Unterdorf, a couple of kilometers downvalley of the Oberdorf. This feature is well known to the local people and has been confirmed by our measurements. A reasonable answer to this phenomenon is an intense mountain wave in the lee of the Raetikon, a high ridge between the Rhine valley and the Walgau, which is often fairly perpendicular to the flow at Alpine crest hight. The location of the mountain wave in a high resolution model (MESO-NH, Lafore, J.P. et al, 1998) run (Lothon, M., 2002) was in very good agreement with the surface pressure profile along the valley axis (see Fig. 29). One of the major tasks of FORM was the test of models with respect to the correct simulation of the behavior of the shallow cold air pool in the lower Rhine valley during foehn. Due to the very dense array of surface automatic stations it was possible to compare directly fields of very high resolution models and fields from observations. For this purpose a model independent objective analysis scheme was utilized (Steinacker, R, et al 2000). It is probably for the first time that conventional observations could be used to carry out a model validation on a horizontal resolution in the order of one kilometer (see Fig. 30).

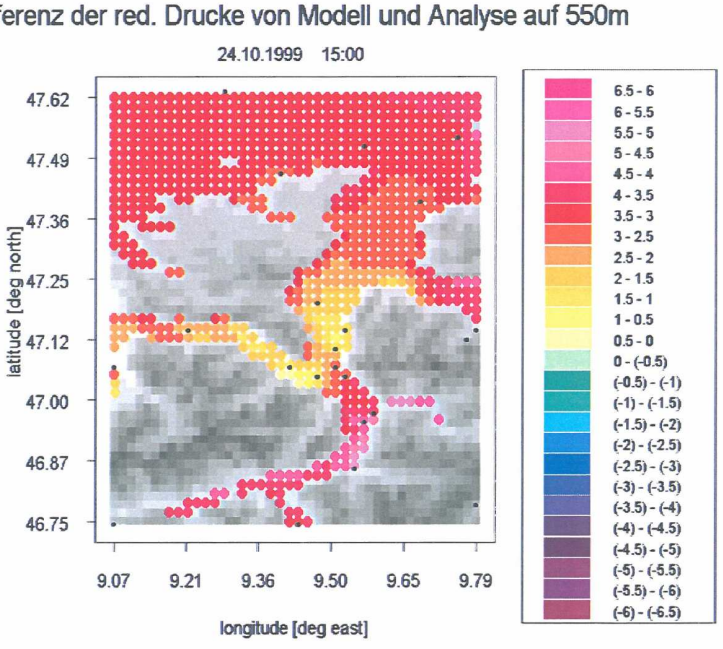

Fig. 30: Very high resolution intercomparison of a simulation model (MM5, 500 m horizontal resolution, courtesy of G. Zaengl, Munich) and observed pressure fields at 550 m msl. The color code indicates the difference in hPa (model minus observation). Dots are only plotted if terrain height is less than 250 m below or above the 550 m level to minimize rduction errors. It is nicely shown that in parts of the valley the model slightly over- or underestimates the actual pressure gradient, especially in the area of the flow splitting (center part of figure).

11 CONCLUSIONS AND OUTLOOK

Thanks to the numerous foehn cases during MAP-SOP the data collecting effort can be seen as a full success. The wealth of data being collected in the area of the Alpine Rhine valley makes it possible, to characterize the foehn flow and its dynamics with a high spatial and temporal resolution. This is an important precondition to conduct further scientific evaluations. A next step consists of the synthesis of the different data into a high resolution gridded format (3D), including the set of observations collected by the international scientific FORM consortium. Then an application of hydro-thermodynamic principles like mass continuity, budgets of humidity, vorticity dynamics and the Bernoulli equation will

be undertaken. This will help to learn more about the specific behavior of the foehn phenomenon, which is so dominant for the weather in many parts of the Alps. Finally, the data fields will be compared with very high resolution prognostic numerical models which have been operated in a test mode during MAP SOP. This will finally allow to find the answer to the question, how well these models are predicting foehn events in Alpine valleys and their temporal evolution.

References

Barry, R., 1992: Mountain weather and climate. Routledge, London, 402 pp.

Baumann, K., H. Maurer, 2000a: Air mass analysis from PBL soundings and trajectories for the Rhine valley – first results of the ROM project. MAP Newsletter, 13

Baumann, K., M. Piringer, 2000b: Continuous PBL measurements of the project ROM during the MAP SOP: Sodar and ultrasonic data. MAP Newsletter, 13

Baumann, K., H. Maurer, G. Rau, M. Piringer, U. Pechinger, M. Furger, A. Prevot, B. Neininger, 200c: ROM project – air mass analysis based on PBL soundings and trajectories. ICAM, Österr. Beiträge zu Meteorologie und Geophysik, 23, No. 392

Baumann, K., E. Polreich, M. Langer, U. Pechinger, 2000c: ROM project – Simulations of the boundary layer – foehn interaction. ICAM, Österr. Beiträge zu Meteorologie und Geophysik, 23, No. 392.

Bougeault, P., P. Binder, J. Kuettner, 1998: MAP Science Plan. SMI Zurich, 64 pp.

Bougeault, P., P. Binder, A. Buzzi, R. Dirks, R. Houze, J. Kuettner, R.B. Smith, R. Steinacker, H. Volkert, 2001. The MAP Special Observing Period. BAMS 82, 433-462

Chimani, B., 2003: Hochaufgelöste Analysen von Druck- und Temperaturfeldern während Föhn im Rheintal. Diploma Thesis, University of Vienna, p. 139

Drobinski, P., A.M. Dabas, C. Haeberli, P.H. Flamant, 2001a: Small scale dynamics of flow splitting in the Rhine Valley during a shallow foehn event. Bound Layer Meteor, in print.

Drobinski, P., A.M. Dabas, C. Haeberli, P.H. Flamant, 2001b: Statistical characterization of the flow structure in the Rhine valley. Bound Layer Meteor, submitted.

Dürr, B., 2000: Föhn heute und gestern – ein interdisziplinäres Forschungsgebiet. Dipl Thesis at Inst Atmos Phys, ETH Zurich.

Häberli, Ch., S. Gubser, B. Dürr, M. Spatzierer, R. Steinacker, T. Gutermann, 2000: Foehn frequencies at surface stations in the Rhine valley during the SOP. MAP Newsletter 13, 40-41.

Lafore, L. P. et al, 1998: The Meso-NH atmospheric simulation system. Part I: Adiabatic formulation and control simulations. Annales Geophys. 16, 90-108.

Lothon, M., 2002: Personal communication

Pechinger, U., K. Baumann, M. Piringer, G. Rau, H. Scheifinger, 2000: ROM: The Rhine valley Ozone study within the MAP foehn campaign FORM – overview and selected results. ICAM, Österr. Beitr Meteor Geophys 23, No. 392.

Piringer, M, K. Baumann, 2000a: Sodar, tethersonde and cable car sonde measurements during the MAP Rhine valley field experiment – first results. MST9 COST 76 workshop, 4.4

Piringer, M., K. Baumann, U. Pechinger, S. Vogt, 2000b: Objectives and first results of the Rhine valley ozone study within MAP. Meteor Zeitschr, subm.

Piringer, M., K. Baumann, U. Pechinger, 2000c: Overview of boundary layer soundings within project ROM during MAP IOPs. MAP Newsletter 13.

Piringer, M., K. Baumann, U. Pechinger, 2000d: An example of continuous measurements by the new tethersonde meteorological tower (TMT) system during the project ROM. MAP Newsletter 13.

Piringer, M., K. Baumann, U. Pechinger, 2000e: Project ROM: The vertical structure of the boundary layer in the Austrian Rhine valley during MAP IOPs. ICAM, Österr Beitr Meteor Geophys 23, No. 392.

Poli, D., G. Seitz, E. Baltsavias, 2000: Cloud top height estimation from satellite stereo pairs for weather forecasting and climate change analysis. ISPRS Archives Vol VII/3

Rau, G., K. Baumann, 2000a: Airborn measurements with the ARAT (STAAARTE 99) over the Rhine valley during deep foehn (IOP 15). MAP Newsletter 13.

Rau, G., K. Baumann, 2000b: Airborn measurements with the ARAT (STAAARTE 99) over the Rhine valley before deep foehn (IOP 18). MAP Newsletter 13.

Rau, G., K. Baumann, 2000c: Comparison of aircraft data (STAAARTE 99) and ground based measurements of ozone (project ROM) before the onset of foehn. ICAM, Österr Beitr Meteor Geophys 23, No. 392.

Rau, G., K. Baumann, 2000d: Aircraft measurements (STAAARTE 99) and cable car soundings (project ROM) during a south foehn event. ICAM, Österr Beitr Meteor Geophys 23, No. 392.

Richner, H., R. Steinacker, 2002: Foehn research in the Rhine valley during MAP: Objectives, concepts and first results. Proceed. 10th Conf Mountain Meteor, Park City, USA, AMS.

Scheifinger, H., R. Werner, K. Baumann, 2000: Ozone measurements in the upper Rhine valley with passive samplers. ICAM, Österr Beitr Meteor Geophys, 23, No. 392.

Seitz, G., E. Baltsavias, 2000a: Cloud mapping using ground based imagers. ISPRS Archives, VII/3.

Seitz, G., E. Baltsavias, 2000b: Satellite and ground based stereo analysis of clouds during MAP. Eumetsat users conf. Bologna, preprints.

Spatzierer, M., 2002: Vergleich der Föhnstruktur in zwei Alpentälern. Diploma Thesis, University of Vienna.

Spatzierer, M., R. Steinacker, 2000: Föhn im Rheintal und Brandner Tal, Rheticus 2, 141-146.

Steinacker, R., 2000a: FORM – Foehn research in the Rhine valley during MAP. MAP Meeting Bohijnska Bistrica, Slovenia, Ljubljana, p 75.

Steinacker, R., I. Groehn, C. Häberli, A. Schmölz, M. Dorninger, M. Spatzierer, 2000b: A comparison of foehn flow in a major valley and its tributaries. ICAM, Österr Beitr Meteor Geophys, 23, No. 392.

Steinacker, R., M. Dorninger, I. Groehn, C. Haeberli, A. Schmoelz, M. Spatzierer, 2000c: A comparison of foehn flow in major valleys and its tributaries – a contribution to MAP.) 9th AMS Conf Mount Meteor. Proceed 67-70.

Steinacker, R., M. Spatzierer, B. Chimani, C. Haeberli, M. Dorninger, S. Tschannett, 2002: What can we learn of surface mesonets in foehn valleys? Proceed. 10th Conf Mountain Meteor, Park City, USA, AMS.

Acknowledgements

Thanks are due to the Austrian Fonds zur Förderung der Wissenschaftlichen Forschung (FWF) for financial support under grant No. P13488-TEC, to Vorarlberger Illwerke for providing their data and to M. Lothon and G. Zaengl for their model results.

Österreichische Beiträge zu Meteorologie und Geophysik

bisher erschienen:

Heft	Publ.Nr.	Fachgebiet	Autor	Titel und Umfang	Preis in Euro
1	329	Meteorologie		*Tagungsbericht EURASAP, Wien, 14.-16. Nov. 1988, Evaluation of Atmospheric Dispersion Models Applied to the Release from Chernobyl.* Wien 1989, 20 Beiträge, 198 S., 100 Abb., 17 Tab.	14,53
2	332	Geophysik		*Tagungsbericht über das 5. Internationale Alpengravimetrie Kolloquium - Graz 1989.* Herausgeber: H. LICHTENEGGER, P. STEINHAUSER und H. SÜNKEL, Wien 1989, 256 S., 100 Abb., 17 Tab.	vergriffen
3	336	Geophysik		*Schwerpunktprojekt S47-GEO: Präalpidische Kruste in Österreich, Erster Bericht.* Herausgeber: V. HÖCK und P. STEINHAUSER, Wien 1990, 15 Beiträge, 257 S., 104 Abb., 17 Tab., 23 Fotos	20,35
4	338	Meteorologie	LANZINGER, A. et al:	*Alpex-Atlas.* FWF-Projekt P6302 GEO, Wien 1991, 234 S., 23 Abb., 2 Tab., 200 Karten	18,17
5	341	Meteorologie	BÖHM, R.:	*Lufttemperaturschwankungen in Österreich seit 1775.* Wien 1992, 95 S., 34 Abb., 24 Tab.	vergriffen
6	343	Geophysik	MEURERS, B.:	*Untersuchungen zur Bestimmung und Analyse des Schwerefeldes im Hochgebirge am Beispiel der Ostalpen.* Wien 1992, 146 S., 72 Abb., 9 Tab.	11,63
7	351	Meteorologie	AUER, I.:	*Niederschlagsschwankungen in Österreich seit Beginn der instrumentellen Beobachtungen durch die Zentralanstalt für Meteorologie und Geodynamik.* Wien 1993, 73 S., 18 Abb., 5 Tab., 6 Farbkarten	23,98
8	353	Meteorologie	STOHL, A., H. KROMP-KOLB:	*Analyse der Ozonsituation im Großraum Wien.* Wien 1994, 135 Seiten, 73 Abb., 8 Tabellen	23,98
9	356	Geophysik		*Tagungsbericht über das 6. Internationale Alpengravimetrie-Kolloquium, Leoben 1993.* Herausgeber: P. STEINHAUSER und G. WALACH, Wien 1993, 251 Seiten, 146 Abb.	23,98
10	357	Meteorologie	ZWATZ-MEISE, V.:	*Contributions to Satellite and Radar Meteorology in Central Europe.* Wien 1994, 169 Seiten, 25 Farbabb., 42 SW-Abb., 13 Tab.	23,98
11	359	Geophysik	LENHARDT W. A.:	*Induzierte Seismizität unter besonderer Berücksichtigung des tiefen Bergbaus.* Wien 1995, 91 S., 53 Abb.	23,98
12	361	Meteorologie	AUER, I., R. BÖHM, N. HAMMER †, W. SCHÖNER., WIESINGER W., WINIWARTER W.:	*Glaziologische Untersuchungen im Sonnblickgebiet: Forschungs-programm Wurtenkees.* Wien 1995, 143 S., 59 SW-Abb., 13 Farbabb., 9 SW-Fotos, 47 Tab.	23,98
13	372	Meteorologie	PIRINGER, M.:	*Results of the Sodar Intercomparison Experiment at Dürnrohr, Austria.* Wien 1996	23,98
14	373	Geophysik	MEURERS, B.:	*Proceedings of the 7th International Meeting on Alpine Gravimetry, Vienna 1996.* Wien 1996	23,98
15	374	Meteorologie	RUBEL, F.:	*PIDCAP - Quick Look Precipitation Atlas.* Wien 1996	23,98

Heft	Publ.Nr.	Fachgebiet	Autor	Titel und Umfang	Preis in Euro
16	378	Meteorologie	DOBESCH, H., KURY G.:	*Wind Atlas for the Central European Countries Austria, Croatia, Czech Republic, Hungary, Slovak Republic and Slovenia,* Wien 1997	23,98
17	382	Meteorologie		*Proceedings of the 9th International Symposium on Acoustic Remote Sensing and Associated Techniques of the Atmosphere and Oceans, Vienna 1998,* 329 Seiten, Wien 1998	23,98
18	383	Meteorologie	RUBEL, F.:	*PIDCAP - Ground Truth Precipitation Atlas.* 84 Seiten, 99 Farbkarten, Wien 1998	36,34
19	384	Meteorologie		*Proceedings of the 2nd European Conference on Applied Climatologie, 19 to 23 Oct. 1998, Vienna.* CD-ROM, Wien 1998	23,98
20	387	Meteorologie		*Proceedings of the 2nd International Conference on Experiences with Automatic Weather Stations, 27 to 29 Sept. 1999, Vienna.* CD-ROM, Wien 1999	23,98
21	388	Meteorologie		*Bericht über den Workshop Umweltforschung im Hochgebirge - Ergebnisse von GAW-Dach und verwandten Projekten, 05. bis 06. Okt. 1999, Wien.* 147 Seiten, Wien 1999	23,98
22	389	Meteorologie	DOBESCH, H., H. V. TRAN:	*The Diagnostic Wind Field Model ZAWIMOD2.* 47 Seiten, 8 Farbabb., Wien 1999	23,98
23	392	Meteorologie		*Proceedings of the 26th International Conference on Alpine Meteorology; 11 to 15 Sept. 2000, Innsbruck.* CD-ROM, Wien 2000	23,98
24	395	Meteorologie	SABO, P.:	*Hochnebelprognose mittels eines objektiven Inversionsindexes für die synoptische Praxis,* 80 Seiten, Wien 2000	23,98
25	397	Meteorologie	AUER, I., R. BÖHM, W. SCHÖNER:	*Austrian long-term climate 1767-2000 - Multiple instrumental climate time series from central Europe,* 160 Seiten, 31 Farbseiten, CD-ROM, Wien 2001	25,00
26	398	Geophysik	MEURERS, B.:	*Proceedings of the 8th International Meeting on Alpine Gravimetry, Leoben 2000,* 240 Seiten, 4 Farbseiten, Wien 2001	25,00
27	399	Meteorologie		*Proceedings of the Deutsch-Österreichisch-Schweizerische Meteorologentagung; 18 to 21 Sept. 2001, Vienna.* CD-ROM, Wien 2001	25,00
28	408	Meteorologie	AUER, I., R. BÖHM, M. LEYMÜLLER, W. SCHÖNER:	*Das Klima des Sonnblicks – Klimaatlas und Klimatographie der GAW Station Sonnblick einschliesslich der umgebenden Gebirgsregion,* 305 Seiten, 130 Farbabbildungen, CD-ROM, Wien 2002	50,00
29	409	Meteorologie		*Scientific Contributions of Austria to the Mesoscale Alpine Programme (MAP), 74* Seiten, 38 Farbseiten, Wien 2003	25,00